

U MATERIAL CHARACTERISATION OF DUCTILE IRONS FOR INDUSTRIAL APPLICATIONS C

BY

HARON O. GEKONDE BSc. ENGINEERING

THIS THESIS HAS BEEN ACCEPTED FOR
THE DEGREE OF M.Sc 1989
AND A COPY ~~TAX~~ BE DEPOSITED IN THE
UNIVERSITY LIBRARY.

A Thesis submitted in partial fulfilment
for the degree of Master of Science in
Mechanical Engineering of the University
of Nairobi.

May 1989

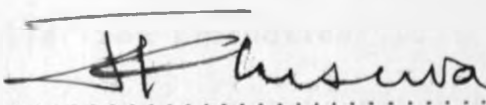
This thesis is my original work and has not been presented for a degree in any other University.

Signature: 

(Haron Ogega Gekonde)

6/11/89

This thesis has been submitted for examination with my knowledge as University Supervisor.

Signature: 

(Prof. J. K. Musuva)

CONTENTS

	Page
CONTENTS	i
ACKNOWLEDGEMENTS	vi
ABSTRACT	vii
NOTATIONS	ix
 <u>CHAPTER ONE : INTRODUCTION</u>	
1.1 History and recent interest in ductile irons	1
1.2 Outline of the work done	3
 <u>CHAPTER TWO : REVIEW OF THE METALLURGY OF DUCTILE IRONS</u>	
2.1 Introduction	7
2.2 Principal types of ductile irons	8
2.3 Raw materials for ductile iron production ..	9
2.4 Melting practices and melting facilities for ductile iron production	9
2.4.1 Cupola	10
2.4.2 Induction furnace	11
2.4.3 Desulphurisation	11
2.5 Solidification of ductile iron	12
2.5.1 Development of graphite spheroids	12
2.5.2 Control of common elements	13
2.6 Production methods and facilities	16
2.6.1 Magnesium treatment processes and facilities for producing ductile iron	16

2.6.1.1	Exact function of magnesium	18
2.6.1.2	Inoculation	19
2.6.1.3	Ladle processes/Open and Covered ladle techniques	20
2.6.1.4	Plunging processes	22
2.6.1.5	Batch treatment vessels	23
2.6.1.6	Inmold process	23
2.7	Metallurgical process control	24
2.7.1	Metal composition considerations	24
2.7.2	Graphite shape	25
2.8	Foundry process control	25
2.8.1	Pouring and gating	25
2.8.2	Riser design	26
2.9	Review of properties of ductile irons	27
2.9.1	Microstructure	27
2.9.2	Hardness	28
2.9.3	Tensile properties	29
2.9.4	Toughness and fracture	30
2.9.4.1	Techniques of assessing fracture toughness	30
2.9.4.2	Impact testing	36
2.9.4.3	Fractography	36
2.9.5	Other properties	37

CHAPTER THREE : EXPERIMENTAL DEVICES AND

DATA ANALYSIS TECHNIQUES

3.1	Experimental devices	46
3.1.1	Induction furnace and treatment ladle	46
3.1.2	Analysis of chemical composition	46
3.1.3	Senstar-Universal Testing Machine	47
3.1.4	Brinell Hardness Number	47
3.1.5	Heat treatment	47
3.1.6	Metallurgical microscope	48
3.1.7	Scanning Electron microscope	48
3.1.8	Testing rig	48
3.1.9	Digital Strain Indicator	49
3.1.10	Measurement of crack length	50
3.1.12	Displacement (clip) gauge	50
3.2	Test specimens	52
3.2.1	Production of ductile iron test specimens ..	52
3.2.2	Heat treatment	53
3.2.3	Fracture toughness specimens	54
3.3	Data analysis techniques	55
3.3.1	Determination of mechanical properties	55
3.3.2	Determination of fracture toughness, K_{IC}	55
3.3.3	Metallography and determination of grain size, nodule count, and mean free path	56

CHAPTER FOUR : EXPERIMENTAL RESULTS

AND DISCUSSION

4.1	Results	65
4.1.1	Mechanical properties	65
4.1.2	Toughness properties	66
4.1.3	Microstructural properties	67
4.2	Discussion	68
4.2.1	Mechanical properties	68
4.2.2	Toughness properties	70
4.2.3	Microstructural properties	71
4.2.4	Fractography	74
4.2.5	Effects of alloying elements	77
4.2.6	Production of ductile iron	79
4.2.6.1	Process control	79
4.2.6.2	Quality control	82
4.2.6.3	Economic factors in production of ductile iron	82

CHAPTER FIVE : CONCLUSIONS AND

RECOMMENDATIONS

5.1	Conclusions	126
5.2	Recommendations	128

APPENDIX A : THE FAMILY OF CAST IRONS

A.1	Definition	130
A.2	Chemical composition	131
A.2.1	White and chilled cast iron	131
A.2.2	Malleable cast iron	132

A.2.3	Gray cast iron	132
A.2.4	Ductile cast iron	133
A.2.5	High alloy cast iron	133
A.3	Microstructure	133
A.3.1	Graphite	134
A.3.2	Cementite	134
A.3.3	Ferrite	135
A.3.4	Pearlite	135
A.3.5	Steadite	136
A.3.6	Austenite	136
A.3.7	Other constituents of cast irons	137
A.4	Summary	137
	<u>REFERENCES:</u>	141

ACKNOWLEDGEMENTS

My first thanks go to my supervisor , Professor J.K.Musuva , for his valuable guidance and advice in the course of this study.

I will not forget Engineer J.K. Chege and the technical staff of the Kenya Railways Corporation's Foundry for their professional contributions and assistance in the production of the test specimens.

I thank the entire Mechanical Engineering Technical workshop staff who assisted in machining the specimens.

I wish to express my appreciation to the Kenya Bureau of Standards and ICIPE for kindly allowing me to use their facilities in analysing the material properties.

I extend my sincere thanks to the members of the Mechanical Engineering Teaching Staff for their encouragement and helpful discussions and mainly to Dr Ubhi for his unlimited assistance.

Finally, I express my gratitude to my wife Mary and my daughter Joan for their warm encouragement and patience during the course of this work.

ABSTRACT

Ductile iron, also known as spheroidal graphite cast iron or nodular cast iron, is an alloy of essentially the same composition as gray cast iron but with the graphite in form of spheroids instead of flake graphite found in gray cast iron.

Recent interest in the development and utilisation of ductile cast irons has resulted in considerable study of the physical metallurgy and mechanical properties to obtain meaningful design data for these materials. Equally important is the identification of process control and quality assurance factors to achieve the desired properties successfully and consistently.

In this study, aspects of the physical metallurgy, production process and properties have been investigated. Results of properties of ductile cast irons from tests performed on cast specimens of a variety of compositions and microstructures are presented. The test specimens were produced from gray cast iron scrap using various magnesium additions in order to obtain alloys with varying amounts of residual magnesium contents and different microstructures. The chemical composition, mechanical properties and microstructural properties were analysed. Tension properties were measured in accordance with ASTM E 8-81 test procedures, fracture toughness was measured using

the compact specimens in accordance with ASTM E 399-81 test procedures and the microstructural properties were measured as per the ASTM E 112 procedures.

The variables studied include: nodule count, nodularity, matrix microstructure, specimen section size, residual magnesium content, alloying elements, matrix grain size, and inter-nodule spacing. After failure, the fracture surfaces were observed visually and by means of the scanning electron microscope, so as to relate microstructure and crack morphology.

The properties were observed to improve as the residual magnesium content increased from 0.004% for gray cast iron to 0.043% for the best ductile iron that was produced. The tensile strength increased from 247 MN/m^2 to 378 MN/m^2 while the average fracture toughness, K_{Ic} , increased from $24 \text{ MN/m}^{3/2}$ to $53 \text{ MN/m}^{3/2}$ for the annealed specimens. The nodule count and nodularity were found to increase with increasing magnesium levels. Annealing heat treatment was found to transform pearlitic matrix structures into ferritic matrix structures from which the highest toughness values were obtained. The ferritic specimens were observed to fracture with ductile tearing while those with pearlitic matrix microstructures fractured with intergranular and partly quasi-cleavage fracture.

NOTATION

- a - effective crack length
- A_c - choke cross-sectional area
- b - vertical distance between the horizontal plane containing the choke and the topmost point of the casting / riser complex
- B - test piece thickness
- C - carbon
- C.E - carbon equivalent
- Cr - chromium
- d - grain diameter
- dS_c - an increment of arc length
- E - Young's modulus
- f_r - friction coefficient
- g - gravitational acceleration
- G - strain energy release rate
- G_{crit} - critical strain energy release rate
- H - vertical distance between the liquid level in pouring basin and the horizontal plane containing the choke
- K - stress intensity factor
- K_I - plane strain stress intensity factor
- K_{Ic} - critical value of K_I or plane strain fracture toughness
- kN - kilo newton

- K_a - a provisional value of K_{Ic}
 K_y - measure of the pinning of dislocations
Mg - magnesium
Mn - manganese
Mo - molybdenum
Ni - nickel
P - phosphorus
 P_a - applied force
 P_a - load at instability of crack
 r_y - radius of plastic zone
S - sulphur
 S_c - crack length around a crack tip
Si - silicon
t - pouring time for a single mould
 T_c - transition temperature
u - surface tractions and displacements along
the contour of a crack
 V_c - volume of cope part of the casting
 V_d - volume of drag part of the casting
W - test piece width
 $Y(\frac{a}{W})$ - calibration function which defines K_I for
the specific body
 ν - Poisson's ratio
 Γ - closed path around a crack tip anticlockwise
r - surface tractions and displacements along
the contour of a crack

- ϵ - strain
- ϵ_{ij} - strain tensor
- ϵ_y - strain at yield
- δ - developed crack opening displacement at the tip of a crack
- μ - micro i.e $\times 10^{-6}$
- σ - applied stress
- σ_F - fracture stress
- σ_{ij} - stress tensor
- σ_{ult} - ultimate tensile stress
- σ_y - yield stress or 0.2% proof stress
- λ - spacing between the nodules (or inter-particle or nodule spacing)

Abbreviations

- AFS - American Foundrymen's Society
- ASM - American Society for Metals
- ASTM - American Society for Testing and Materials
- ASTM STP - American Society for Testing and Materials Standard Testing Procedures
- BCIRA - British Cast Iron Research Association
- BHN - Brinell Hardness Number
- BSI - British Standard Institution
- COD - crack opening displacement

- ICIPE - International Centre of Insect Physiology
and Ecology
- INCO - International Nickel Company
- J.Mat.Sci.- Journal of materials science
- LEFM - Linear elastic fracture mechanics
- SEM - Scanning Electron Microscope
- Trans.AFS Transactions of the American Foundrymen's
Society
- Trans.AME Transactions of the American Institute of
Mechanical Engineers
- UNIDO United Nations Industrial Development
Organisation

CHAPTER ONE

1.0 INTRODUCTION

1.1 HISTORY AND RECENT INTEREST IN DUCTILE IRON

The phrases "Strategic Metals" and "Critical Metals" are now commonly used to describe a group of metals on which a country can have heavy import dependence and that it would have hard time getting along without, from an economic stand point. With adequate "Substitution Technology" available, the ability to switch quickly to new materials in non-critical applications will help minimise the impact of import dependence and increase the value of our existing supplies. However "Substitution Technology" has its minimum requirements which lie in the hands of the producer and the consumer.

The predominant materials in current industrial and automobile engines are cast iron and steels. Ductile iron, which is also known as spheroidal graphite cast iron or nodular iron, was first announced to the foundry industry as a new engineering material at the 1948 annual meeting of the American Foundrymen's Society [1]. The BCIRA discovered it by the process of adding cerium to molten, hypereutectic cast irons of the same analysis as gray cast iron while the INCO

discovered it by similarly employing magnesium addition to either hypo or hypereutectic cast irons.

At present ductile iron is taken as a new material by researchers [2,3,4,5] because its properties have not been fully exploited. However, there has been increased interest in the properties and applications of this material especially in the automobile industry and in 1983 it formed 21% of the world's production of ferrous castings [1], while in 1984 it formed 24.8% of the world production of ferrous castings as calculated from Table 1.1 [6].

Ductile iron has been shown [7] to comprise a large number of cast irons with tensile strengths ranging from about 400 N/mm^2 with 17% elongation to over 1000 N/mm^2 with 2-3% elongation.

Donaldson [8] has described some of the many applications of spheroidal graphite cast iron in the automobile industry. Gratton [9] has also suggested industrial applications of ductile irons. Recent efforts [10] have been to use ductile irons in components for which fracture toughness is a concern e.g turbine casings and automotive components.

Many theories have been proposed [11,12,13,14] to describe how spheroidal graphite nucleates in ductile iron and the subsequent production of the material, but so far very little work has been done to produce the

material in Kenya and from scrap metal.

In view of the increased use of ductile iron by the foundry industry in the world and for critically stressed components, particularly in industrial and automobile components, it is necessary to obtain meaningful design data which enables fail-safe behaviour prediction for this material.

As well as being cost competitive with forged and cast steels, ductile iron may offer considerable flexibility in the design of industrial components if the attractive combinations of tensile, fatigue, toughness, fracture and damping properties are explored and fully utilised. This requires a considerable study of the physical metallurgy and the properties of these high strength high toughness cast irons. Equally important is the identification of process control and quality assurance to achieve the desired properties successfully and consistently.

1.2 OUTLINE OF THE WORK DONE

A suitable process for the production of ductile iron was determined and used to produce the specimens that were tested in this study.

Ductile iron was produced from gray cast iron scrap by the use of magnesium ferrosilicon in the spheroidising treatment.

Four heats of alloys with varying amounts of residual magnesium content were produced.

The chemical compositions and mechanical properties of the alloys were determined. Investigation of the fracture characteristics of the alloys was done by determining the plane strain fracture toughness.

The effects of the microstructure, residual magnesium content, heat treatment, alloying elements and process control on the properties of these alloys was determined. The fracture behaviour of the alloys was analysed metallographically using optical as well as scanning electron microscopy.

WORLD CASTING PRODUCTION - 1984

COUNTRIES	GRAY Ton	DUCTILE Ton	ROLLABLE Ton	STEEL Ton	TOTAL IRON Ton	TOTAL Ton	POPULATION	GDP/PER \$	IRON/PER. kg	TOTAL/PER kg
ARGENTINA	161,440	68,082					30,104,000	2,230		
AUSTRALIA	320,000	68,000	5,000	75,000	393,000	468,000	15,962,000	11,400	25,294	30,673
AUSTRIA	95,500	44,900	12,800	21,900	193,200	175,100	7,527,000	9,140	20,353	23,243
BELGIUM	130,900	11,300	200	75,000	142,400	217,400	9,856,000	8,430	14,444	22,058
BRAZIL	963,069	273,214	37,756	133,689	1,274,035	1,407,724	132,582,000	1,710	9,609	10,414
CANADA	492,245	289,118	6,639	77,745	768,032	865,777	25,183,000	13,140	31,292	34,379
CHINA	939,000	32,740	31,110	34,720	602,940	637,660	1,030,150,000	310	0,585	0,419
CHINA TAIWAN	640,000	80,320	27,060	50,850	727,180	778,030	n.a.	n.a.	n.a.	n.a.
CZECHOSLOVAKIA	1,044,274	27,706	32,056	328,000	1,104,036	1,432,036	15,464,000	n.a.	71,394	82,605
Denmark	66,837	17,175	n.a.	9,979	84,012	93,988	5,110,000	11,290	16,437	18,392
EGYPT	n.a.	n.a.	n.a.	24,265	n.a.	n.a.	46,172,000	720	n.a.	n.a.
FINLAND	56,600	14,000	2,000	10,600	72,600	83,200	4,902,000	10,830	14,61	16,973
FRANCE	1,014,300	669,900	35,500	135,000	1,719,700	1,655,600	55,089,000	9,660	31,217	33,654
GERMANY, DEM.	2,343,300	802,000	126,400	229,000	3,271,700	3,500,700	16,701,000	n.a.	105,698	200,61
GERMANY, FED.	2,268,100	769,000	132,400	217,800	3,189,500	3,387,300	61,205,000	11,090	51,785	55,744
HUNGARY	201,030	4,274	45,472	47,000	250,776	297,776	10,492,000	2,050	23,455	27,85
INDIA	241,315	87,998	n.a.	n.a.	n.a.	n.a.	749,880,000	260	n.a.	n.a.
ISRAEL	16,100	1,250	3,000	3,000	21,250	25,150	4,172,000	5,100	5,093	6,028
ITALY	1,163,200	129,100	20,900	86,800	1,313,200	1,400,000	57,033,000	6,440	23,025	24,547
JAPAN	3,180,000	1,765,000	290,000	545,000	5,235,000	5,780,000	120,075,000	10,390	43,598	48,137
KOREA, REP.	540,000	170,000	33,000	105,000	743,000	848,000	40,576,000	2,090	16,311	20,809
LUXEMBURG	n.a.	n.a.	n.a.	n.a.	n.a.	n.a.	385,000	13,650	n.a.	n.a.
MALAYSIA	29,030	5,443	n.a.	n.a.	34,473	n.a.	15,206,000	1,990	2,267	n.a.
MEXICO	330,000	45,000	n.a.	57,800	375,000	432,500	76,949,000	2,060	4,873	5,821
NETHERLANDS	188,000	28,900	9,400	3,000	220,300	229,300	14,411,000	9,430	15,703	15,911
NEW ZEALAND	n.a.	n.a.	n.a.	n.a.	n.a.	n.a.	3,249,000	7,240	n.a.	n.a.
NORWAY	96,500	18,000	11	4,000	86,000	90,000	4,151,000	13,750	20,716	21,621
PERU	12,000	800		5,200	13,000	18,200	10,770,000	980	0,711	0,609
PHILIPPINES	745,000	n.a.	n	265,000	745,000	1,010,000	60	660	13,945	12,912

Table 1.1 - World casting production - 1984 [6].

POLAND	1,427,000	373,766	51,200	258,000	1,496,966	2,154,966
PORTUGAL	37,000	10,000	15,500	9,000	62,500	71,500
ROMANIA	1,130,270	31,370	19,830	370,000	1,181,470	1,551,470
SOUTH AFRICA	129,000	20,700	17,600	107,300	107,100	274,400
SPAIN	510,000	130,000	28,000	112,000	668,000	780,000
SWEDEN	214,000	46,000	7,000	14,600	267,600	281,600
SWITZERLAND	115,300	69,300	n.a	5,200	184,600	189,600
TURKEY	380,000	14,000	6,000	80,000	400,000	460,000
UNIT KINGDOM	1,000,100	304,900	82,600	114,300	1,376,200	1,400,500
USA	7,400,000	2,360,000	329,000	879,000	10,029,700	10,908,000
USSR	0,162,720	1,860,667	n.a	n.a	n.a	n.a
VENEZUELA	19,959	2,722	n.a	n.a	22,680	n.a
YUGOSLAVIA	279,418	62,597	32,300	96,000	374,315	470,315
ZAMBIA	931	n.a	n.a	25,232	931	26,163

Table 1.1 - Cont.

36,918,000	a. a	51,383	58,371
10,202,000	1,070	6,126	7,008
22,628,000	a a	761,519	66,564
32,722,000	2,260	5,107	8,366
38,523,000	4,470	17,34	20,248
8,337,000	11,880	32,026	33,777
6,572,000	15,990	26,080	28,68
48,266,000	1,200	6,287	9,531
56,327,000	6,530	24,432	26,462
236,961,000	15,490	42,323	46,033
275,029	a a	a. a	a. a
17,820,000	3,220	1,272	a a
22,955,000	2,120	16,306	20,484
6,477,000	470	a. a	4,039

CHAPTER TWO

2.0 REVIEW OF THE METALLURGY OF DUCTILE IRONS

2.1 INTRODUCTION

Ductile cast iron has the range of chemical composition shown in Table 2.1.

Formation of ductile iron involves the nucleation of the carbon in gray iron in the form of spheroids or nodules. This process is very sensitive to the composition and impurities [4] and therefore requires a molten iron of very restricted content of minor elements. Alloying elements are also essential to provide sufficient mechanical and microstructural properties and response to heat treatment for heavy sections, but it has been found [4] that excessive alloying imposes difficulty in obtaining sound castings.

Therefore, the production of ductile iron involves complex physical metallurgy and requires the use of special melting, pouring techniques and close process control. This has since been tried and several methods have been suggested [15] and the original methods have been improved [16], in order to produce sound ductile iron castings.

2.2 PRINCIPAL TYPES OF DUCTILE IRONS

Depending on solidification conditions and heat treatment offered to ductile cast irons, several types with a range of different properties can be obtained as summarised in Table 2.2 and also specified by the ASTM standards [17].

Ductile irons have been classified as follows:

- (i) Ferritic type: These have a microstructure consisting of ferrite matrix and graphite spheres, and possess high ductility, excellent machinability and moderate yield strength.
- (ii) Pearlitic type: These have a matrix microstructure primarily of pearlite, have good yield strength and machinability, but moderate ductility. They provide excellent response to flame or induction hardening.
- (iii) Heat treated type: These are normalised or quenched and tempered. They have exceptionally high tensile and yield strength, while retaining ductility.

2.3 RAW MATERIALS FOR DUCTILE IRON PRODUCTION

The main raw materials commonly used for production of ductile iron are:

- (i) The material for the molten metal usually referred to as the charge of the furnace. In most cases the materials charged into the furnace are pig iron, mild steel and gray iron. The gray iron and mild steel may be obtained from scrap, but the composition of the charge must be known so that the composition of the molten metal can be adjusted to bring the elements to the required levels before the magnesium treatment for spheroidisation. Other additions may be silicon, manganese or silicon carbide in form of briquets which improve the properties.
- (ii) Ladle additions which are referred to as the treatment alloy or nodularising agent. These may be a magnesium alloy or cerium, but the former has been proved [18] to be more effective.

2.4 MELTING PRACTICES AND MELTING FACILITIES FOR DUCTILE IRON PRODUCTION

There are several types of furnaces that are used in foundries. The commonly used are, cupolas, open hearths, air furnaces, electric arc furnaces,

electric induction furnaces, crucible furnaces, reverberatory furnaces and non-crucible furnaces.

The cupola and electric induction furnaces are the common methods of melting for ductile iron production. More so the induction furnace is less prone to impurities in the metal, and offers enough holding time for metal composition adjustments to be made before the spheroidising treatment to obtain ductile iron.

2.4.1 THE CUPOLA

It has been found [5] that to produce one ton of molten iron, the materials needed are as listed in Table 2.3. Pig iron is used to increase the silicon, carbon and manganese level in the molten metal before treatment with magnesium. Proper proportioning of pig iron, gray iron scrap and steel scrap is usually performed by charge calculation and experience with the materials.

Composition adjustments and alloying are an important step in the melting of ductile irons. The silicon and manganese contents of the cupola charge are increased by adding briquets of ferrosilicon and ferromanganese, or silicon carbide. Alloy addition can be done in the ladle.

2.4.2 INDUCTION FURNACES

The most widely used induction furnaces for ductile iron production are the low frequency, 60-cycle type. Superheating can be achieved using these furnaces along with close control of composition and temperature for high quality product.

2.4.3 DESULPHURISATION

As will be explained in section 2.6.1 magnesium first reacts with sulphur before it causes any spheroidising. Kalph [16], in his study of the magnesium treatment processes for production of spheroidal graphite cast iron proved that an appreciable amount of high-cost magnesium alloy is consumed before graphite spheroidisation can occur if the sulphur content is not reduced prior to treatment.

Heine [19] and Gertman [20] have concluded that a reduction of 0.01% sulphur requires approximately 0.01% magnesium while injection of calcium carbide into the melt causes desulphurisation from 0.12% to 0.02% and soda ash addition reduce the sulphur level of the melt, causing desulphurisation from 0.14% to about 0.06%, which with further addition of soda ash can be reduced to between 0.03% and 0.025%.

A recent innovation [5] is the development of the "shaking ladle". In this process, desulphurisation occurs by the reaction of lime with the sulphur of the melt. Shaking the ladle increases the contact of the iron with the lime, resulting in sulphur levels as low as 0.02% with 70 to 75 per cent efficiency.

2.5 SOLIDIFICATION OF DUCTILE IRON

The base chemistry of gray and ductile iron can be the same as given in Table 2.1. The only exception is in the sulphur and magnesium content and that the alloys solidify according to quite different models.

2.5.1 DEVELOPMENT OF GRAPHITE SPHEROIDS

Unlike gray iron [5,21], solidification of the spheroidal graphite eutectic in ductile iron has been reported to start at temperatures above those of the flake-graphite eutectic for similar carbon equivalents.

Murthy and Seshan [15] have found that the number of graphite spheroids is determined at an early stage of solidification and subsequent cooling of the solidified ductile iron is accompanied by graphite precipitation on the existing spheroids at temperatures down to the eutectoid range.

For fully spheroidal graphite structures therefore, an adequate number of spheroids is required at the start of solidification (See Figures 2.1 and 2.2).

2.5.2 CONTROL OF COMMON ELEMENTS

As it is well known, ductile iron is a quality product and therefore requires strict control of its composition which affects the properties.

CARBON:- The carbon contents for commercial ductile iron is 3% - 4%. It has been shown [3] that increasing the carbon content from 3% to 4% results in high nodule count, increased castability by improved fluidity and feeding, and progressive increase in the tensile strength upon heat treatment.

Carbon equivalent is given by [5],

$$\left. \begin{aligned} \text{C.E} &= \%C + \frac{1}{3} \%Si \\ &\text{(for low phosphorus contents)} \\ \text{C.E} &= \%C + \frac{\%Si + \%P}{3} \\ &\text{(for high phosphorus contents)} \end{aligned} \right\} \dots\dots (2.1)$$

In order to promote development and growth of graphite spheroids the carbon equivalent should be in excess of 4.3 and therefore the composition range of carbon has been restricted to 3.5% - 3.7% [4].

SILICON:- Silicon in ductile cast iron offers satisfactory response to ferritising anneal and provides improvement in fracture toughness, K_{Ic} , of these alloys.

The normal range is 2.5% - 2.9% . Silicon is more influential in spheroidal graphite control when the additions are made after the magnesium treatment, a process referred to as late inoculation or post-inoculation [22].

SULPHUR:- As it has been shown in section 2.4.3, high sulphur levels make the production of ductile iron difficult and expensive. For good results and low costs, the sulphur level of the melt should be reduced to 0.015% before magnesium treatment.

PHOSPHORUS:- A maximum of 0.05% phosphorus is usually specified [21] since it adversely affects toughness and ductility by forming the very hard and brittle structure known as steadite in ductile iron.

MANGANESE:- Manganese increases hardenability of ductile irons, but reduces tensile strength, hardness and elongation if increased beyond 0.6%.

Vasudevan et al [23] have concluded that in austenitic ductile irons, nickel may be partially replaced by manganese at a lower cost,

accompanied by increased hardness and some loss in corrosion resistance, formation of carbides and a decrease in nodule count.

Argo et al [24] have concluded that as the section size of a bar cast decreases, the amount of nodular graphite, carbides and pearlite increases for any given manganese content.

NICKEL:- This element imparts corrosion resistance, heat resistance and hardenability to ductile iron when present in the range of 14% to 36% without appreciable amounts of manganese or chromium [23].

COPPER:- Copper suppresses formation of carbides, increases fluidity and hence improves fracture toughness, machinability and castability when present in ductile iron at about 1.5% by weight.

MOLYBDENUM:- Additions of up to about 0.3% are most effective in increasing hardenability but reduce tensile strength, hardness and ductility. It also promotes formation of carbides.

VANADIUM AND CHROMIUM:- They both impart heat resistance, high hardness, corrosion resistance but should be kept below 0.05% because they readily cause segregation of carbides.

ALUMINIUM, TITANIUM AND BORON:- They all increase casting soundness. In addition, boron increases surface hardness and refines the structure of ductile irons.

2.6 PRODUCTION METHODS AND FACILITIES

Ductile iron has predominantly nodular shaped graphite in the as-cast condition. To enhance the formation of nodular cast iron, many methods have been proposed [15], and most of them are based on the effective treatment alloy and ladle treatment process. A review of the common methods and facilities is given below.

2.6.1 MAGNESIUM TREATMENT PROCESSES AND FACILITIES FOR PRODUCING DUCTILE IRON

Although a number of elements can be used to promote at least partial spheroidization of graphite in cast irons, magnesium is by far the most effective and economical element.

The cost of the nodularising addition and the suitability of many treatment processes are affected by the sulphur content of the base metal, this being an important factor in process selection. Magnesium combines readily with sulphur present in molten metal.

This reaction lowers the nodularisation reaction and the sulphur content should be kept below 0.01% by the methods given in section 2.4.3.

In general, a minimum retained magnesium content of between 0.015 and 0.05 percent has been considered adequate [18]. Magnesium is a very volatile element at the high temperature at which spheroidising is done and a lot of it escapes into the air in form of fumes. The amount of magnesium which does the actual spheroidising is referred to as the "magnesium recovery" and is dependent on the depth of the liquid through which the vapour rises before escaping into the air.

To reduce reaction-violence magnesium is alloyed. Several forms of magnesium alloys have been suggested [16], but the most widely used alloy is magnesium ferrosilicon, with a magnesium content of 5%. There also has been an increase in the use of the alloys which contains lower magnesium (2.5% - 3.5%) with varying amounts of cerium (1%-2%). Such alloys have been found to reduce reaction-violence and with high cerium contents are often claimed [16] to give fully nodular graphite structures at otherwise marginal magnesium contents.

2.6.1.1 EXACT FUNCTION OF MAGNESIUM

The functions of magnesium have been reported to be[16]:

- (i) deoxidising and desulphurising of the molten metal,
- (ii) to promote development of graphite spheroids,
- (iii) to prevent nucleation of flake graphite during the solidification process and thereby promote the growth of graphite spheroids.

Else et al[18], in their study of the magnesium treatment of cast iron for the production of spheroidal graphite, have given the following explanation about the reaction of magnesium and the molten metal. The first effect of magnesium is desulphurisation where it reacts with the sulphur present to form magnesium sulphide which tends to float to the surface of the liquid iron bath. When desulphurisation is complete, the true residual magnesium content tend to increase and at a level of 0.01/0.02%, the ends of the graphite flakes start rounding and the eutectic cell size reduces so that the flakes become more chunky and assume a sausage like configuration.

Increasing the free magnesium content to 0.03/0.04% changes the graphite progressively to spheroidal shape. A further function of magnesium, which is detrimental to the fracture properties of ductile iron, is to act as a carbide meta-stabiliser in the as-cast condition, but this carbide phase readily breaks down on heat treatment to give spheroids of secondary graphite. Only 0.05% residual magnesium is necessary to achieve spheroidisation.

The process of spheroidisation has not been fully explained, however, it is thought [15] that due to the addition of magnesium to the melt, magnesium oxide is presumed to act as the nuclei. Apart from nucleation, it has been shown [15] that surface tension plays an important role in determining the shape of graphite. While an increase of the surface tension, which favours spheroidisation, is obtained by adding magnesium, the presence of sulphur has been reported [25,26,27] to decrease the surface tension drastically.

2.6.1.2 INOCULATION

Inoculation or postinoculation refers to the practise of making an addition to the melt in order to increase the number of spheroids formed during solidification.

In ductile iron, inoculation is employed to counteract the carbide stabilising effect of the spheroidising alloy and to increase the graphite nodule count (See section 2.6.1.1).

Typical inoculants are ferrosilicon, silicon carbide, calcium silicate, silicomanganese and aluminium. These are usually added as postinoculants by reladling the treated iron into the inoculant placed in the bottom of the ladle or at times the inoculant can be added to the metal stream.

2.6.1.3 LADLE PROCESSES/OPEN AND COVERED LADLE TECHNIQUES

The most common techniques are those which reduce or eliminate fume emission and metal ejection during treatment, as well as achieve good magnesium recovery.

To achieve good magnesium recovery;

- (i) The filling rate of the ladle must be high.
- (ii) The alloy pocket must be of suitable size to contain the alloy preferably a cover of small steel scrap or granular low silicon content ferrosilicon.
- (iii) A correctly graded ferrosilicon magnesium alloy to give a high packing density in the pocket is required.

- (iv) A ladle of high H:D ratio is required about 1:5 or 2:1 (See Figure 2.3).

Treatment ladles are designed to be deep and narrow so that the violent reaction of magnesium vapour with the liquid iron is confined to the ladle. Magnesium vapour can permeate a greater depth of molten iron before it escapes to the air.

Open ladle treatment is cheap and offers minimum loss in temperature.

The commonly used open ladle techniques are:

- (i) Overpour:- In this technique, the transfer of magnesium to the liquid iron is inefficient and considerable volumes of magnesium oxide white smoke are evolved into the atmosphere.
- (ii) Sandwich process:- In this process, the alloy is covered with some steel scrap or ferrosilicon or sand whilst the molten iron is poured into the ladle. This ensures that the magnesium alloy has to travel up through the liquid iron bath, treating as it goes.

(iii) Trigger process:- This process is the same as the sandwich process, but the magnesium reaction is initiated and controlled by external factors as desired. The cover of the alloy is usually calcium carbide, sand or cast iron borings. This achieves both delayed treatment and delayed nucleation, both being desired features.

(iv) Tundish ladle process:- In this process, the ladle has either a fixed or a pneumatically operated lid incorporating a tundish/pouring basin which has a controlled orifice. The time to fill the ladle is adjusted to be equal to the reaction time of the iron with the treatment alloy.

(v) Other ladle techniques:- The injection of pure magnesium [27], the pressure magnesium treatment wire [28,29], and porous plug ladle are other techniques whose advantages have not been fully utilised.

2.6.1.4 PLUNGING PROCESSES

Plunging involves placing the magnesium alloy into a container positioned within a vented graphite or refractory bell. The bell is then plunged into a ladle filled with iron.

It offers a higher magnesium recovery than open-ladle method.

2.6.1.5 BATCH TREATMENT VESSELS

The Flotret [30] and Imconod [31] are the batch treatment processes widely used. Less fumes are emitted in these processes.

2.6.1.6 INMOLD PROCESS

The magnesium ferrosilicon is added in the mould. The process has been said to offer many advantages [16,18,32]. It is virtually smokeless, efficient in alloy usage and offers a pronounced inoculating effect with freedom from carbides formation and a high nodule number at costs equivalent to conventional ladle treatment.

The mould design, pouring rate, pouring time and base metal sulphur content are critical in this process. It requires rigid moulds and sulphur contents of less than 0.01%.

A common problem is the wash over of ferrosilicon magnesium during mould tilling.

2.7 METALLURGICAL PROCESS CONTROL

Production of ductile iron is a process highly sensitive to process variables. Methods of control are designed to provide and maintain reliability of the cast product and to ensure the effectiveness of the magnesium treatment and inoculation.

2.7.1 METAL COMPOSITION CONSIDERATION

Important points to consider in selection and control of the metal composition are:

- (i) Sufficient alloying to avoid transformation to pearlite during quenching, but not over-alloying to the extent of increasing the time required for transformations during heat treatments.
- (ii) The structure should be free from intercellular carbides and phosphides.
- (iii) The segregation effects of different alloying elements should be minimised by their balanced selection, thereby ensuring that response to heat treatment is uniform throughout the section (See section 2.5.2).

2.7.2 GRAPHITE SHAPE

Quality ductile iron is enhanced by producing it such that the graphite has high nodularity (See Figure 2.1).

It has been reported [5] that low pouring temperature, heavy section sizes, insufficient magnesium addition, lack of inoculation and low carbon equivalent lead to poor graphite shapes.

2.8 FOUNDRY PROCESS CONTROL

Pouring rate, pouring time, pouring temperature, choke design, feeding methods and riser design have been reported [33,34] to be factors on which quality ductile iron depend.

2.8.1 POURING AND GATING

The pouring rate of liquid ductile iron into the moulds should be high:

- (i) to minimise temperature loss and its effects on shrinkage tendency.
- (ii) to minimise metallurgical deterioration of the liquid iron following the spheroidising and inoculation treatments.
- (iii) to minimise dross formation.

Anderson and Karsay [34] have related the cross-section of the choke and pouring rate by the following expression.

$$A_c = \frac{1}{t \cdot f_r \sqrt{2g}} \left[\frac{V_d}{H} + \frac{1.5 \cdot V_c \cdot b}{H^{3/2} - (H-b)^{3/2}} \right] \dots (2.2)$$

Roeder [35] has given a method of pressure-control feeding for ductile iron castings. He has also given the riser and feeder shape that offer higher efficiency. In order to produce ductile iron having good metallurgical quality, a pouring temperature of 1480°C or higher is preferred to avoid dross formation.

2.8.2 RISER DESIGN

Roeder [35] has suggested riser dimensions. It has been reported [5] that ductile iron solidifies by the growth of graphite spheroids surrounded by a shell of austenite. It does not freeze in layers from the surface inward as gray cast iron and steel do. Instead, solidification takes place with liquid and solid metal throughout the casting. This type of solidification emphasises the need for rigid moulds, hard-rammed, to prevent bulging of the casting.

2.9 REVIEW OF PROPERTIES OF DUCTILE IRON

In general, ductile iron combines the principal advantages of gray iron of low melting point, good fluidity and castability, excellent machinability and good wear resistance with the engineering advantages of steel of high strength, toughness, ductility, hot workability and hardenability to achieve its superior properties.

2.9.1 MICROSTRUCTURE

The structural components of cast irons which also apply to ductile iron are presented in appendix A.

Perhaps the most significant structural property of ductile iron is that the graphite in it is spherical and this forms the main difference between ductile iron and gray iron

Microstructural examination is one of the quality control techniques used in foundry. For ductile iron the degree of spheroidisation, the size of the graphite nodule, the inter-particle or nodule spacing, and ferrite grain size have been found [36] to be closely related to the ductile - brittle transition behaviour, and both tensile strength and 0.2% proof stress.

This relation is well presented by the Hall-petch's equation [37] as,

$$\sigma_y = \sigma_0 + K_y d^{-1/2} \dots\dots\dots(2.3)$$

Nishi et al [[36] have shown that the yield strength can be related to the spacing between graphite nodules and the ferrite grain size as

$$\sigma_y = L + M \lambda^{-1} + N d^{-1/2} \dots\dots\dots(2.4)$$

Where L,M and N are constants.

Conrad [38] has, in addition to equation (2.4), shown the relation between interparticle spacing, the grain size and the transition temperature to be,

$$T_c = L - M \lambda^{-1} - N d^{-1/2} \dots\dots\dots(2.5)$$

Where L,M, and N are constants.

2.9.2 HARDNESS

The hardness of ductile iron can be directly related to other properties and the Brinell hardness is preferred [21] for this material.

The relationship between the hardness and strength has been found [39] to be,

$$\text{strength} = K \cdot \text{BHN} \dots\dots\dots(2.6)$$

where,

$$K = 2.90 \text{ N/mm}^2 \text{ for as-cast or annealed ductile irons}$$

$$K = 3.27 \text{ N/mm}^2 \text{ for normalised or bainitic ductile irons}$$

2.9.3 TENSILE PROPERTIES

Tension testing is one of the quick methods of determining properties and has been used as a tool for quality control in ductile iron production. The tensile properties are used to specify the standard grades of ductile iron [1, 17].

By the use of linear regression analysis Salzbrenner [10] has developed the following relations between the chemical composition and the mechanical properties of ductile iron.

$$\left. \begin{aligned} \sigma &= 135 + 118(\%Ni) + 105(\%Si) \\ \sigma_{UTS} &= 286 + 85.6(\%Ni) + 84.6(\%Si) \end{aligned} \right\} (2.7)$$

2.9.4 TOUGHNESS AND FRACTURE

Diesburg [40] has proved that fracture toughness is sensitive to changes in microstructure.

Measurement of fracture toughness can serve the following purposes:

- (i) In research and development to establish service performance, effects of metallurgical variables such as composition or heat treatment, or fabrication operations such as welding or forming on the fracture toughness of new or existing materials.

- (ii) In service evaluation to establish suitability of a material for specific application given maximum flaw sizes.

- (iii) For applications of acceptance and manufacturing quality control.

2.9.4.1 TECHNIQUES OF ASSESSING FRACTURE TOUGHNESS

- (i) Griffith's Theory :- The present methods of measuring a material's fracture toughness have evolved from Griffith's works [41] .

It has been shown that Griffith's principle of relating crack extension to change in energy of regions relatively remote from the crack tip is followed in all the methods of determining fracture toughness, but changes in energy are derived differently.

- (ii) Linear Elastic Fracture Mechanics (LEFM) :- This method supposes the pre-existence of a significant crack-like defect that will lead to failure. It can be used in selection of the optimum material or heat treatment for a particular job.

- (iii) Compliance methods :- Compliance, C , (the reciprocal of the load deflection curve at a particular value of crack length) offers a means of determining the potential energy release rate, G , which is used as a fracture quantity. However, the compliance cannot be used for the large structures to which fracture toughness measurements are applied.

- (iv) Stress intensity approach :- Through Westergaard's [41] stress functions, the strain energy release rate, G , has been related to the stress intensity factor, K , as:

$$\left. \begin{aligned} G &= \frac{K^2}{E} (1-\nu^2), & \text{plane strain} \\ G &= \frac{K^2}{E}, & \text{plane stress} \end{aligned} \right\} \dots\dots\dots(2.8)$$

In general stress intensity factor is represented in the form [41]

$$K_I = \sigma \sqrt{a} Y\left(\frac{a}{W}\right) \dots\dots\dots(2.9)$$

(v) Quasi-brittle fracture:- This refers to situations where small amounts of local plastic flow precede crack extension. For this situation it has been shown [41] that G_{crit} can be related to failure stress by linear elastic methods.

The presence of a small plastic zone of total extent $2r_y = \frac{k^2}{\pi\sigma_y^2}$ produces a crack of half-length $(a + r_y)$.

In plane strain, fracture stress, σ_F , is given by

$$\sigma_F = \sqrt{\frac{E G_{crit}}{\pi (a + r_y)}} \dots\dots\dots(2.10)$$

$$\text{or } K_{crit} = \sigma_F \sqrt{\pi a \left[1 + \frac{\sigma_F^2}{2\sigma_y^2} \right]} \dots\dots\dots(2.11)$$

Using Dugdale's model for plastic zone size,

$$K_{crit} = \sigma_F \sqrt{\pi a \left[1 + \frac{\sigma_F^2 \pi^2 a}{16 \sigma_y^2} \right]} \dots\dots\dots(2.12)$$

(vi)The J-Integral:- The J-integral is a path independent integral, derived for non-linear elastic materials as an expression for the rate of change of potential energy per unit thickness with respect to an incremental extension of the crack [43] .

J is defined by the expression given by

$$J = \int_{\Gamma} W_{\circ} dy - \tau \frac{du}{dx} dS \dots\dots\dots(2.13)$$

where,

$$W_{\circ} = \int \sigma_{ij} d\epsilon_{ij} \dots\dots\dots(2.14)$$

(See Figure 2.4).

In a linear elastic material, the above equation can be integrated on substitution of the stress, strain and displacements associated with a singular region of a sharp crack to yield,

$$J = \frac{K^2}{E} = G \dots\dots\dots(2.15)$$

in the case of mode I plane stress condition (See Figure 2.5).

- (vii) The crack opening displacement (COD):- The COD is a measure of the resistance of materials to fracture initiation under conditions where gross plastic deformation occurs. Failure is likely to occur when the COD attains a critical value.

The near tip values of COD may be related to the applied stress and crack length by an expression which follows Dugdale's [43] analysis as,

$$\delta = \frac{8\varepsilon_y}{\pi} \text{Log Sec} \left(\frac{\pi \sigma}{2 \sigma_y} \right) \dots\dots\dots(2.16)$$

(viii) Plane strain fracture toughness :- There are three modes of fracture [41] .These are explained by Figure 2.5. The critical stress intensity factor under opening mode, that is mode I, is usually referred to as fracture toughness, K_{Ic} .

K_{Ic} has been found [44] to decrease as specimen thickness increases and beyond a certain point surface influence becomes unimportant and essentially plane strain conditions apply and the minimum value of K_{Ic} is referred to as the plane strain fracture toughness of the material (See Figure 2.6).

In most engineering applications it is plane strain conditions that apply and hence knowledge of K_{Ic} is important for design of components where toughness is a design criterion.

2.9.4.2 IMPACT TESTING

Shockey et al [37] have, by varying grain size and determining values of the parameters describing microstructure nucleation and growth, established quantitative relationships between microstructural features and dynamic fracture behaviour. They found that the effect of grain size in the fracture toughness was indicated by work-to-fracture (the area under the load-displacement curve normalised by the minimum specimen cross-section), measurements in notched tensile bars.

2.9.4.3 FRACTOGRAPHY

Fractography provides an insight into the microstructural and metallurgical factors that steer the course of crack growth and is used in failure investigations. This method of study has been used [45,46] to show that at the crack tip there is an inter-play between two conflicting mechanisms, cleavage and ductile fracture, and consequently a simple model proposed in the following as a description of the interaction on microscopic and submicroscopic levels.

- (i) Cleavage is a relatively rapid process which, for activation, requires a stress concentration that is very high on the microscopic level.

There is relatively little flow of material on the fracture surface.

- (ii) Ductile rupture is a relatively slow process taking time and involving substantial flow of the material on the fracture surface.

2.9.5 OTHER PROPERTIES

For ductile iron compression strength is usually greater or equal to its yield strength in tension. The ultimate strength in torsion is about 0.9 times the tensile strength [21]. Young's modulus is usually constant up to the elastic limit and lies between 158 and 172 GN/m².

Poisson's ratio for ductile irons in both tension and compression is about 0.28 [5].

Ductile iron has dynamic elastic properties between those of gray cast iron and steel.

	GRAY CAST IRON	DUCTILE IRON
C	2.5 - 4.0	3.0 - 4.0
Si	1.0 - 3.0	1.8 - 2.8
S	0.05 - 0.25	0.03 max.
P	0.05 - 1.00	0.10 max.
Mn	0.4 - 1.0	0.15 - 0.90
Mg	0.001-0.01	0.01 - 0.05

Table 2.1 - Composition range for gray and ductile cast irons [5].

Type No*	BHN	Characteristics	Applications
80-60-03	200-270	Pearlitic matrix, high strength as-cast	Heavy-duty machinery, gears, dies, rolls
60-45-10	140-200	Ferritic matrix, excellent machinability and good ductility	Pressure castings, valve and pump bodies shock-resisting parts
60-40-15	140-190	Fully ferritic matrix, maximum ductility and low transition temperature	Navy shipboard and other uses requiring shock resistance
100-70-03	240-300	Fine pearlitic matrix, normalised and tempered or alloyed. Excellent combination of strength, wear resistance, and ductility	Pinions, gears, crankshafts, cams, guides, track rollers
120-90-02	270-350	Matrix of tempered martensite. May be alloyed to provide strength and wear resistance	

Table 2.2 - Principal types of ductile iron [5].

* The type numbers indicate the minimum tensile strength, yield strength in kpsi, and per cent elongation.

Cupola input	Cupola output
1.0 ton pig iron, steel	0.98 ton molten iron
0.15 ton coke	0.05 ton molten slag
0.03 ton flux	1.35 tons tack gases
1.20 tons air	
2.38 tons total	2.38 tons total

Table 2.3 : Approximate amounts of materials per ton of iron in cupola melting [5]

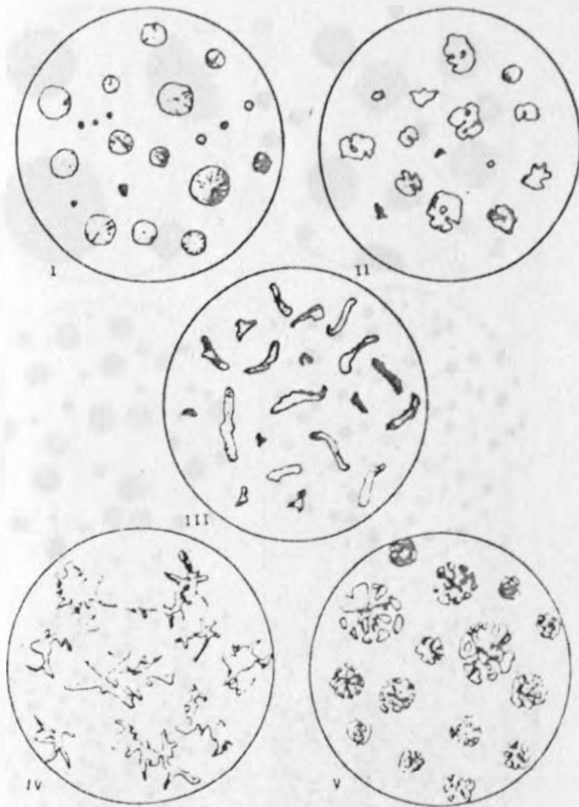


Figure 2.1 - Proposed classification of graphite shapes in ductile iron. X 100 [5]

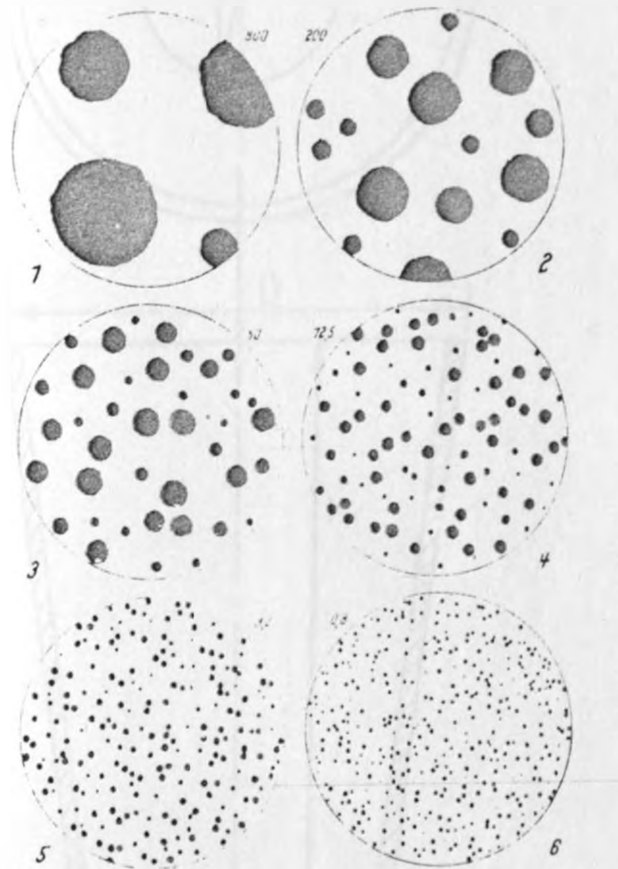


Figure 2.2 - Proposed classification of spheroidal graphite sizes based on size of spheroid at X 100 [5].

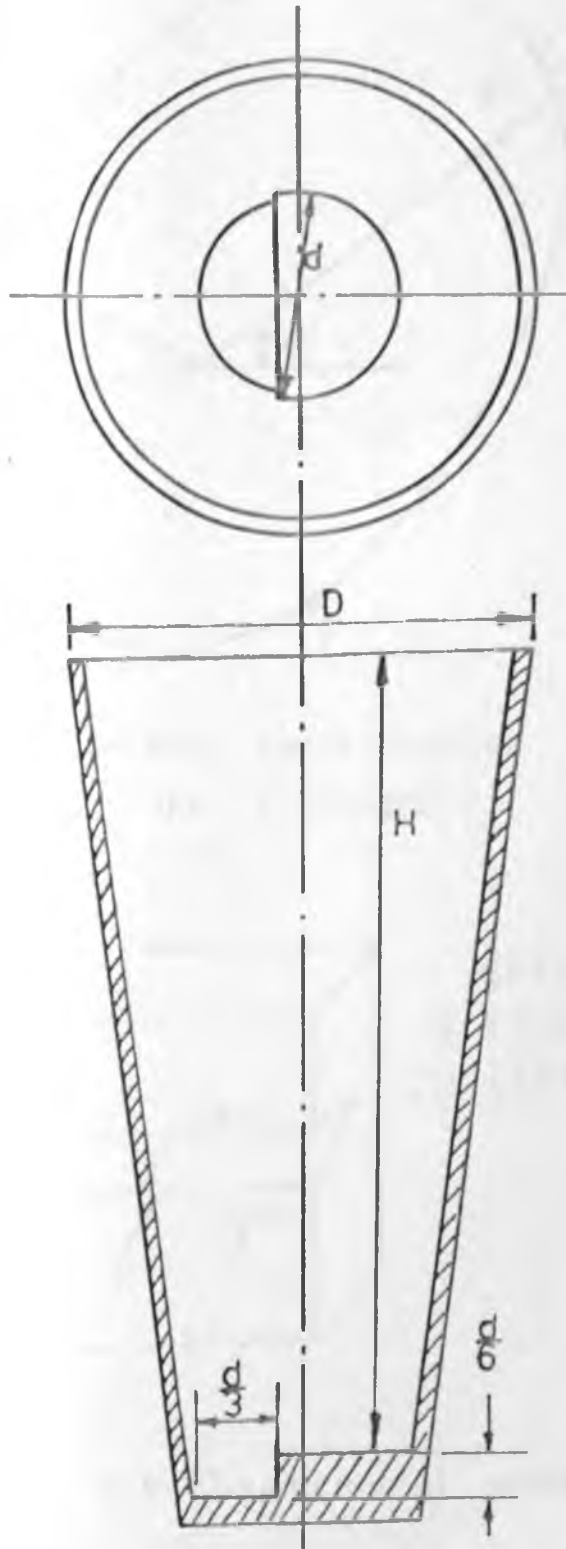


Figure 2.3 - Typical overpour treatment ladle.

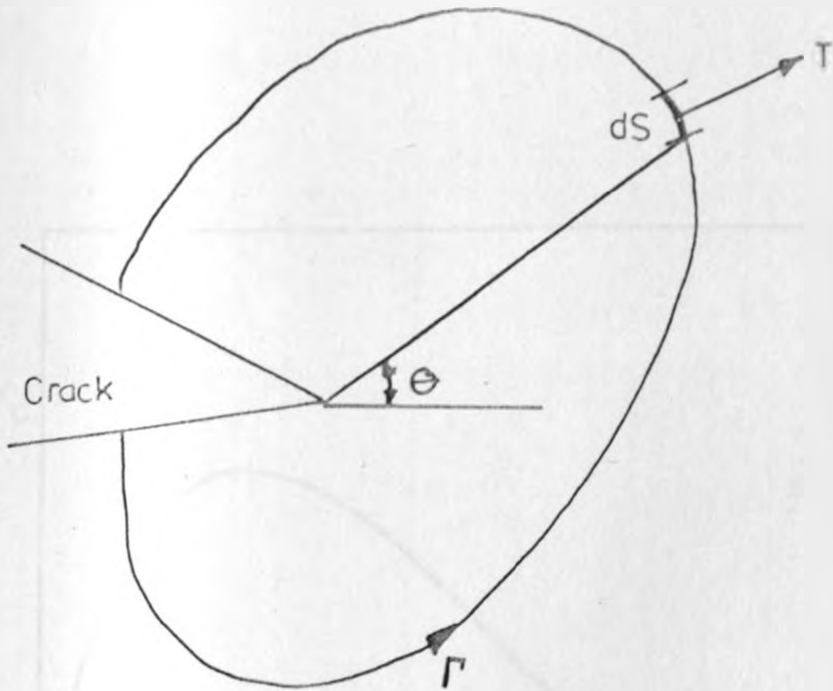
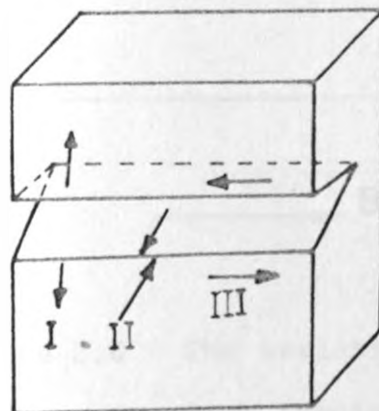


Figure 2-4- Path for evaluation of the J-Integral.



- I OPENING MODE
- II EDGE SLIDING MODE
- III SHEAR MODE

Figure 2.5-Displacement modes.

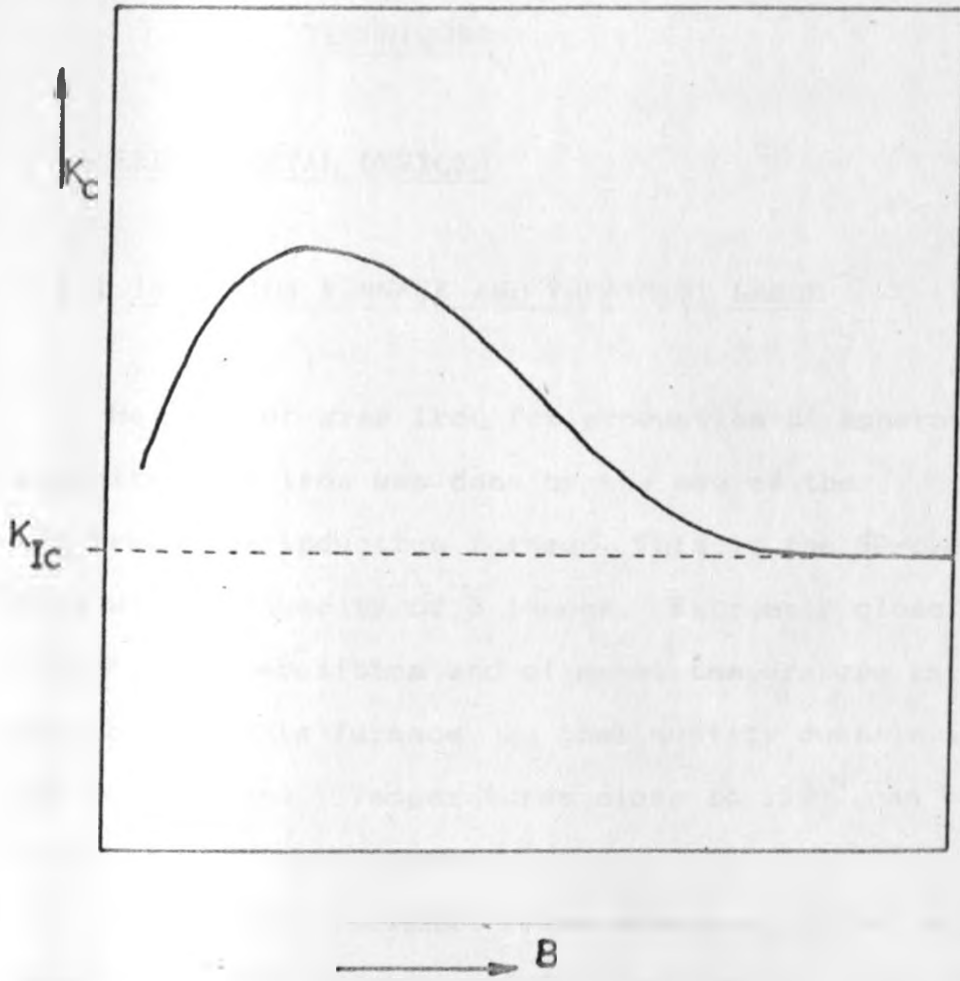


Figure 2.6 - The variation of fracture toughness with specimen thickness.

CHAPTER THREE

3.0 EXPERIMENTAL DEVICES AND DATA ANALYSIS TECHNIQUES

3.1 EXPERIMENTAL DEVICES

3.1.1 INDUCTION FURNACE AND TREATMENT LADLE

Melting of gray iron for production of spheroidal graphite cast iron was done by the use of the low-frequency induction furnace. This is the 60-cycle type with a capacity of 3 tonnes. Extremely close control of composition and of metal temperature is possible in this furnace, so that quality ductile iron can be produced. Temperatures close to 1550^o can be achieved with this furnace.

A specially designed ladle with a top cover and capacity of 250 kg was used for treating the melt with magnesium ferrosilicon to obtain ductile iron (See Figure 2.3).

3.1.2 ANALYSIS OF CHEMICAL COMPOSITION

Quantitative analysis of chemical composition by weight was done at the Kenya Bureau of Standards laboratories. The weight percentages of the elements

were determined as per the BS handbook No 19 [47] .

3.1.3 SENSTAR - UNIVERSAL TESTING MACHINE

The tension and toughness properties were obtained using the Senstar - universal testing machine of capacity 100 kN.

3.1.4 BRINELL HARDNESS NUMBER (BHN)

Brinell hardness test was used in this study because the impression of the ball is large enough to average the heterogeneous structures such as graphite, ferrite, pearlite and cementite with widely different hardness. Brinell hardness of the materials was obtained by the use of the Avery type 6403 hardness tester. A 10 mm diameter ball was used with a 3000 kg load.

3.1.5 HEAT TREATMENT FURNACE

Annealing of the specimens was done using a 2.1 kW electric furnace. The maximum operating temperature for this furnace is 940°C.

3.1.6 METALLURGICAL MICROSCOPE

The Olympus Inverted metallurgical microscope, model PME, was used to observe and take the photographs of the microstructures. The microscope is fitted with a 35 mm camera.

3.1.7 SCANNING ELECTRON MICROSCOPE

The optical microscope could not be used to give details of the fracture appearance of the specimens so the SEM was used to examine and take photographs of the fracture surfaces.

3.1.8 TESTING RIG

A test rig, consisting of a motor rated at 5.5 Horse power, 940 r.p.m. (15.7 Hz), was used to initiate and propagate the required length of fatigue crack from the starter notch (See Figure 3.1).

Power from the motor is transmitted through a universal coupling to a crank with an eccentric arm, which converts circular motion into oscillatory motion of the force transmitting lever through a piston-cylinder-connecting lever mechanism. The lever amplifies the force, depending on the position of the pivot.

The specimen is secured through a multi-pin assembly connected to the upper and lower clevis by pins. The whole specimen assembly is supported by the specimen support frame which was modified to accommodate the type and size of specimens that were used.

A load cell in line with the specimen was used. The load cell was connected to a digital strain indicator (see section 3.1.9) for read out of the strain corresponding to the load which was applied by tightening the lock nuts on top of the load cell. Prior to usage the load cell was calibrated using the digital strain indicator and the senstar. The following calibration equation was obtained for the load cell (See also Figure 3.2).

$$P_a = 0.0985 \epsilon \times 10^6 \dots\dots\dots(3.1)$$

where P_a is in KN and ϵ is in microns.

3.1.9 DIGITAL STRAIN INDICATOR

The type V/E 25 digital strain indicator was used for read-out of strain in both pre-cracking the specimens and testing to fracture. This strain indicator has a direct-reading display representing microstrain and a printing device. It has immunity to electrical noise on the output.

3.1.10 MEASUREMENT OF CRACK LENGTH

There are several methods for monitoring the crack length [48].

The commonly used are:

- (i) Microscopy techniques
- (ii) Acoustic methods
- (iii) Mechanical methods
- (iv) Electrical techniques
- (v) Eddy currents, and
- (vi) Ultrasonics

In the present investigation a microscope of X10 magnification mounted on a travelling base was used for crack length measurement. This was used to measure crack length only at the surface of the specimen. Measurement of the crack length was completed with a meter rule after fracturing the specimens.

3.1.11 DISPLACEMENT (CLIP) GAUGE

The clip gauge, which was used for the measurement of the opening displacement of the crack, was designed and fabricated. The design is based on the BS 5447 [49] and the ASTM E 399 [50] standards. The design is given in Figure 3.3 .

The material used for the gauge arms was a hack-saw blade made from high speed steel. The blade was softened at 500°C for one hour in order to make it machinable.

Calibration of the gauge was done in accordance to the BS 3846 [51]. This was done using the Senstar and the digital strain indicator. Six sets of readings of displacement and the corresponding strain were taken and the average of the values was used to obtain the calibration equation. A linear regression program was used on a micro-computer to obtain the calibration equation for the clip gauge. A plot of the data is presented in Figure 3.4 .

The equation for the straight line is

$$V_g = 0.003213 \epsilon - 0.01491 \dots\dots\dots(3.2)$$

where V_g is in mm and ϵ is in microns.

The calibration equation is valid for V_g values ranging from 0 to 10 mm.

3.2 TEST SPECIMENS

3.2.1 PRODUCTION OF DUCTILE IRON TEST SPECIMENS

Owing to the experience and capabilities of Kenya Railways Corporation Foundry, all test specimens of the metallic materials investigated in this study were produced from scrap metal. The induction furnace and treatment ladle described in section 3.1.1 were used.

A known quantity of magnesium ferrosilicon in form of small pellets was placed at the bottom of the ladle and then covered with steel stampings. Then a steel tube covered with refractory material was placed in the ladle with its mouth pointing at the magnesium ferrosilicon. The tube was connected to an argon cylinder, which had a pressure regulator. The alloy was covered in order to prevent the spheroidising reaction before the ladle was filled with the molten metal.

Molten metal at 1460°C was poured quickly into the ladle and this was followed, immediately, with the removal of the steel stampings, by stirring, in order to start the spheroidising reaction. At the instant of stirring the argon valve was also slowly opened to allow the argon gas to bubble through the metal. The spheroidising reaction was accelerated by bubbling argon gas through the molten metal.

Argon also contributes in the spheroidisation of the graphite flakes and in refining the grain structure.

The ductile iron obtained was then poured into moulds. Dried sand moulds were used to cast the ductile iron samples. Specific attention was paid to the design of the feeders, risers and gating systems. The feeder was made wide enough to provide effective feeding in the liquid contraction of the casting. Round feeders with diameters ranging between 100 mm and 150 mm, and height 1.5 times the diameter were used. The lengths of the risers were made to be $\frac{2}{3}$ the feeder diameter while the feeder gates were made to be 0.68 times the feeder diameter [34, 35].

Four master heats of cast irons with different additions of magnesium, were produced beginning from gray cast iron obtained without any addition of magnesium ferrosilicon (See tables 4.1 and 4.2).

Round bars of 25.4 mm and 50.8 mm diameter, and flat bars of 27 mm x 90 mm and 15 mm x 90 mm cross-sections were obtained from each heat. The section thickness was varied in order to vary the nodule size and the mean free path.

3.2.2 HEAT TREATMENT

The specimens were tested in both as-cast and annealed conditions.

Annealing involved heating to 920°C and holding at this temperature for 4 hours in order to dissolve the carbide phase into the austenitic matrix.

The solutionising (carbon decomposition) treatment was followed by a slow furnace cooling (at about 10°C per hour) to 700°C , which allowed the carbon in the austenite matrix to precipitate at pre-existing graphite nodules. The sample material was held at 700°C for 24 hours to ensure a (nearly) complete graphitisation. Cooling of the sample to room temperature was performed slowly to avoid introduction of residual stresses. The heat treated materials in this study were a combination of essentially two phases; ferrite and graphite.

3.2.3 FRACTURE TOUGHNESS SPECIMENS

The specimens were machined to size as given in the BS 5447 [49] and the ASTM E 399-81 [50] with some little modification to give allowance for them to fit in the clevises on the test rig that was used for pre-cracking.

The compact type of specimen was used in this study (See Figure 3.5). It was machined by the use of a shaper. A 3.2 mm cutter was used to machine the notch. A parting tool machined to a V-shape was used for cutting the V-notch on a shaper.

The final sharp notch was obtained by the use of a junior hack-saw blade with its teeth ground to the required V-shape. The specimen was then surface ground using the surface grinder to smoothen the surface. In order to facilitate crack measurement, the specimen surface was hand-polished using fine emery paper until a mirror finish was obtained.

The specimen was then tested in accordance to the BS 547 [49] and the ASTM E 399-81 [50] standard methods.

3.3 DATA ANALYSIS TECHNIQUES

3.3.1 DETERMINATION OF MECHANICAL PROPERTIES

Brinell hardness was measured for each heat and condition, as per the ASTM E 10-78 [52]. The tension properties were determined as per the ASTM E 8-81 [53], using a 13.85 mm diameter specimen with 50.8 gauge length.

3.3.2 DETERMINATION OF FRACTURE TOUGHNESS, K_{Ic}

The critical stress intensity factor under opening mode is usually referred to as the fracture toughness,

K_{Ic}

The relationship between the stress intensity factor, K , and applied stress, σ , crack length, a , and geometric factor, $Y(\frac{a}{W})$, is called a K-calibration.

For the compact specimen used in this study the K-calibration is given by [49];

$$K_{\alpha} = \frac{P_{\alpha}}{BW^{1/2}} Y\left(\frac{a}{W}\right) \dots\dots\dots(3.3)$$

where,

$$Y\left(\frac{a}{W}\right) = 29.6\left(\frac{a}{W}\right)^{1/2} - 185.5\left(\frac{a}{W}\right)^{3/2} + 655.7\left(\frac{a}{W}\right)^{5/2} \\ - 1017\left(\frac{a}{W}\right)^{7/2} + 638.9\left(\frac{a}{W}\right)^{9/2} \dots\dots\dots(3.4)$$

The load P_{α} was determined from the load-loadline displacement curves shown in Figures 4.1 to 4.8, by the offset procedure given by the BS 5447 [49] standard.

3.3.3 METALLOGRAPHY AND DETERMINATION OF GRAIN SIZE, NODULE COUNT AND MEAN FREE PATH

Details of the structure of the specimens were observed and photographs taken using the metallurgical microscope.

The specimens were prepared and etched according to the metallographic procedures recommended in the ASTM E 3 [54].

The grain diameter and the mean free path (or inter-particle spacing) were determined using the procedures described in the ASTM E 112 [55]. The photomicrographs used for estimation of the grain diameter and the inter-particle spacing were prepared in accordance with the ASTM E 2 [56]. The specimens were cut and mounted using resin. Then they were polished with grade 220,320,400 and 600 emery paper. The final polishing was done with 1/4 micron diamond paste. The specimens were then etched in 2% Nital before examination with the microscope.

The circular intercept procedure was used in estimating the grain size and the mean free path. This procedure was preferred to the straight test lines because the circular arrays automatically compensate for departures from equiaxed grain shapes, and also because it eliminates ambiguous intersections at ends of test lines. A 500-mm circular pattern was used. This consisted of three concentric circles with diameters of 79.53 mm, 53.05 mm and 26.53 mm, whose circumferences give a total length of 500 mm. The three concentric circles were drawn in five different fields and the intercepts of the grain boundaries with the lines were counted. Five fields were tested with the 500-mm pattern, yielding five counts. The average of the five counts was used to estimate the grain diameter from the graphs given in the ASTM E 112 [55].

The inter-nodule spacing was estimated by similarly employing the circular intercept method, but the intercepts of the nodule's circumference and the line drawn were counted instead of intercepts with the grain boundaries.

The nodule count was estimated by counting the number of nodules on the micrograph to obtain the number of nodules per square millimetre and then multiplying this number by the magnification.

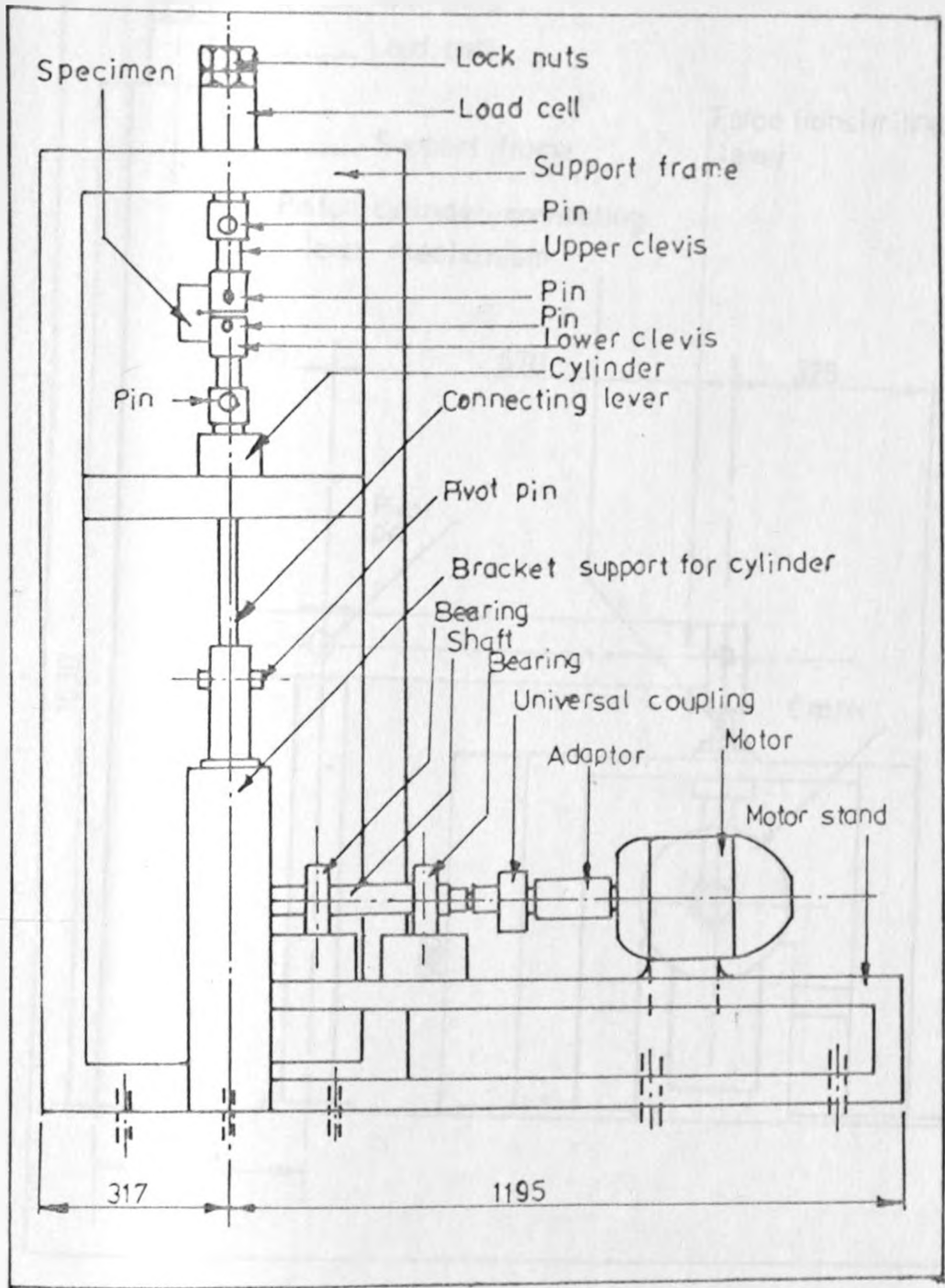


Figure 3.1(a) - Test rig assembly drawing

Front elevation

Scale 1:10. All dimensions in mm.

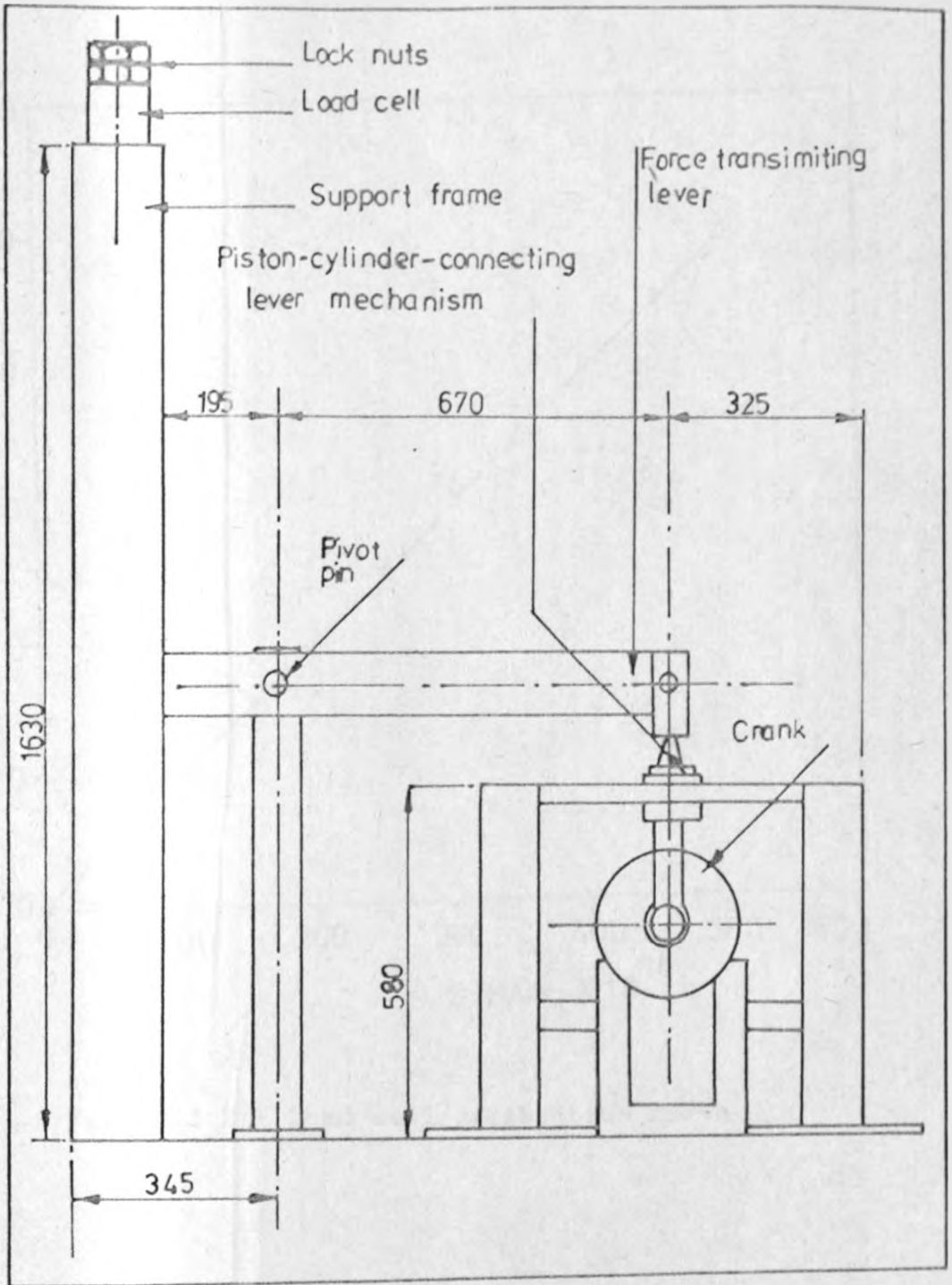


Figure 3.1(b) - Test rig assembly drawing

Left hand side elevation

Scale 1:10. All dimensions in mm.

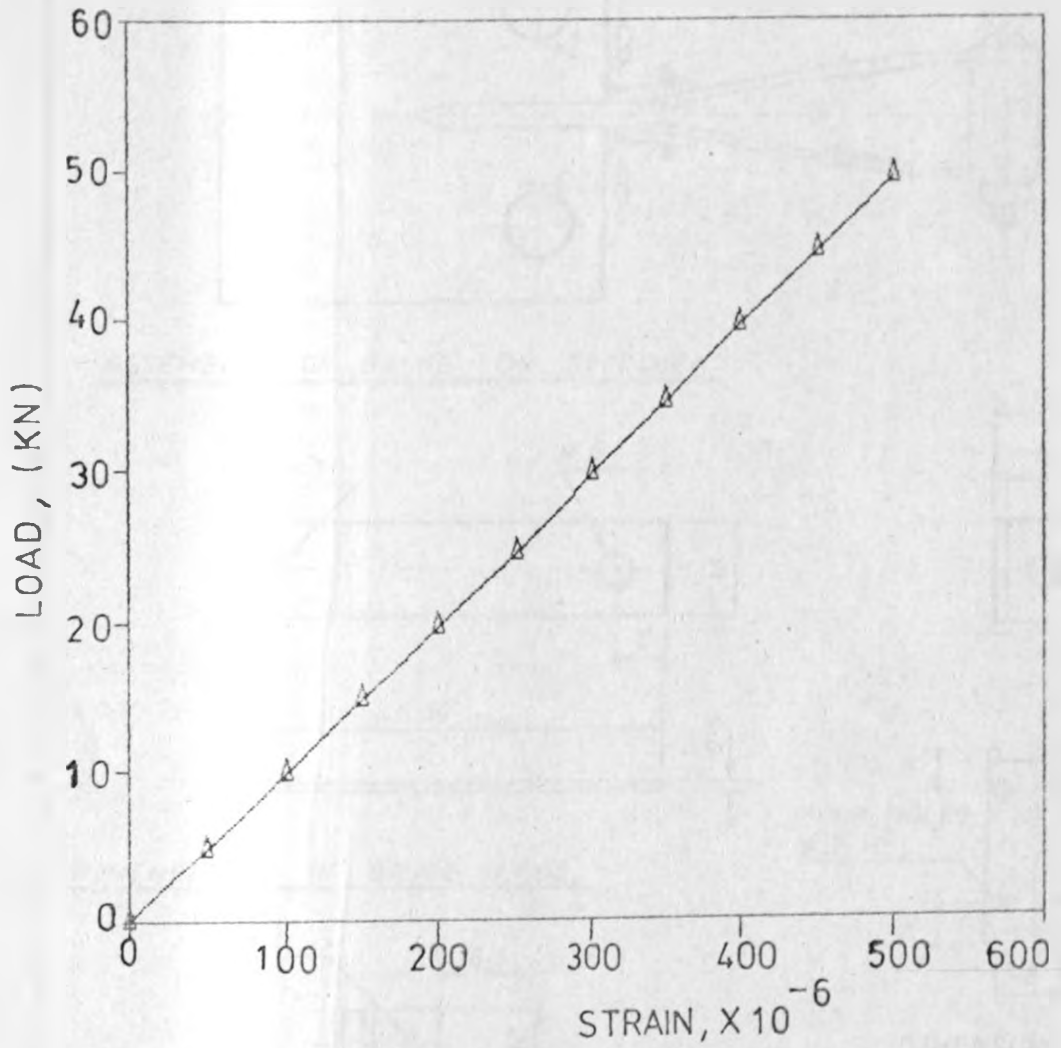


Figure 3.2 - Load cell calibration curve.

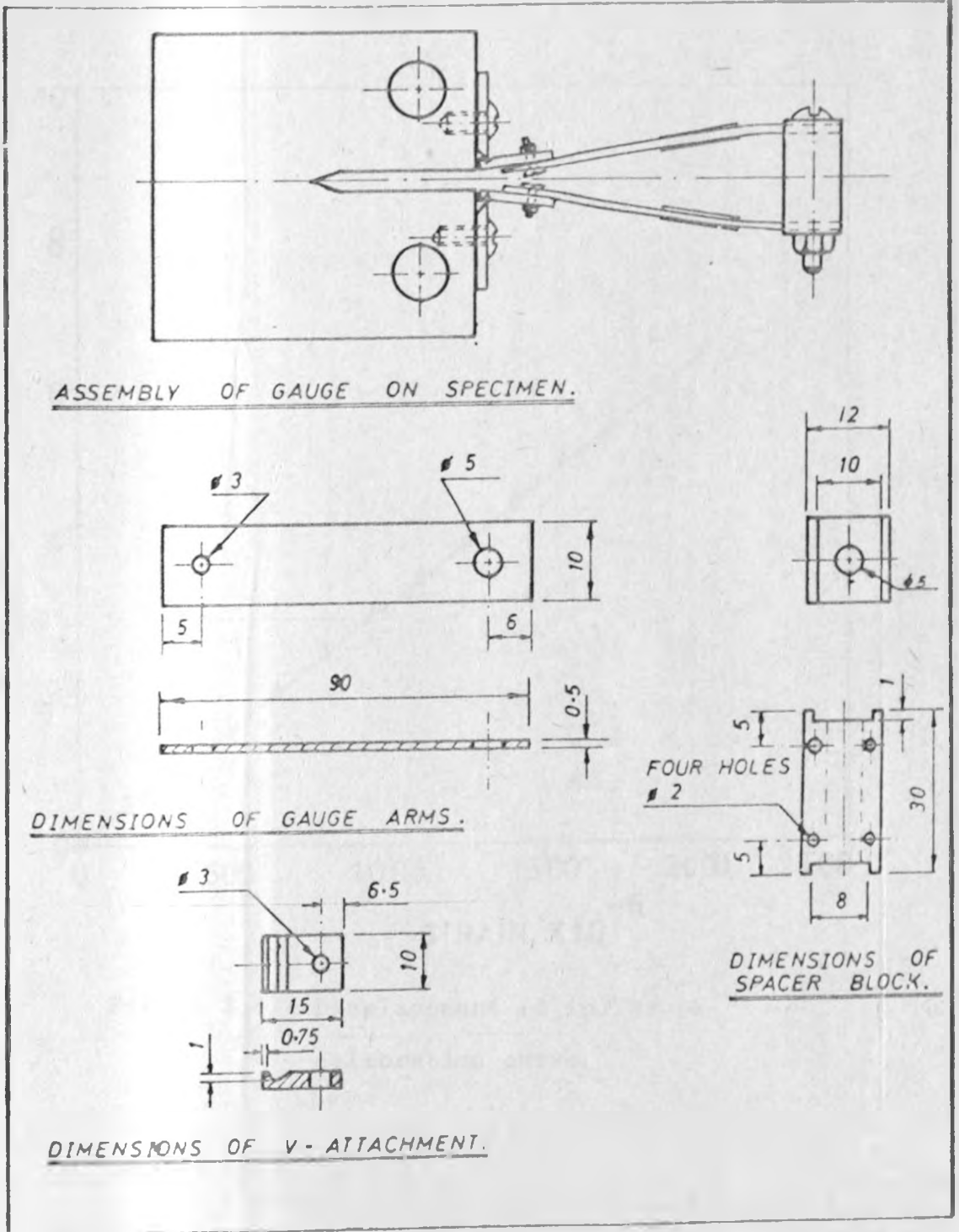


Figure 3.3 - Details of displacement (clip) gauge.

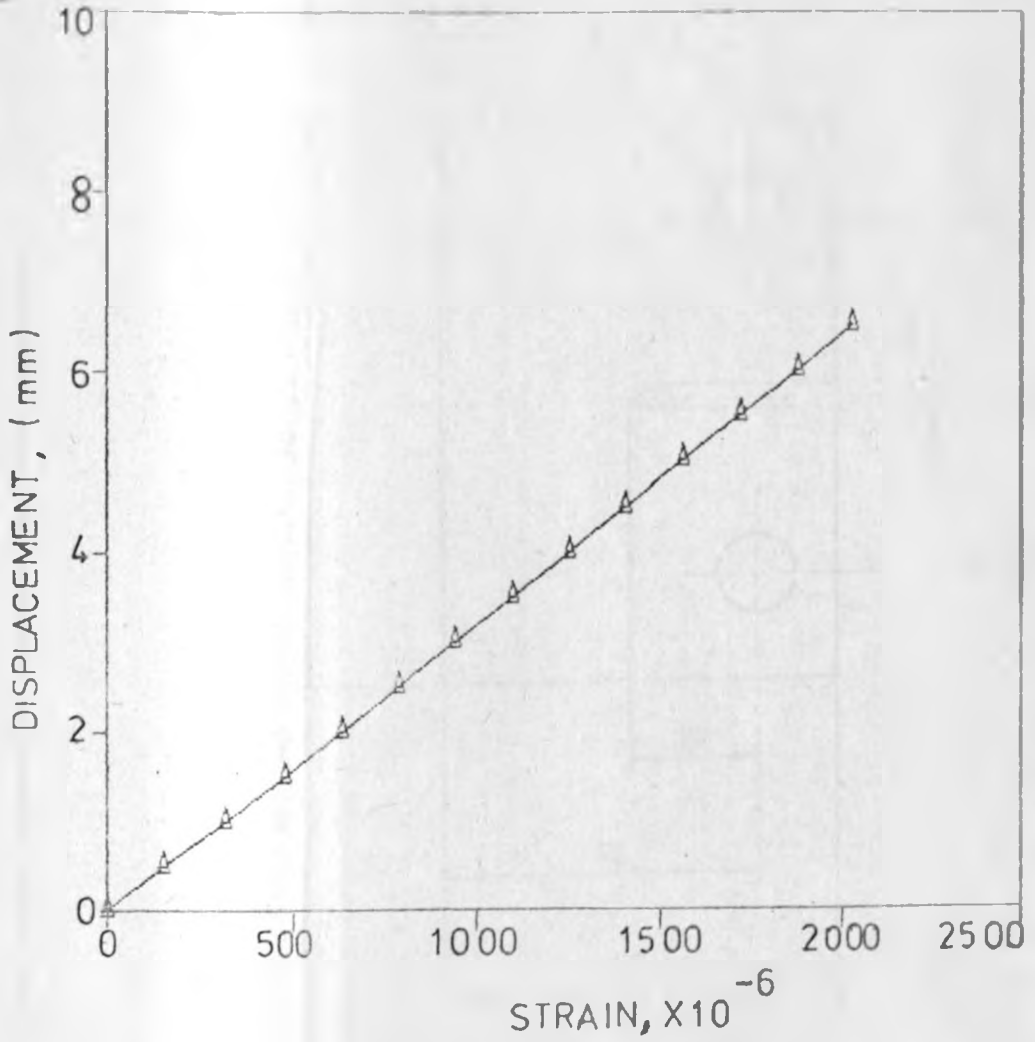


Figure 3.4 - Displacement (clip) gauge calibration curve.

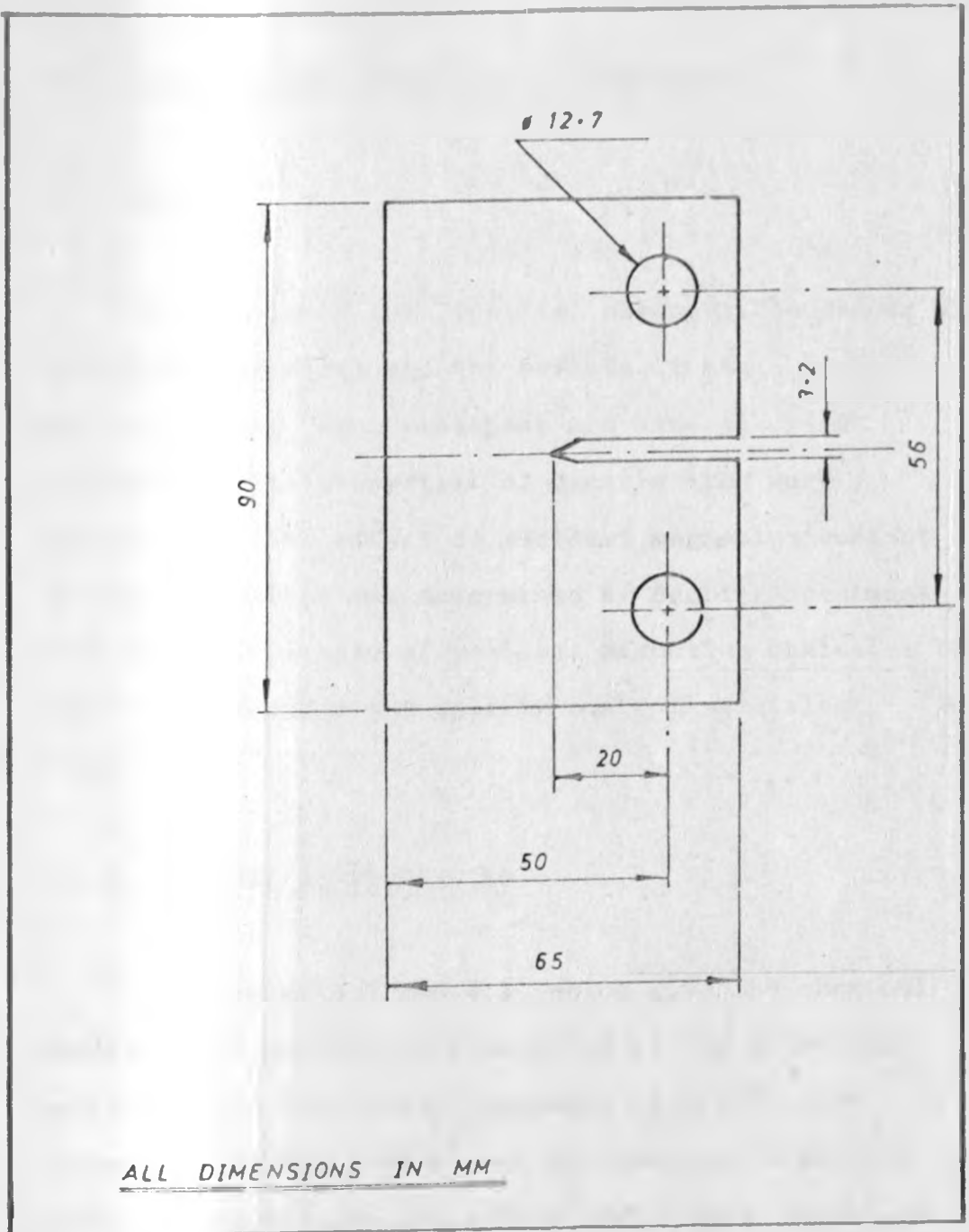


Figure 3.5 - Compact specimen

CHAPTER FOUR

4.0 EXPERIMENTAL RESULTS AND DISCUSSION

4.1 RESULTS

In this study the tensile, hardness, toughness and fracture properties and the effects of the microstructure, heat treatment and some alloying elements on the properties of ductile iron were determined. The effect of residual magnesium content on the properties was determined by testing specimens with varying amounts of residual magnesium content. The production process and quality control were also reviewed.

4.1.1 MECHANICAL PROPERTIES

From tables 4.2 and 4.3, which give the chemical analysis and mechanical properties of the materials respectively, the tensile strength is observed to increase from 246.9 MN/m^2 , at low residual magnesium content (0.004%), to 378.4 MN/m^2 , at higher levels of magnesium (0.043%). The percentage elongation similarly increases from 0.85 to 2.3 while the Brinell hardness number ranges between 114 and 241. The Young's modulus was found to be about 185 GN/m^2 .

4.1.2 TOUGHNESS PROPERTIES

The plane strain fracture toughness was determined and is here reported as the conditional fracture toughness, K_{Ic} . Two thicknesses of compact specimens were used and it was observed that there was no effect of thickness on the fracture toughness for thicknesses above 13 mm. The values of fracture toughness for all the specimens tested in this study are given in Table 4.4.

From Table 4.4 K_{Ic} for gray cast iron, heat GI, was found to be in the range of 19.34 $\text{MN/m}^{3/2}$ to 25.72 $\text{MN/m}^{3/2}$. Heat SGA ductile iron was observed to have K_{Ic} values between 31.3 $\text{MN/m}^{3/2}$ and 68.48 $\text{MN/m}^{3/2}$, heat SGB had K_{Ic} values between 23.16 $\text{MN/m}^{3/2}$ and 29.87 $\text{MN/m}^{3/2}$ while heat SGC had K_{Ic} values between 18.81 $\text{MN/m}^{3/2}$ and 28.03 $\text{MN/m}^{3/2}$.

The above values clearly show that as the residual magnesium content increases from 0.004% in gray cast iron to 0.043% in heat SGA ductile iron, the fracture toughness increases progressively. This observation is also illustrated by Figure 4.10. K_{Ic} for mild steel was also determined and found to be about 57 $\text{MN/m}^{3/2}$. Typical load versus displacement curves from which the load P_{Ic} was obtained are shown in Figures 4.1 to 4.8.

4.1.3 MICROSTRUCTURAL PROPERTIES

The microstructural properties are given in table 4.5.

The effects of sulphur, phosphorus, residual magnesium and silicon content on the mechanical and the microstructural properties of the alloys are illustrated in Figures 4.9 through to 4.23.

As the residual magnesium content is increased the sulphur content is observed to decrease and the graphite shape factor, which is a measure of nodularity, increases from 0.10 to 0.91 (Figure 4.15 and Table 4.2 and 4.5). The graphite types change from flake to type I graphite as it is seen in plates 2 through to 12. The shapes of graphite commonly formed in ductile iron are shown in Figure 2.1.

The nodule count increases from 43 per mm^2 to 145 per mm^2 as the residual magnesium is increased as illustrated by Figure 4.14. The nodule size ranges between 13.07 and 17.73 micrometres but does not seem to have any correlation with the other properties, however, it is thought that small nodule sizes improve properties [39].

The matrix grain size is in the range of 31 to 71 micrometres and has effect on the properties, as will be explained in section 4.2.3. This is illustrated by Figure 4.18 and 4.21.

4.2 DISCUSSION

4.2.1 MECHANICAL PROPERTIES

The values obtained for the mechanical properties of the materials under study are given in section 4.1.1.

The materials therefore correspond to grade 60-40-18 of ASTM A 536-84 [17]. The types of ductile irons are given in Table 2.2. The chemical analysis of the specimens reveals that as the residual magnesium content is increased from 0.008% for heat SGC to 0.043% for heat SGA, the mechanical properties improve. It is also observed that the microstructure changes progressively and thus this shows that changes of the microstructure affect the mechanical properties of ductile iron.

Else and Dixon [18] also observed that as the magnesium content of a ductile iron increased to a level of 0.01-0.02% modifications in the flake graphite structure were observed metallographically. When they increased the residual magnesium content to between 0.03 and 0.04%, the graphite shape changed progressively to the spheroidal form. Similar observation was made in this study, by increasing the magnesium content from 0.004% to 0.043%.

It has been observed, in this study, that annealing changes pearlitic matrix into ferritic matrix structures. This had the effect of slightly reducing the tensile strength, but increased machinability and ductility (Table 4.3). The continuous increase of graphite shape to nodular form is observed to cause continuous increase in ductility (Table 4.3 and 4.5).

Segregation of carbides to grain boundaries is observed in plates 3, 6, and 10. This has the effect of reducing ductility, tensile strength and toughness. (Table 4.3 and 4.4) Annealing heat treatment was observed to have the effect of breaking the pearlite and the inter-cellular carbides and thus increasing ductility. The effect of annealing on the microstructure is observed by comparing plate 6 with plates 7 and 8 and also plate 10 with plates 11 and 12. From these plates it is observed that the matrix changes to ferritic as a result of annealing, hence the increase in ductility observed in Table 4.3.

Argo and Gagne [24] have reported that increasing the manganese content from 0.025% to 0.78% cause the tensile strength to increase from 348 to 441 MN/m^2 and the yield strength from 266 to 301 MN/m^2 , while from the present study it is observed, from Table 4.2 and 4.3, that as the manganese content increases from 0.3 to 0.77% the tensile and the yield strengths

increase from 253.5 to 378.4 MN/m^2 and 236.7 to 250.3 MN/m^2 respectively.

4.2.2 TOUGHNESS PROPERTIES

In this study, the values of the fracture toughness, K_{Ic} , for gray iron and ductile iron have been given in section 4.1.2.

The microstructure of the gray cast iron was found to be pearlitic as it can be observed in plate 2. Verma and Perry [46] used thicknesses between 12.5 mm and 25 mm and found K_{Ic} for pearlitic gray cast irons to be in the range of 12.8 $\text{MN/m}^{3/2}$ to 28.3 $\text{MN/m}^{3/2}$. This shows appreciable scatter in the fracture toughness of gray cast iron. The scatter is due to the inhomogeneity of the microstructure of cast irons.

The microstructures of the ductile irons were found, in this study, to range from pearlitic to ferritic matrices. The ferritic matrix structures were observed to exhibit higher K_{Ic} values than the pearlitic matrix while the pearlitic-ferritic structures had K_{Ic} values between those of pearlitic and ferritic structures. This clearly shows that the fracture toughness of these materials depend on the matrix.

Karsay [39] has reported K_{Ic} values for as-cast ferritic and pearlitic ductile irons to be 41.88 $\text{MN/m}^{3/2}$ and 37.7 $\text{MN/m}^{3/2}$ respectively.

Kei-Feng et al [57] measured the fracture toughness of an ASTM A 536 as-cast pearlitic nodular iron with thicknesses of 8, 12.7, 18 and 25.4 mm and found K_{Ic} to be insensitive to the specimen thickness in the above range and to have a value of approximately $33 \text{ MN/m}^{3/2}$. Nonstad et al [58] have reported K_{Ic} values of between $28.6 \text{ MN/m}^{3/2}$ (for low nodularity, ferritic) and $41.8 \text{ MN/m}^{3/2}$ (for high nodularity, pearlitic) nodular cast irons, while Little and Heine [59] have obtained toughness values of between 33 and $44 \text{ MN/m}^{3/2}$ for ductile iron and between 22 and $35.7 \text{ MN/m}^{3/2}$ for malleable cast iron. From the present study the values of K_{Ic} obtained ranged between 31.3 and $68.48 \text{ MN/m}^{3/2}$ for the annealed ductile irons.

From the above it can be concluded that the fracture toughness of ductile irons depends on the nodularity and the matrix structure, and the values obtained in this study are within the range of values obtained by the researchers mentioned above.

4.2.3 MICROSTRUCTURAL PROPERTIES

In ductile iron it has been observed that the microstructure governs the mechanical properties and mainly the fracture behaviour. The matrix structure was found to have the greatest effect on the properties of ductile iron.

Pearlitic matrix structures have high strength but low toughness and ductility. Structures with a ferritic matrix were found to have low strength but high toughness and ductility. Structures with inter-mediate matrix, that is, pearlitic-ferritic matrix have properties between the two. The values are given in tables 4.3 and 4.4 and the observations can be made in plates 10, 11, and 12. It was observed that annealing can be used to obtain either fully ferritic or pearlitic-ferritic matrix structures from pearlitic structures.

In addition to the matrix structure, the degree of spheroidisation (graphite shape factor), the size of the inter-particle (nodule) spacing, the nodule count, and the ferrite grain size have been found, from this study, to be important microstructural variables which control the other properties. The effects are illustrated in Figures 4.13 through to 4.23.

In this study the graphite shape was found to improve from flake to nodular as the magnesium was increased (Figure 4.15). It was observed that continuous improvement of properties occurred with increasing graphite shape factor (Figure 4.16 and 4.23). The nodule count was also observed to have significant effect on the properties.

The highest toughness values were obtained from samples with high nodule counts and graphite shape factor and with ferritic matrix structures. These effects are illustrated in Figure 4.13, 4.14, 4.22, and plate 11 and 12.

The presence of a ferrite ring around the graphite nodule was observed in an annealed sample of alloy SGA (See plate 12). The highest toughness value of 68.48 $\text{MN/m}^{3/2}$ was obtained from this sample. This ferrite ring is the characteristic "bull's-eye" appearance of ferritic ductile irons.

The mean free path or inter-particle spacing was also noted to have control over the toughness (Figure 4.19). Uniform distribution of the nodules and smaller spacing between the nodules improve the quality and properties of ductile iron. The effect of inter-nodule spacing on the tensile strength is illustrated by Figure 4.20.

In this study it is observed from Figure 4.21, that the yield and tensile strengths increase with decrease of the ferrite grain size.

The presence of carbides was observed to cause decrease in tensile strength, elongation, nodule count, nodularity and toughness.

Physical examination of the fracture surfaces of the specimens revealed defects with a dark gray appearance within the light gray fracture appearance of ductile iron. This resulted in fractures at relatively low loads and is the result of the inhomogeneity exhibited by ductile irons as shown in plates 8 and 9.

4.2.4 FRACTOGRAPHY

Analysis of the fracture behaviour of the alloys was done by using the fracture surfaces of the compact specimens.

Physical examination revealed modification from the dark gray fracture of gray cast iron to the light gray fracture appearance of ductile iron as the residual magnesium content increased.

Areas of internal imperfections were also observed macroscopically. These imperfections, which appeared dark gray as compared to the light gray fracture of ductile iron, were found to be the cause of the significant scatter in the fracture toughness of specimens machined from the same bar. These imperfections are thought to be the result of non-uniform distribution of the magnesium ferrosilicon in the molten metal.

The scanning electron micrograph of the as-cast specimens from heat SGA, shown in plate 13, reveals that these specimens fracture by transgranular failure of the pearlitic matrix. The annealed specimens from the same heat show ductile fracture as can be seen in the SEM photos in plates 14 and 15. This fracture is characterised by the concave structure of the dimples shown in plate 15(b).

As noted in previous studies [9,59], the fracture of fully ferritic ductile cast irons at room temperature takes place by micro-void coalescence. The initiation of fracture is shown to depend on the mean void-initiating particle spacing within the matrix, which is reflected by the fracture surfaces. Direct evidence of this is shown in plate 15(a) which is typical of ferritic ductile irons.

It has been observed [59] that the the ductile behaviour of the ferrite ring around the nodules can be attributed to the lack of constraint present at the nodule interface, and that the combined features of a thin section of ferrite adjacent to a soft compressible graphite nodule create a plane stress situation in which tearing takes place, rather than cleavage. This mode of crack propagation results in substantial energy absorption and hence high toughness values.

The specimens from heats SGB and SGC show the characteristic spotted dark gray surfaces of chunk graphite deterioration in ductile irons. Examination with the SEM revealed that the deteriorated graphite causes "branching" on the crack tip as shown in plates 16 and 17. This is also observed by the presence of "channels" on the fracture surfaces of these low nodularity specimens. The fracture surfaces consist of mainly intergranular fracture with partly quasi-cleavage fracture modes which are characterised by the tongues and river patterns seen in the SEM micrographs in plates 16 and 17.

Gray cast iron, heat GI, exhibits its characteristic dark gray and flat fracture surface, with tongues and river patterns as shown in the SEM photograph in plate 18. It therefore fractures by cleavage.

The characteristic smell of a fresh ductile iron fracture exposed to moisture was also noted by the author. This can be a quick way of identifying better quality ductile iron.

4.2.5 EFFECTS OF ALLOYING ELEMENTS

Carbon and silicon:- Karsay [39] has concluded that carbon and silicon strongly promote carbide-free as-cast structures, silicon being the stronger of the two. He has also found that high silicon contents result in reduced impact energy, increased impact transition temperature and has therefore suggested that the silicon level be maintained between 2.5% and 2.8%. Low silicon has been found, from this study, to have the effect of low graphitisation as shown by plate 4, while high silicon has been found [39] to improve nodule count, but promote chunky-type graphite deterioration in heavy section ductile irons. A chunky-type graphite deteriorated structure is shown in plate 9.

Morgan [3] has also suggested strict carbon and silicon contents for ductile irons. In his report, he has concluded that increasing the carbon content from 3% to 4% results in progressive increase of tensile strength with negligible change of the percent elongation and hardness. He has suggested a carbon content in the range of 3.5 to 3.7% for better casting soundness.

In the present investigation the carbon and silicon levels achieved were below the ones suggested above but it has been observed that as the carbon and silicon contents increase the nodule count increases due to the improved graphitisation.

Manganese:- Vasudevan et al [23] have observed that increase of manganese results in formation of as-cast carbides and decrease in nodule count. The authors have recommended manganese contents within 0.3-0.5%. In the present study it was observed that the tensile strength increased with increase of manganese content (See also section 4.2.1).

Magnesium and sulphur :- In the present investigation it was observed as, given in table 4.2, that the sulphur content decreases as the residual magnesium content increases. From Figures 4.10 and 4.12 it is deduced that the fracture toughness and the tensile properties are improved by the above observation. It was also observed that magnesium levels beyond 0.05% might result in stability of carbides and thus reduce the properties. Most investigators have recommended sulphur and magnesium contents of less than 0.005% and a maximum of 0.05% respectively.

Phosphorus :- It is revealed in the literature that phosphorus forms carbides and reduces the mechanical properties of ductile cast irons. It is observed in Figure 4.9 that as the phosphorus content decreases from 0.3% to 0.03% the fracture toughness increases considerably, from an average of 20 to 55 $\text{MN/m}^{3/2}$.

4.2.6 PRODUCTION OF DUCTILE IRON

In promoting ductile iron, emphasis is often given to its ductility and toughness. In this study the test specimens were produced from 100% gray cast iron scrap by effecting spheroidisation with magnesium ferrosilicon. Process control, quality control and production costs were found to be the major factors in production of ductile cast irons, as detailed below.

4.2.6.1 PROCESS CONTROL

The technique of adding magnesium to the molten metal, to achieve spheroidisation, has been found [16] to be important in obtaining high quality ductile iron and control of the process. However, the technology available in a foundry dictates the process to be used.

In this study the ladle addition of magnesium ferrosilicon described in section 2.6.1.3 was used together with argon bubbling. This was found to be very effective and easy to control. In order to achieve homogeneity in the castings a ladle of special design, with a diameter to height ratio of 1:2, was used. This type of ladle allows time and proper mixing of magnesium ferrosilicon with the metal as it travels up. Paulo et al [60] have shown that bubbling an inert gas through a molten metal refines the grains. In this study argon gas was bubbled through the molten metal.

All test specimens that were produced in this study were observed to have gas holes and porosity at the surfaces. The microstructure of the regions close to the surface of the castings consisted of chunky graphite as compared to spheroidal graphite at the interiors. The above observation shows the importance of feeding of ductile irons into moulds and the design of the moulds, feeders and risers in the production of ductile iron.

Roeder [35] has shown that high integrity castings of ductile iron can be obtained by pressure-control feeding techniques. The method utilises the volume changes which take place during the solidification and cooling of graphitic cast irons allowing the use of small but effective feeder heads.

The level of impurities has also been observed to play an important role in the production of high quality ductile irons. The most important of all is sulphur, which reacts with magnesium and thus prevents the spheroidisation reaction, if present in magnitudes above 0.01%. However, it was found that if high magnitudes of magnesium are added spheroidisation can be achieved (See Table 4.1).

Tables 4.1 and 4.2 show that as the magnesium added increases the sulphur content decreases. The presence of sulphur, therefore, requires large quantities of magnesium to be added in order to achieve spheroidisation. This might not be economical.

Morgan [3] has suggested a strictly controlled composition for high quality ductile iron. He has shown that silicon improves graphitisation and hence the nodule count, but on the other hand high silicon results in formation of exploded graphite in ductile iron and lower impact strengths, while low silicon has the effect of refractory wear. Therefore production of ductile iron requires a careful control of silicon.

High treatment temperatures were observed to result in reaction violence and spiling of the metal. Low temperatures are known [35] to result in formation of exploded graphite and gas holes in ductile iron. Temperatures close to 1500°C were found to be adequate for the spheroidisation reaction.

4.2.6.2 QUALITY CONTROL

High quality ductile iron is one which has high nodule count, high nodularity and low intercellular carbide segregation.

In this study it was found that under-treatment with magnesium produces poor quality ductile iron, with properties close to those of compacted graphite cast iron, which is essentially half-way between gray cast iron and spheroidal graphite cast iron and has a microstructure between flakes and spheroids. This is shown in plate 4 .

It was found that the presence of carbide forming elements like phosphorus or excess magnesium, low solidification rates and ineffective postinoculation results in segregation. Therefore heavy section sizes are susceptible to formation of exploded graphite, low nodule count, large blow holes and segregation of carbides. Porosity was also observed in some of the specimens that were tested (See plate 16(b)). The porosity may be the result of trapped air due to turbulent flow of metal, created gases or volumetric shrinkage, which form voids. Such defects reduce the tensile properties but may increase the fracture toughness by blunting and/or arresting a crack and consequently reducing the stress intensity.

4.2.6.3 ECONOMIC FACTORS IN PRODUCTION OF DUCTILE IRON

Ductile iron should be considered as a quality product. In its production the practical aspects which affect the costs are the melting, desulphurisation and heat treatment.

Desulphurisation is not always necessary if charge selection is strictly controlled, but in cupola melting and when a high percent of scrap is charged, desulphurisation becomes absolutely necessary.

In the present study desulphurisation was not done. Only gray cast iron was used and spheroidisation was achieved by the use of large quantities of magnesium ferrosilicon. Due to increased costs inoculation, after the spheroidising treatment was not done.

It can be concluded, from this study, that desulphurisation and proper charge selection can be used to lower the production costs.

Alloy	Amount of magnesium ferrosilicon added to 0.25 ton metal (Kg)	Graphite Type
GI	None	Flake
SGA	5.0	I
SGB	3.5	II
SGC	2.0	III

Table 4.1 - Quantity of magnesium added and resulting graphite types.

	C %	S %	Si %	Mg %	Mn %	P %
Gray iron	3.34	0.08	1.88	0.004	0.43	1.13
SGA	2.38	0.04	1.70	0.043	0.77	0.10
SGB	2.73	0.05	1.76	0.030	0.35	0.20
SGC	3.33	0.07	1.50	0.008	0.30	0.17

Table 4.2 - Chemical composition of the specimens.

Specimen and condition	σ_{uts} MN/m ²	σ_y MN/m ²	Percent Elong- ation	BHN	Young's modulus GN/m ²
GI As-cast	265.5	—	0.85	199	—
GI annealed	250.4	—	0.95	172	—
SGA As-cast	378.4	250.3	1.50	241	184.0
SGA Annealed	355.9	227.2	2.30	183	189.1
SGB As-cast	301.2	236.7	0.92	221	—
SGB Annealed	289.3	213.6	1.67	146	—
SGC As-cast	253.5	—	1.20	216	—
SGC Annealed	246.9	—	1.57	114	—
Mild steel	516.0	364.5	28	129	207

Table 4.3 - Mechanical properties of the specimens in both as-cast and annealed condition, including mild steel.

Specimen	Thickness B, mm	Fracture toughness K_{Ic} , MN/m ^{3/2}
GI	24.56	21.24
	24.52	23.56
	24.53	19.34
	15.61	19.54
SGA	13.15	31.30
	13.15	39.35
	13.15	29.35
SGB	23.73	25.29
	23.73	26.30
	23.73	21.56
	23.73	23.16
	13.62	27.22
	13.62	28.11
	13.62	24.21
SGC	24.62	21.10
	24.62	19.92
	24.62	18.81
	24.62	23.14
	13.64	20.78
	13.64	23.69
	13.64	24.70
	13.64	21.12

Table 4.4(a) - Fracture toughness of the specimens in as-cast condition.

Specimen	Thickness B, mm	Fracture toughness K_{Ic} , MN/m ^{3/2}
GI	24.50	25.72
	24.32	23.88
	24.33	24.40
	15.01	21.83
SGA	13.68	23.55
	13.68	68.48
	13.80	36.44
	13.80	41.84
	13.80	48.62
SGB	22.57	29.52
	22.57	29.64
	22.57	24.93
	22.57	19.72
	13.57	29.87
	13.57	32.01
	13.57	21.48
SGC	23.05	23.36
	23.05	26.23
	23.05	21.08
	23.05	25.39
	13.42	28.03
	13.42	27.72
	13.42	19.43
	13.42	26.72
Mild steel	15.00	54.33
	14.78	59.63

Table 4.4(b)- Fracture toughness of the annealed specimens, including mild steel.

Alloy	Graphite shape Factor	Nodule count /mm ²	Nodule size μm	Grain size		Mean inter-nodule spacing μm
				ASTM size No.	Normal diam. μm	
SGA As-cast	0.91	145	13.07	7.1	31	18.71
SGA Annealed	0.91	145	13.07	4.7	71	18.71
SGB As-cast	0.80	75	17.73	6.0	45	27.33
SGB Annealed	0.80	75	17.73	4.8	69	27.33
SGC As-cast	0.25	43	15.24	5.8	50	35.42
SGC Annealed	0.25	43	15.24	—	—	35.42

Table 4.5 - Microstructural properties of the specimens.

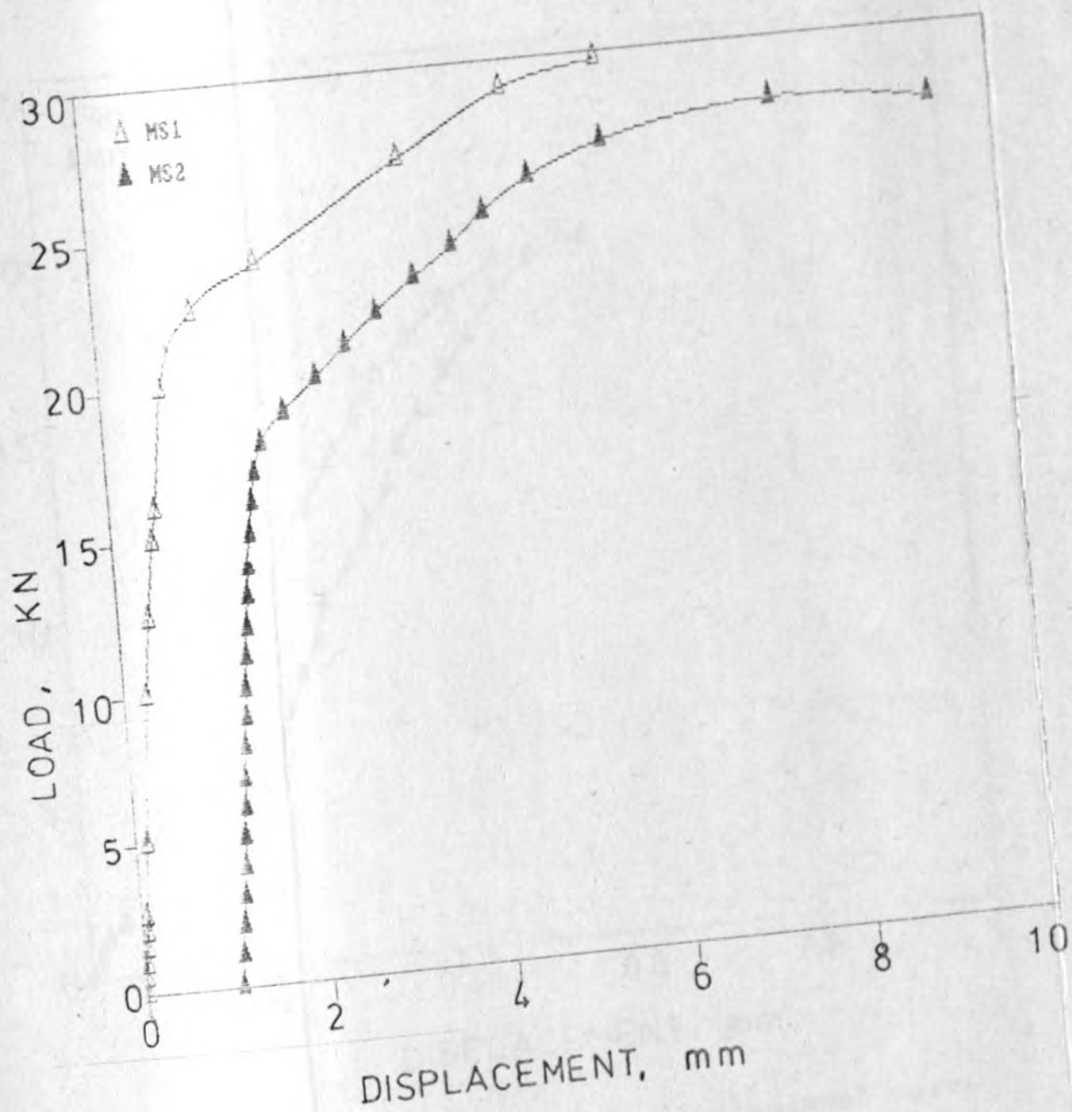


Figure 4.1 - Load-loadline displacement curve for mild steel.

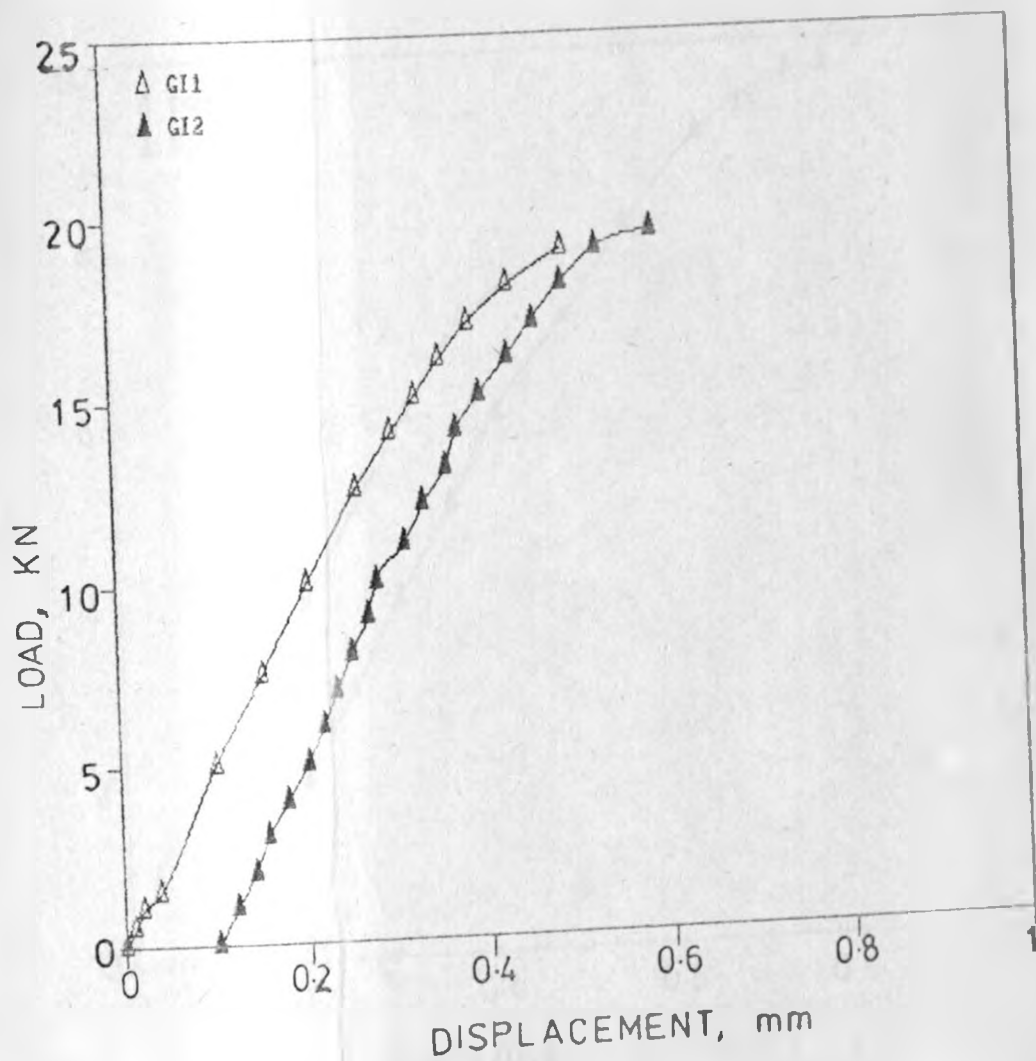


Figure 4.2 - Load-loadline displacement curve for specimen GI (as-cast).

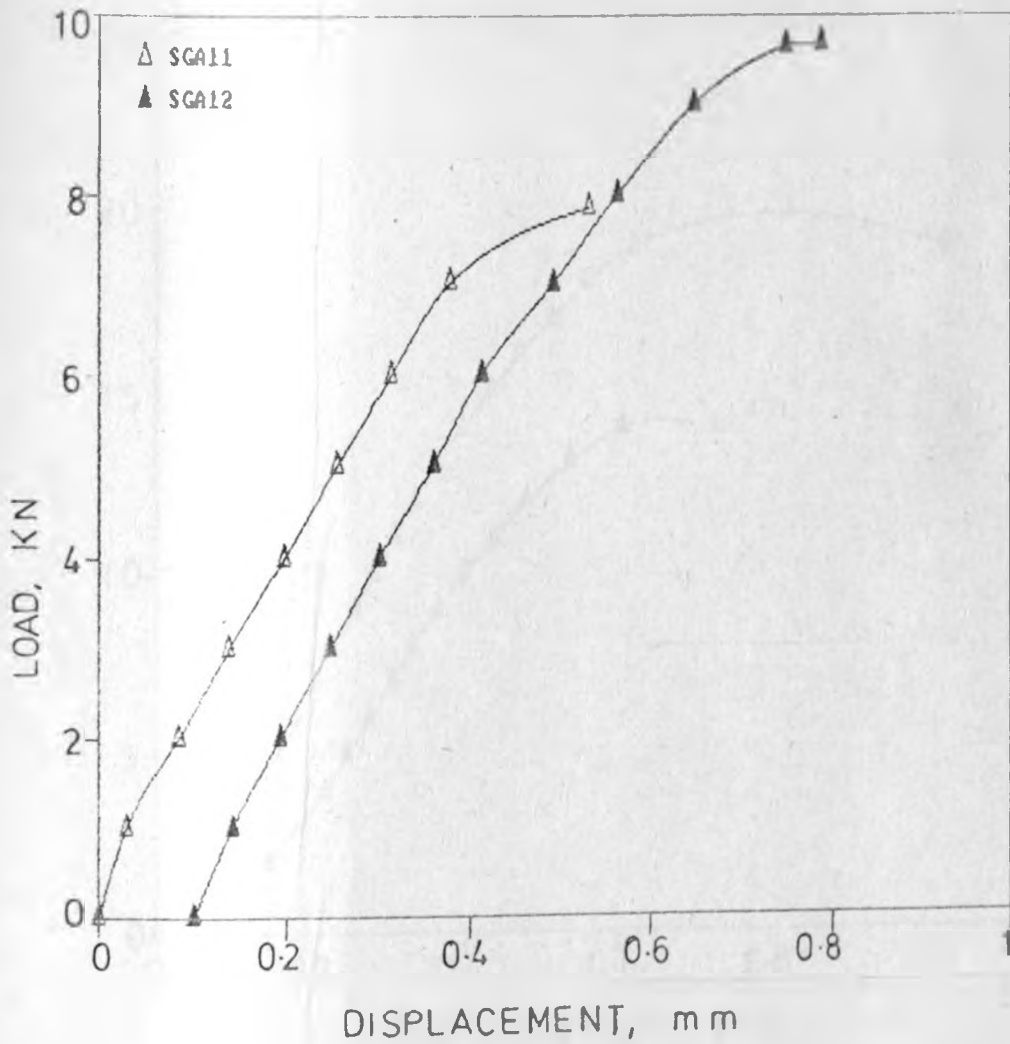


Figure 4.3 - Load-loadline displacement curve for specimen SGA (as-cast)

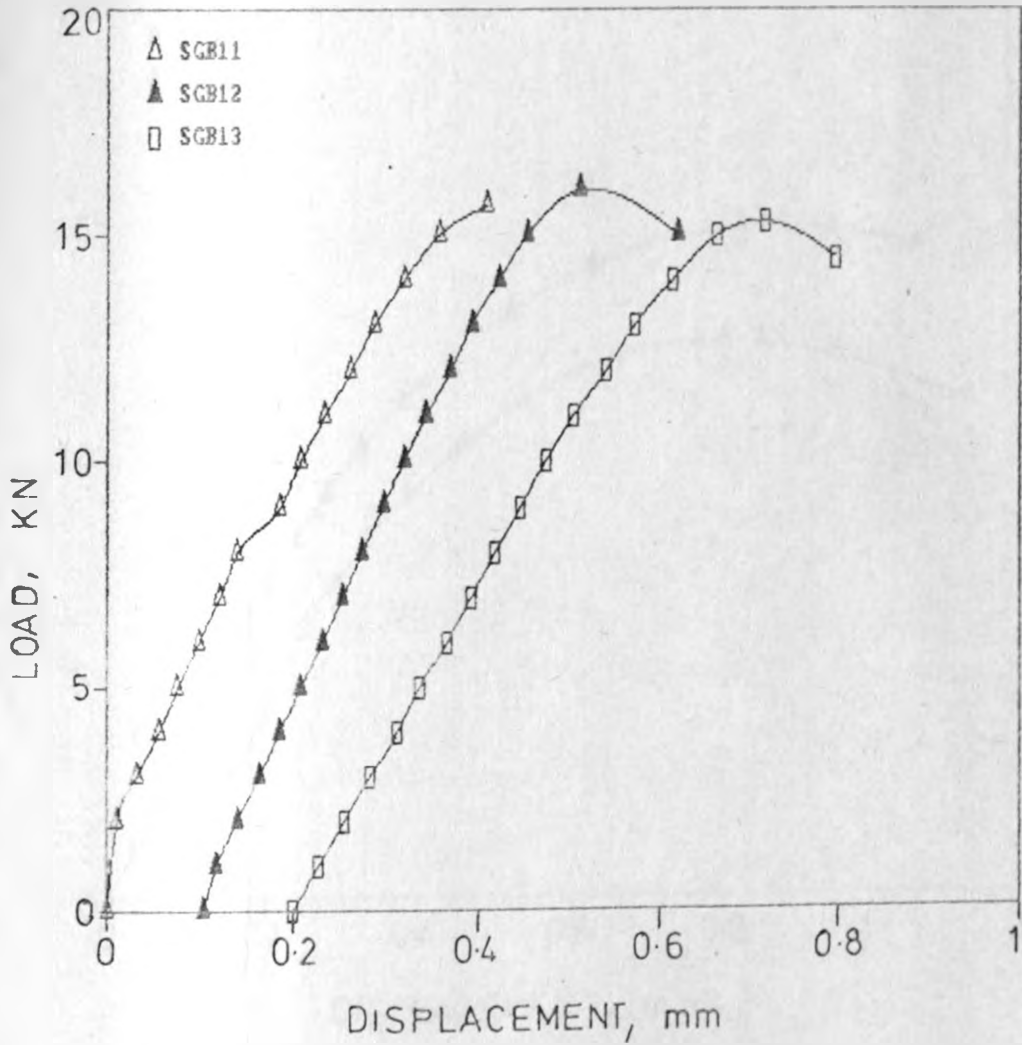


Figure 4.5 - Load-loadline displacement curve for specimen SGB (as-cast)

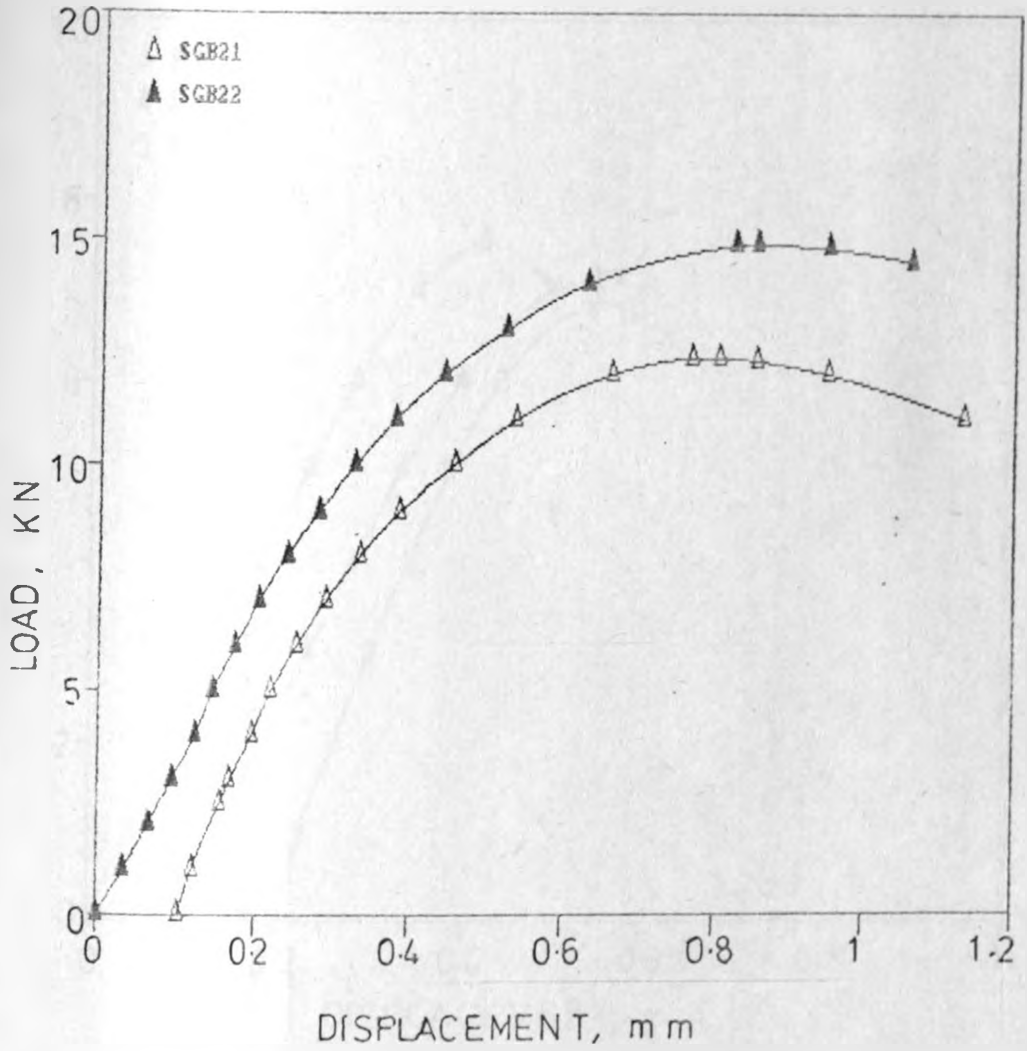


Figure 4.6 - Load-loadline displacement curve for specimen SGB (annealed)

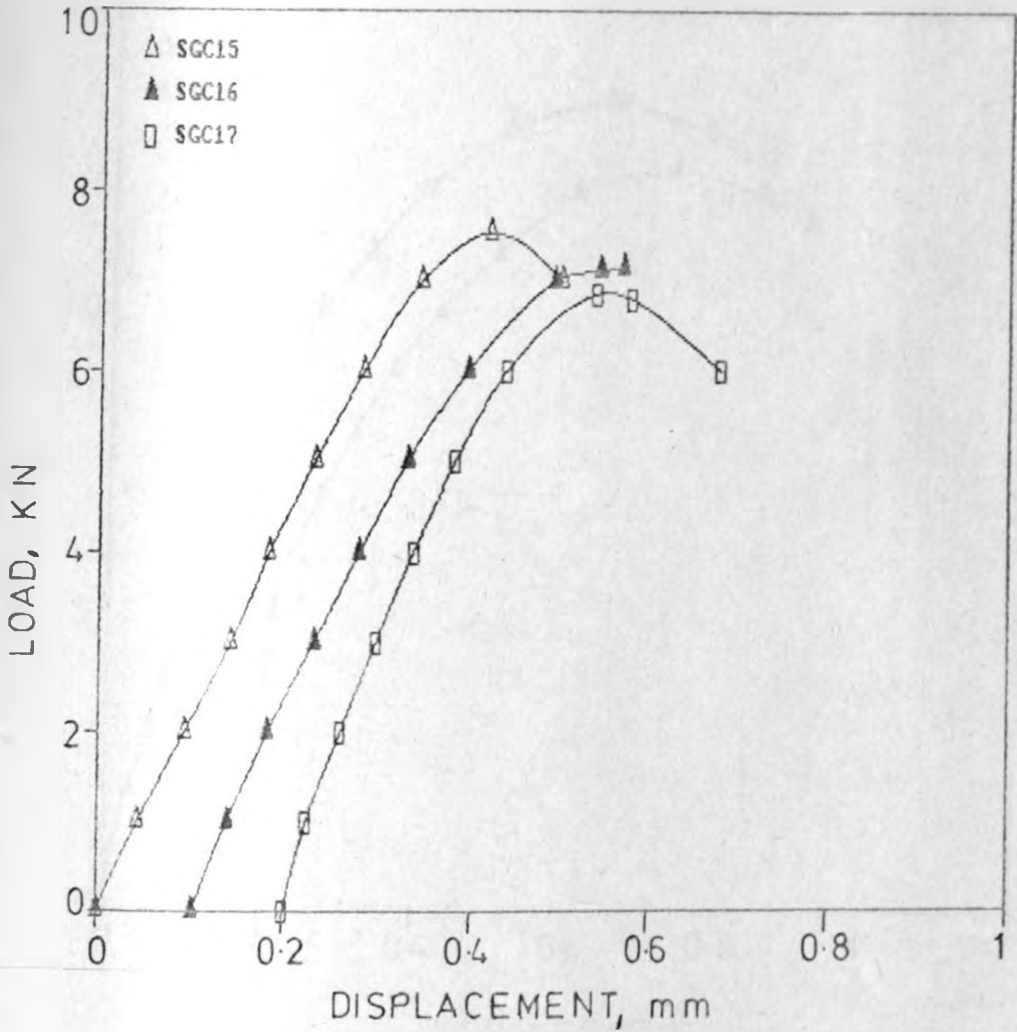


Figure 4.7 - Load-loadline displacement curve for specimen SGC (as-cast)

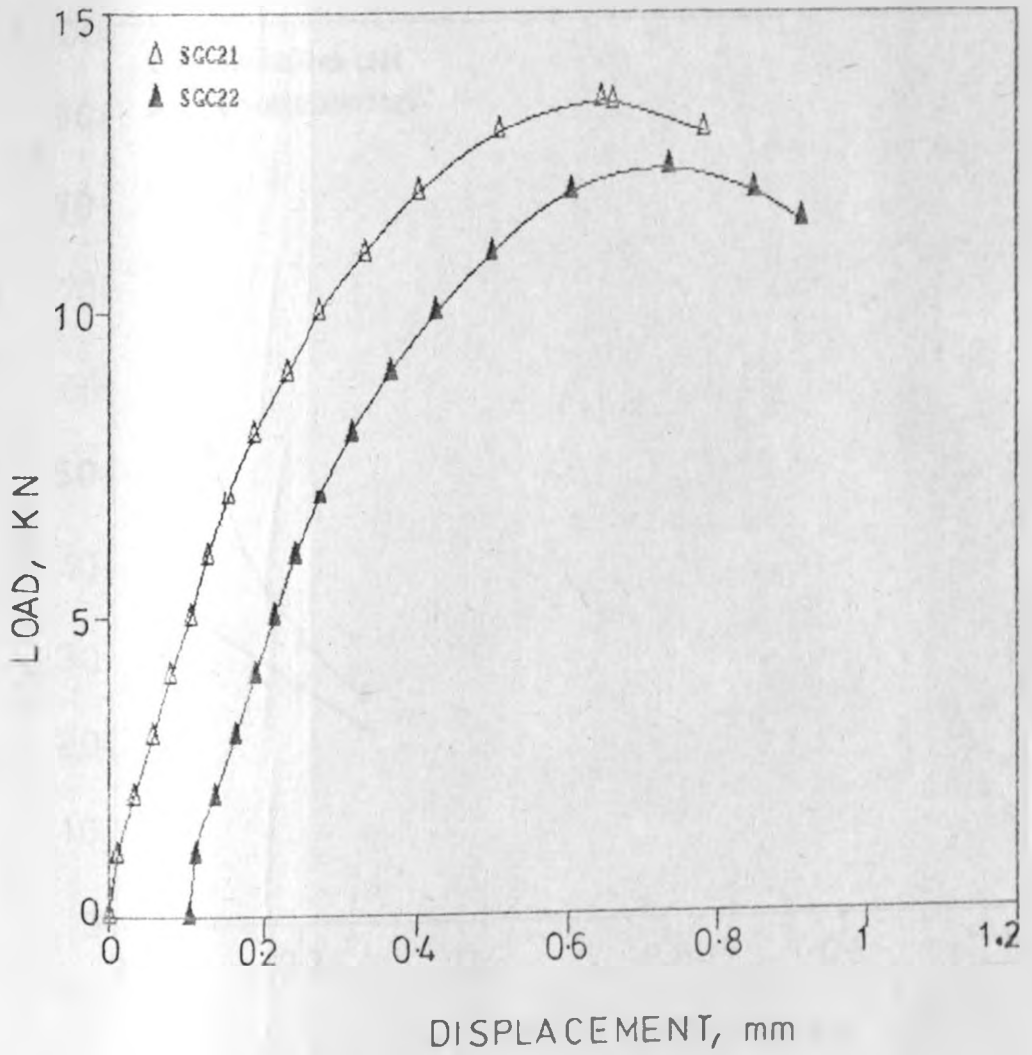


Figure 4.8 - Load-loadline displacement curve for specimen SGC (annealed)

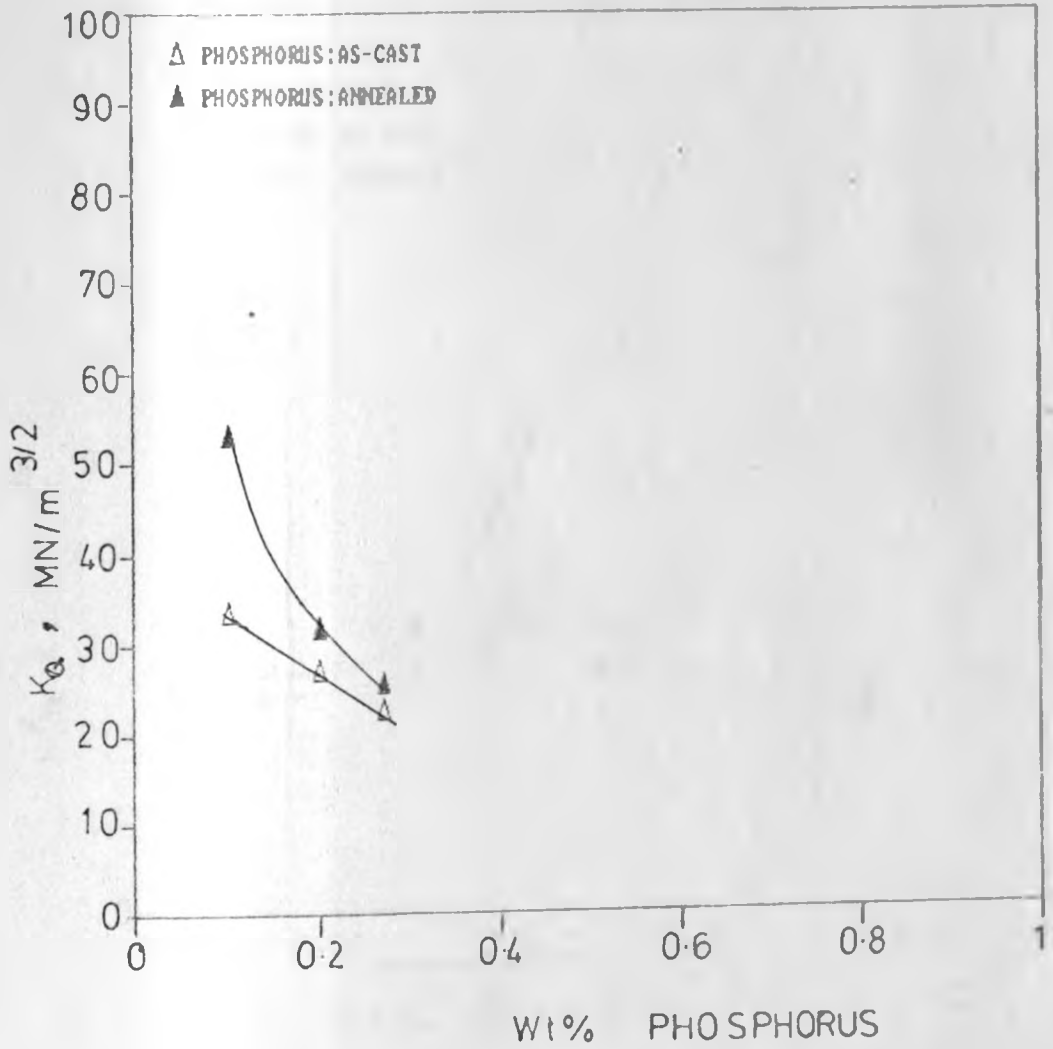


Figure 4.9 - Fracture toughness versus phosphorus content

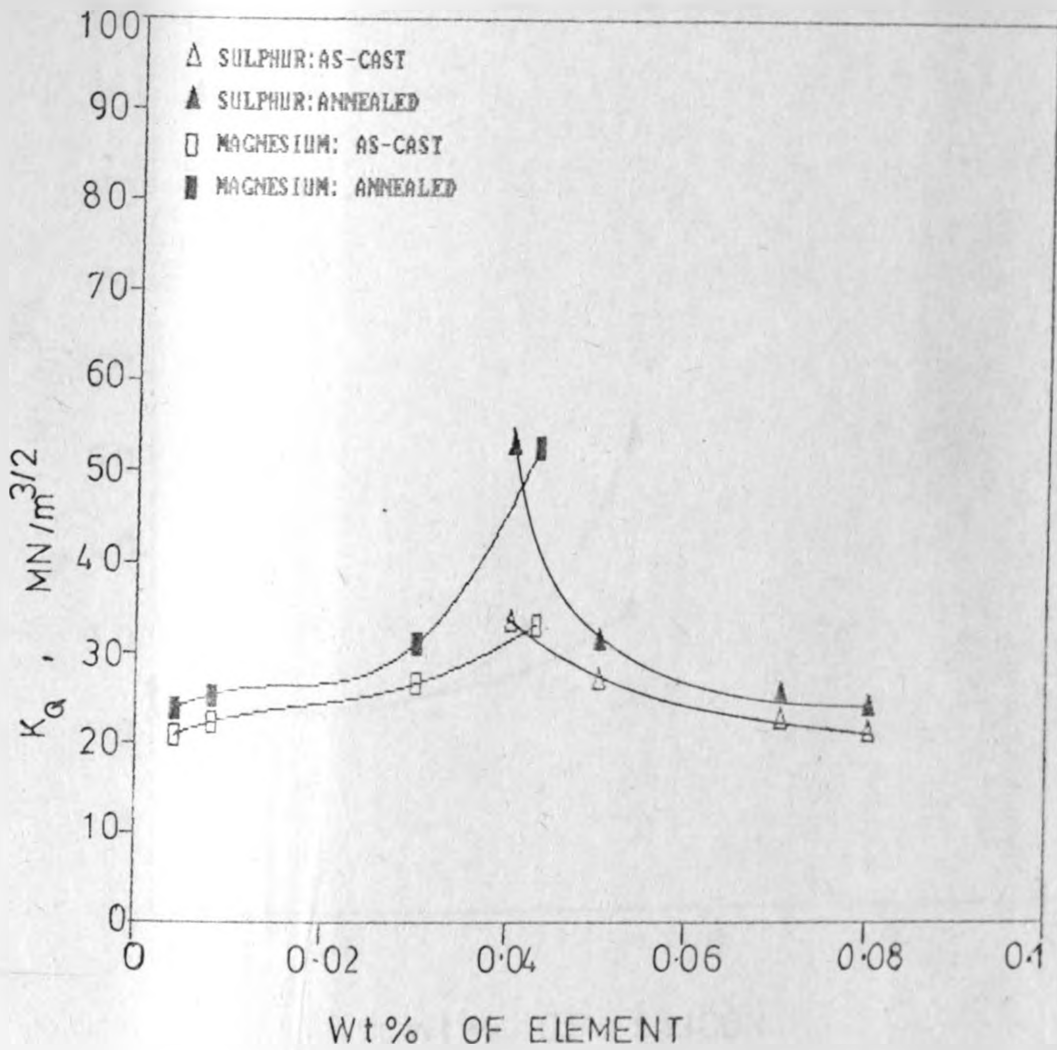


Figure 4.10 - Fracture toughness versus sulphur and magnesium content

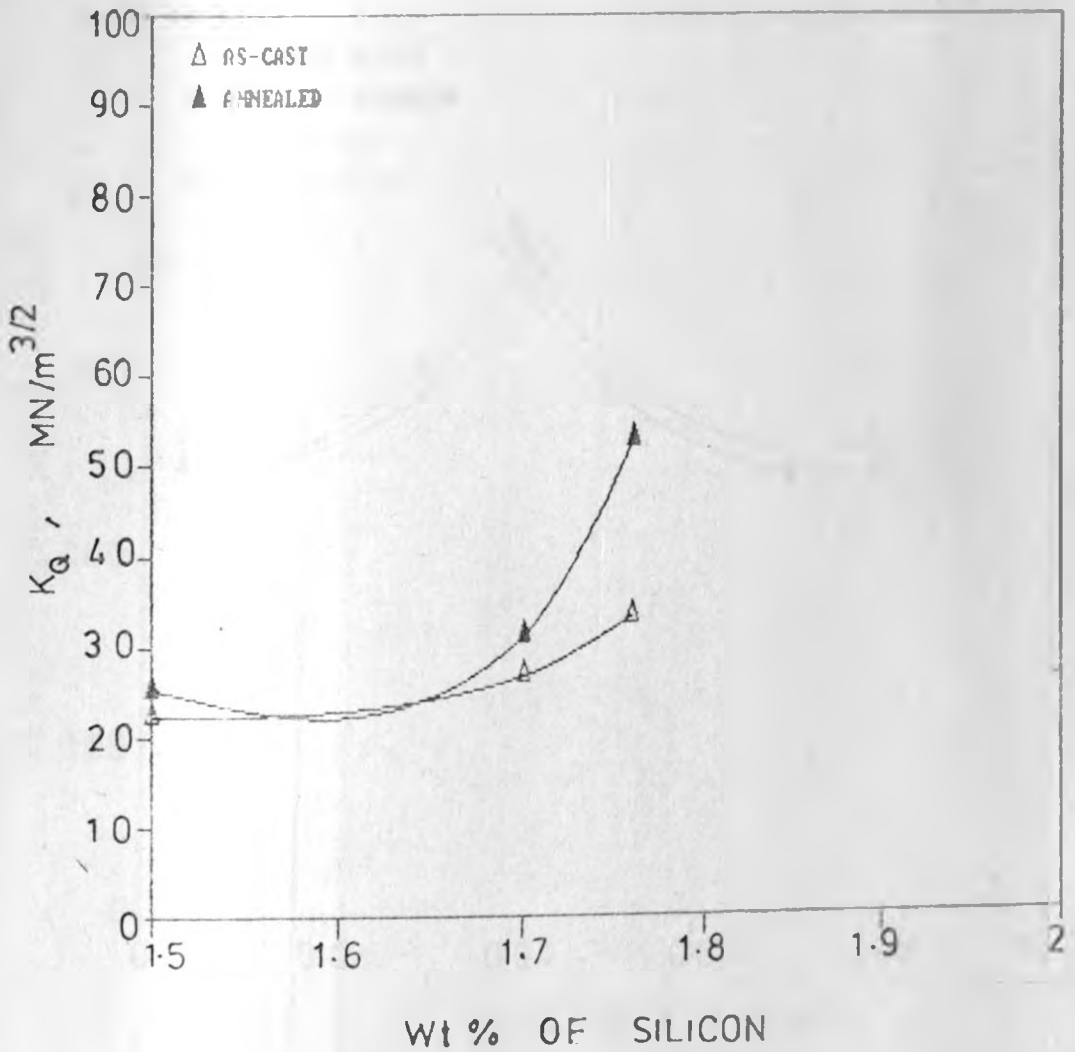


Figure 4.11 - Fracture toughness versus silicon content

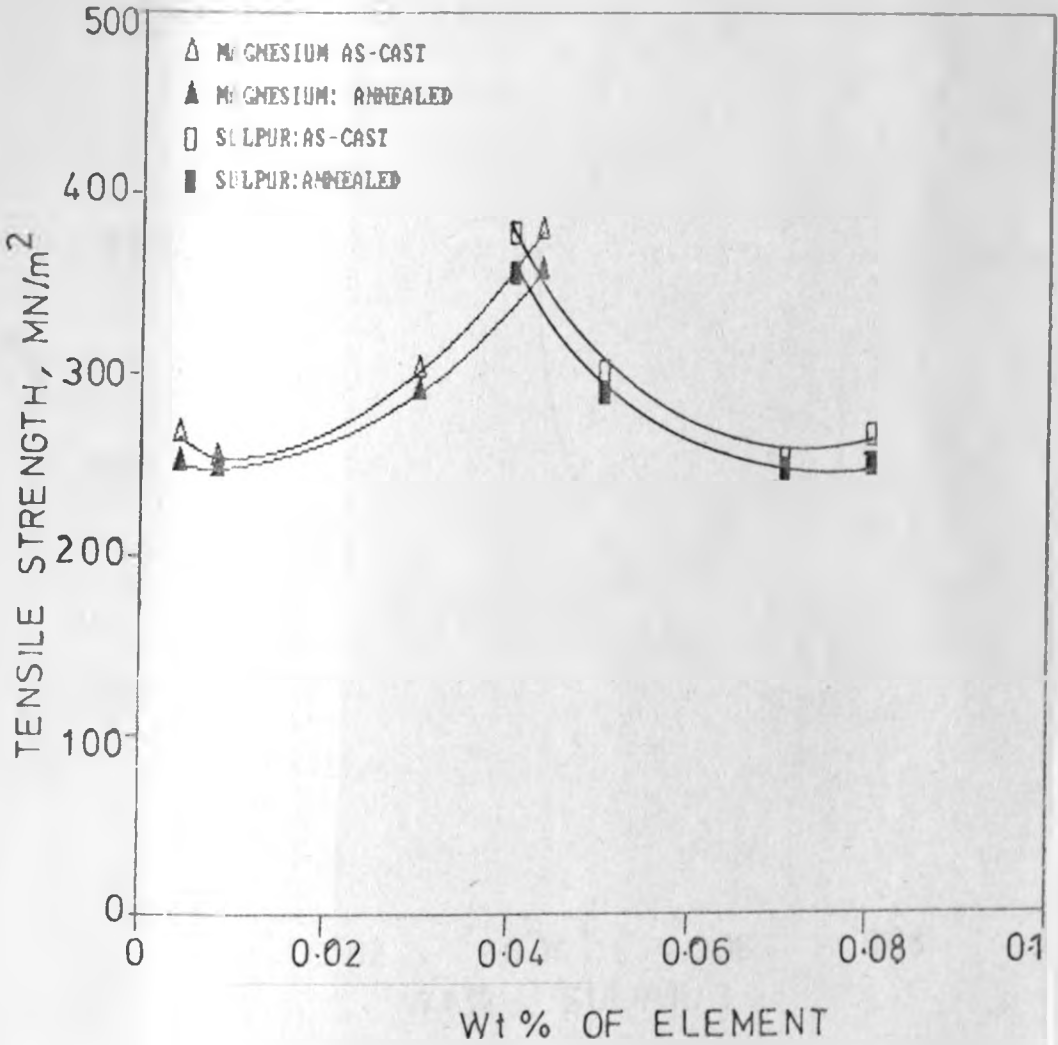


Figure 4.12 - Tensile strength versus magnesium and sulphur content

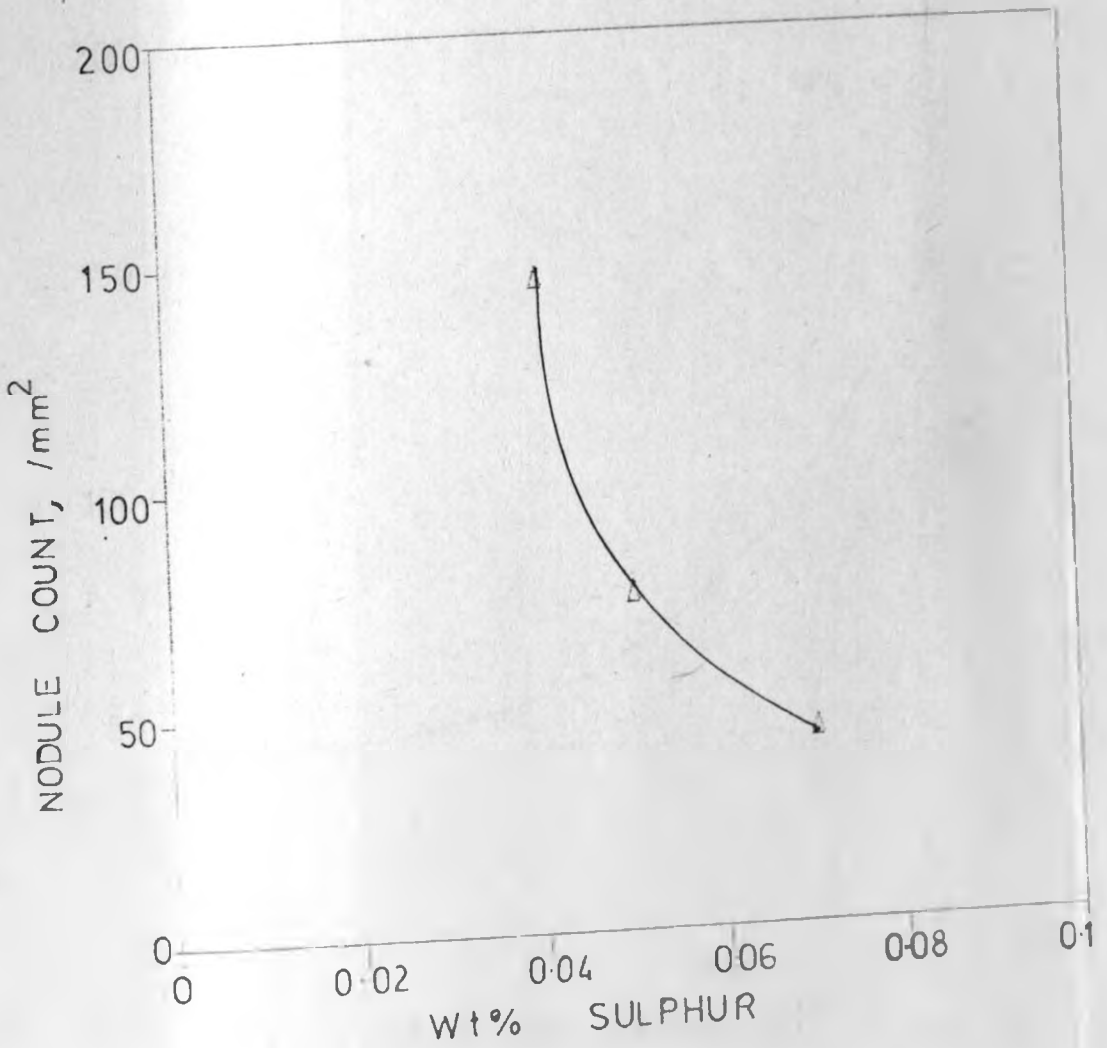


Figure 4.13 - Nodule count versus sulphur content

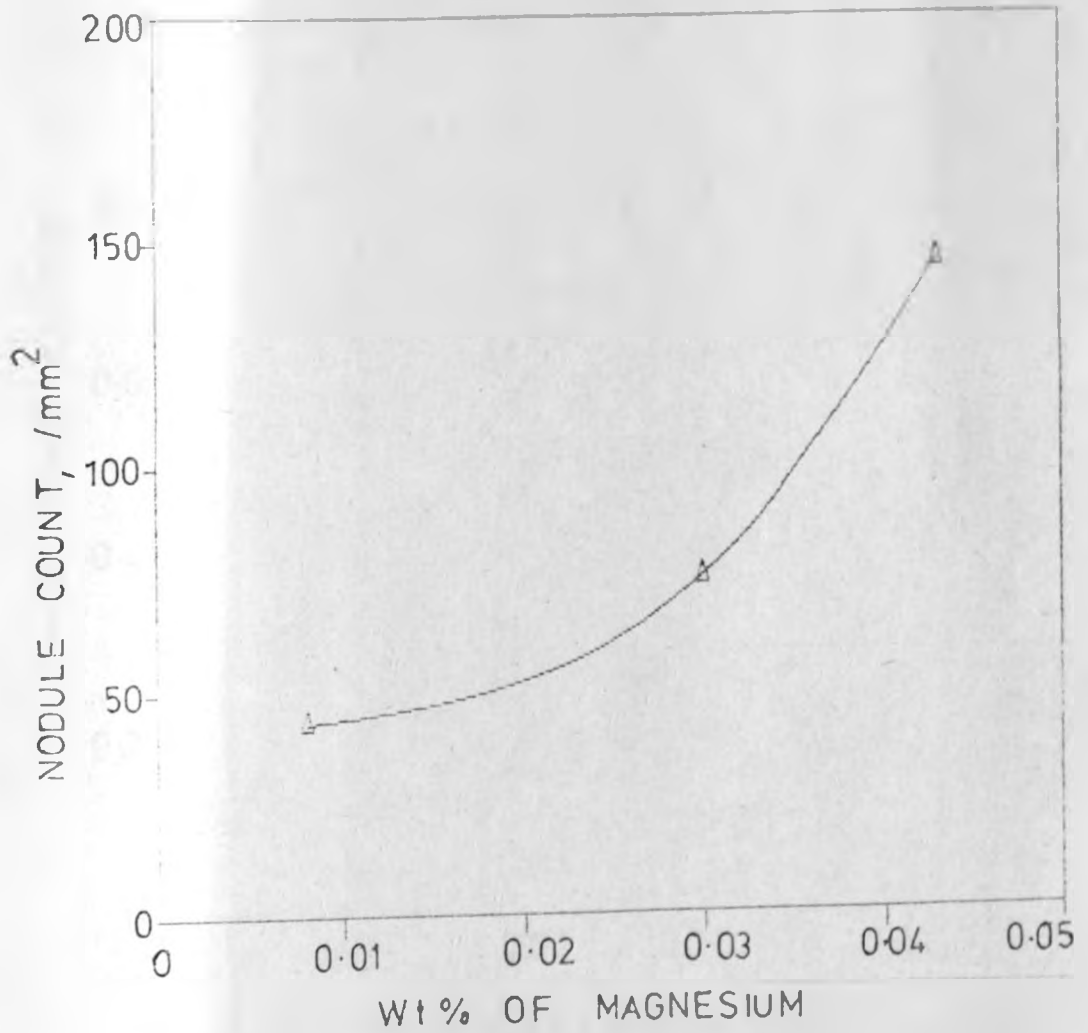


Figure 4.14 - Nodule count versus magnesium content

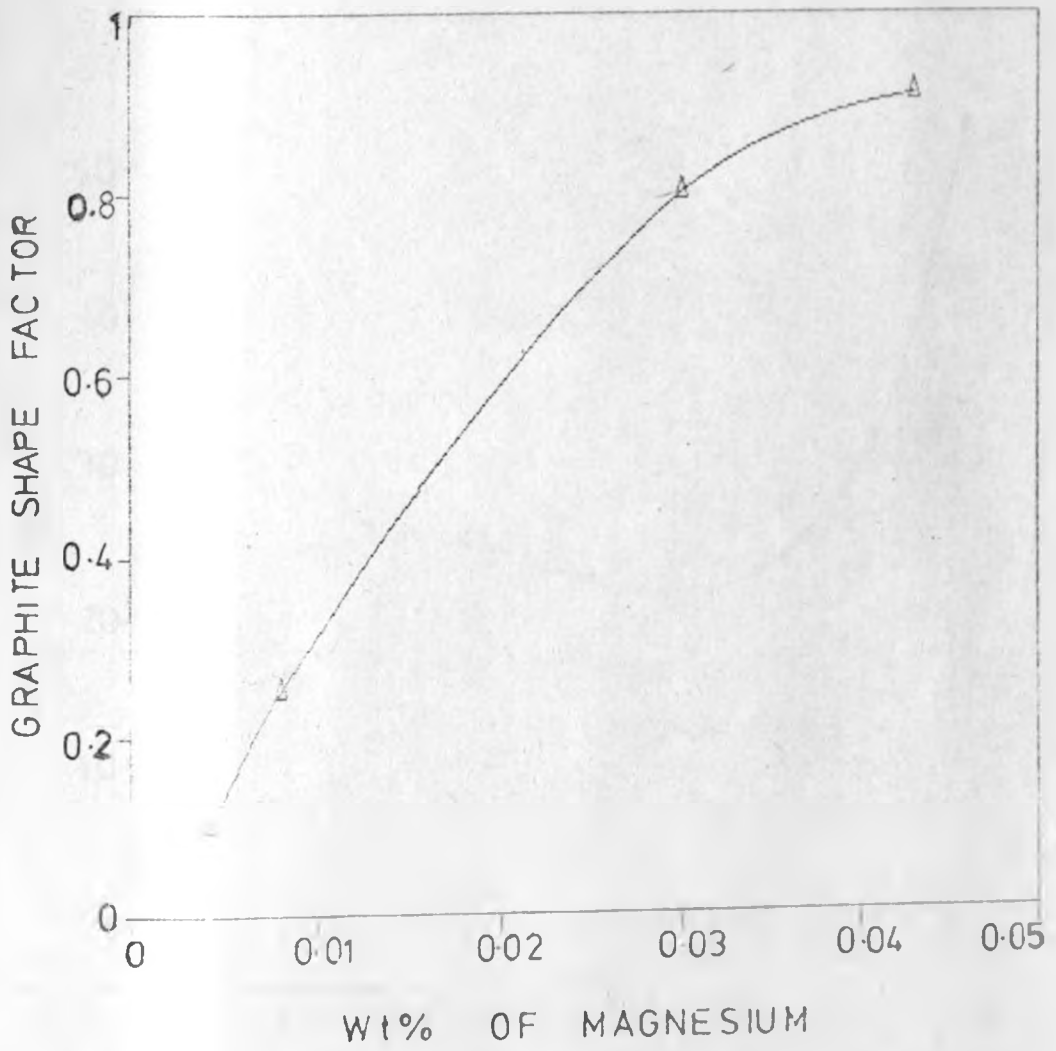


Figure 4.15 - Nodularity (graphite shape factor) versus magnesium content.

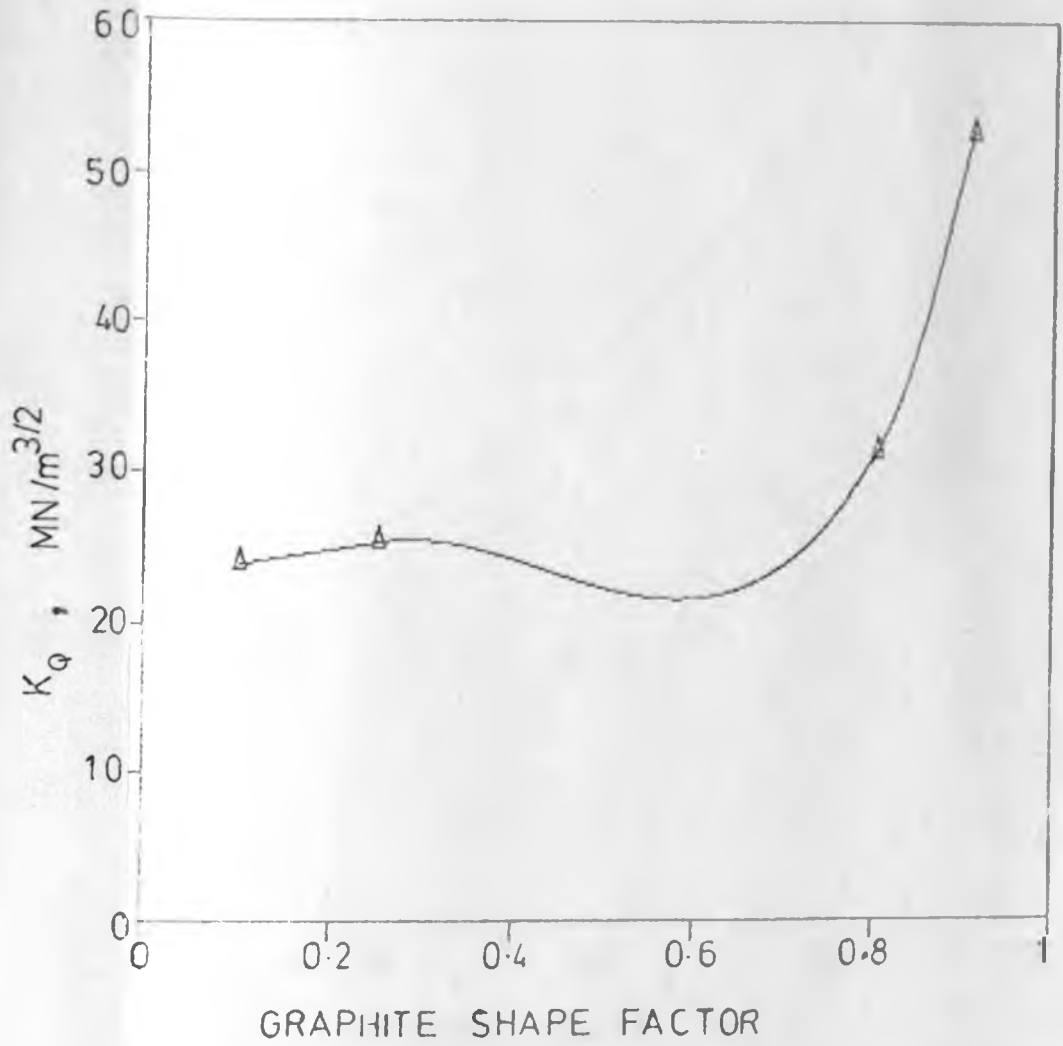


Figure 4.16 - Fracture toughness versus nodularity (graphite shape factor)

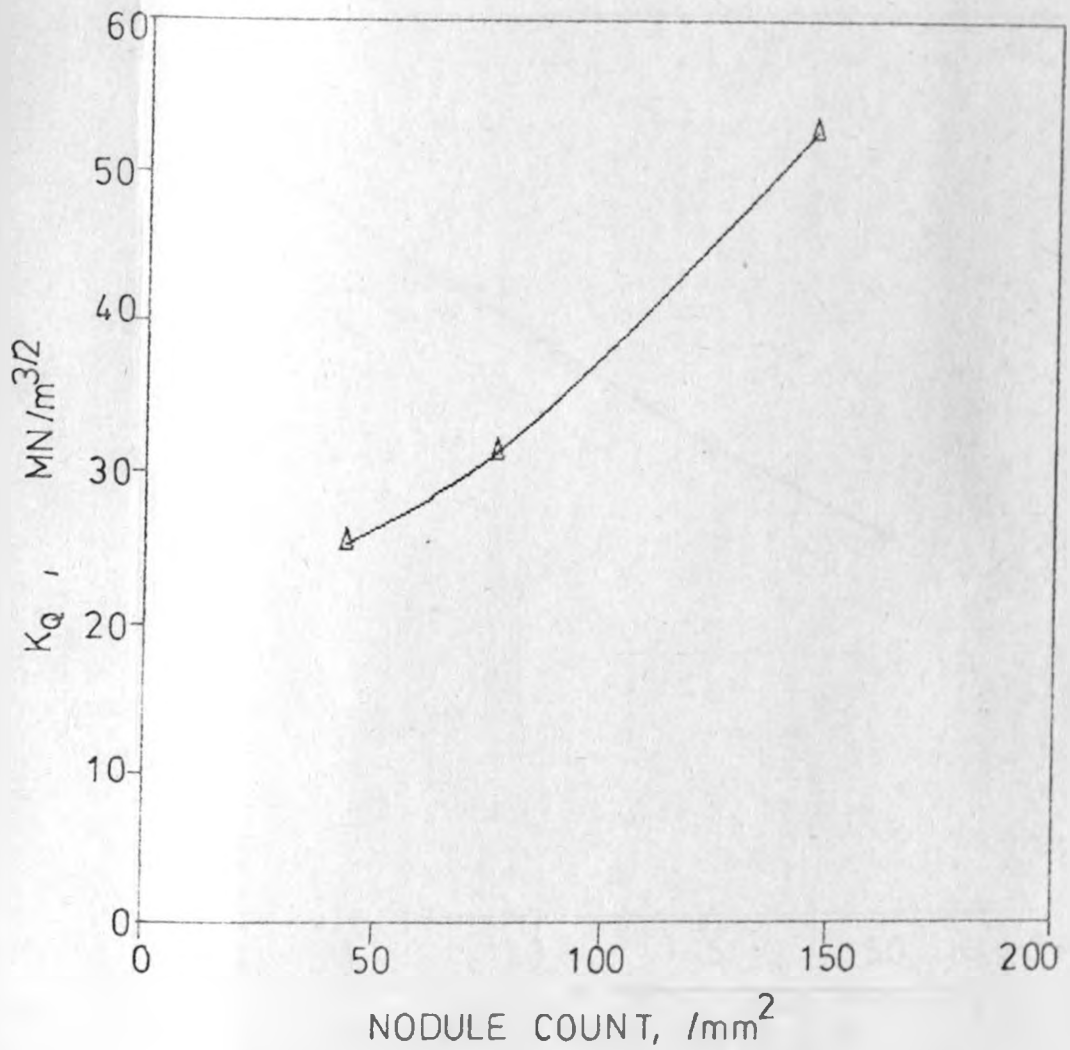


Figure 4.17 - Fracture toughness versus nodule count

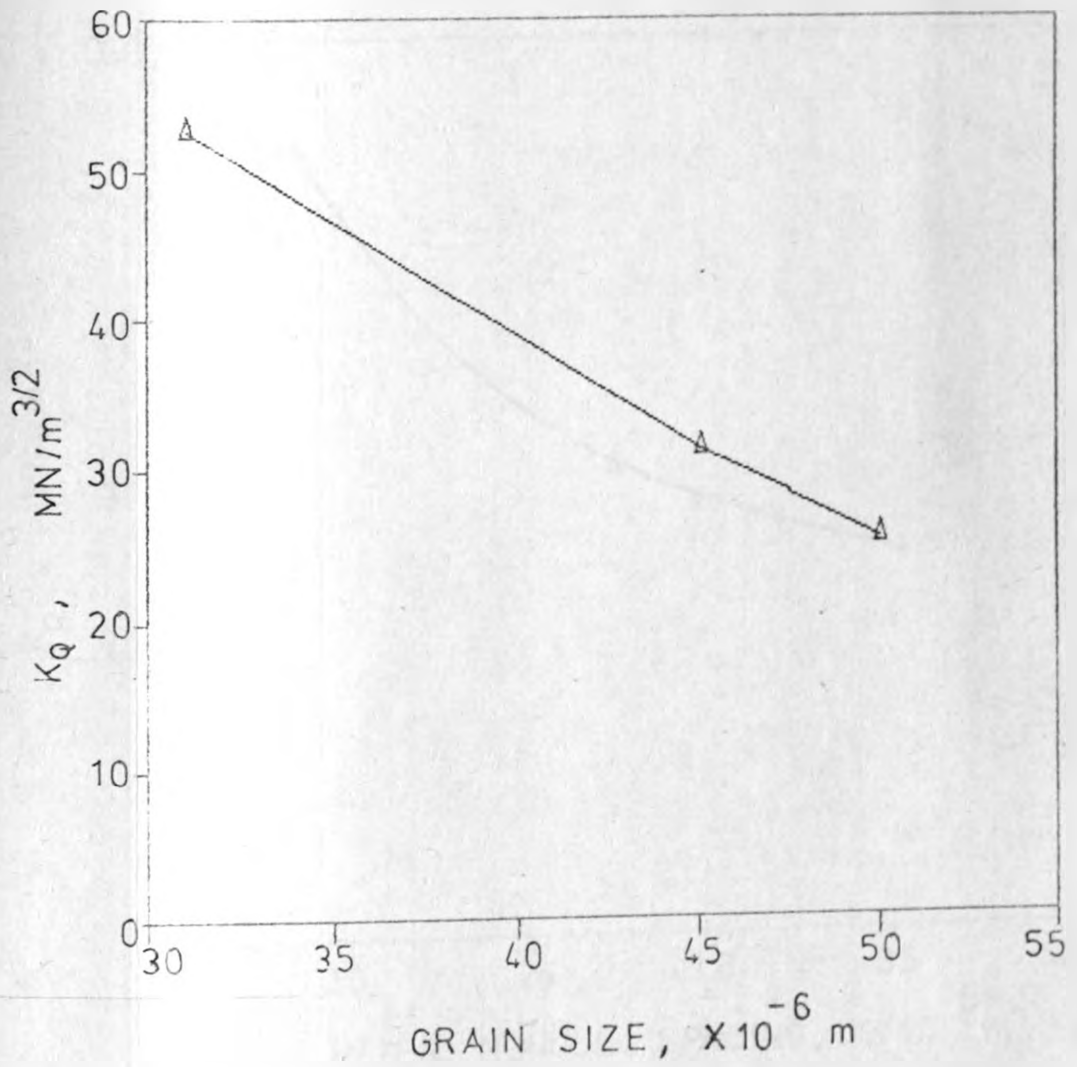


Figure 4.18 - Fracture toughness versus matrix grain size

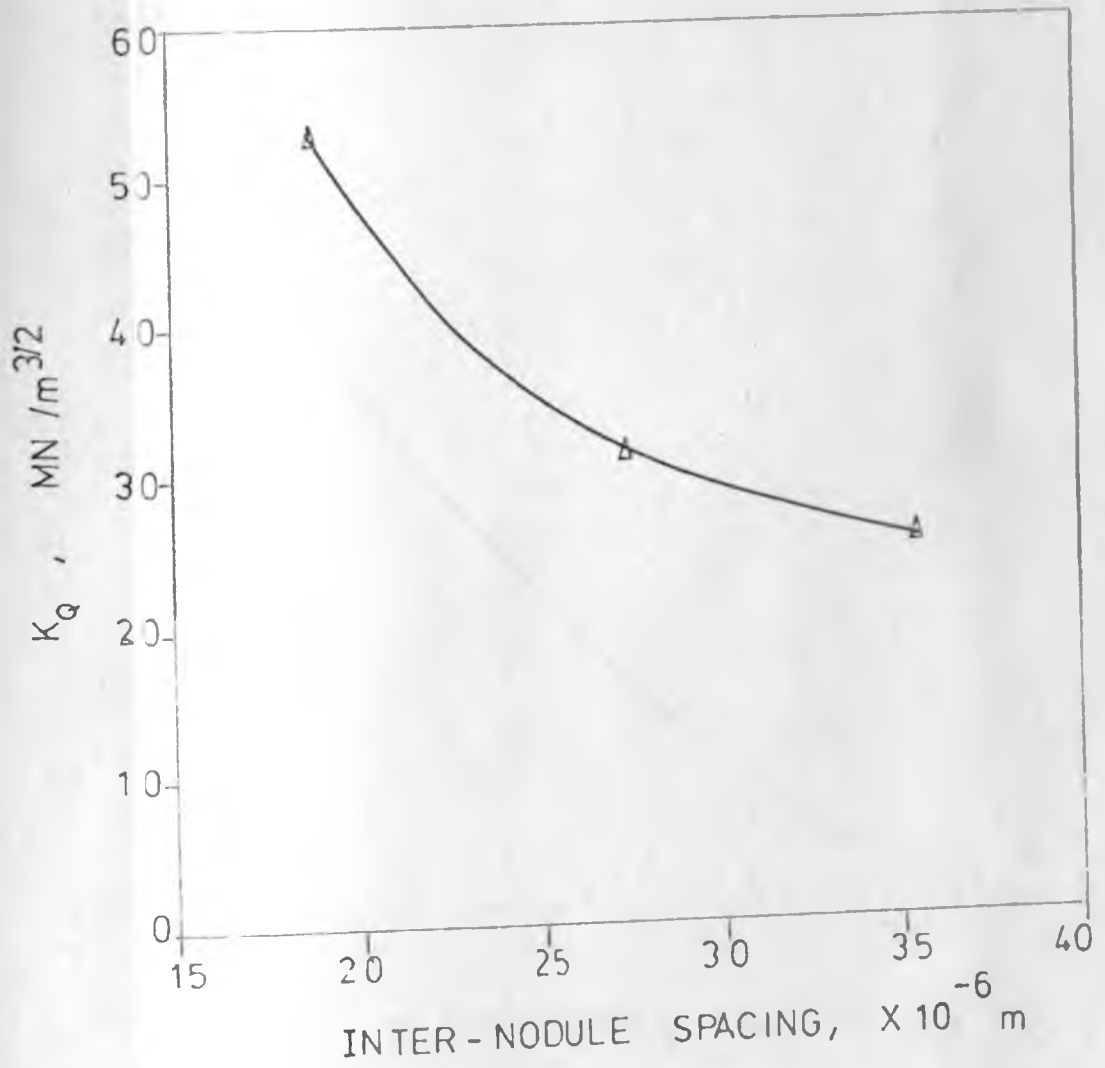


Figure 4.19 - Fracture toughness versus inter-nodule spacing

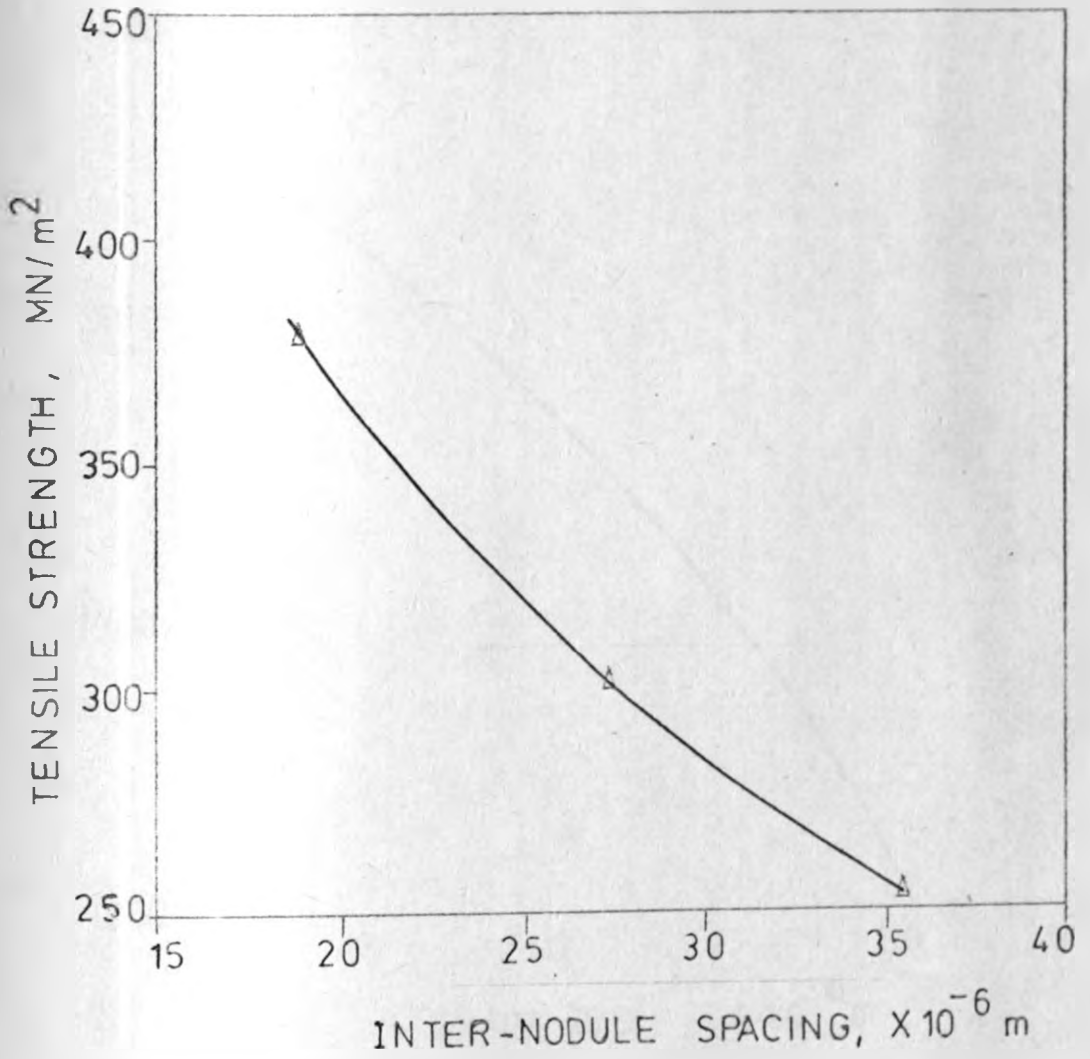


Figure 4.20 - Tensile strength versus inter-nodule spacing

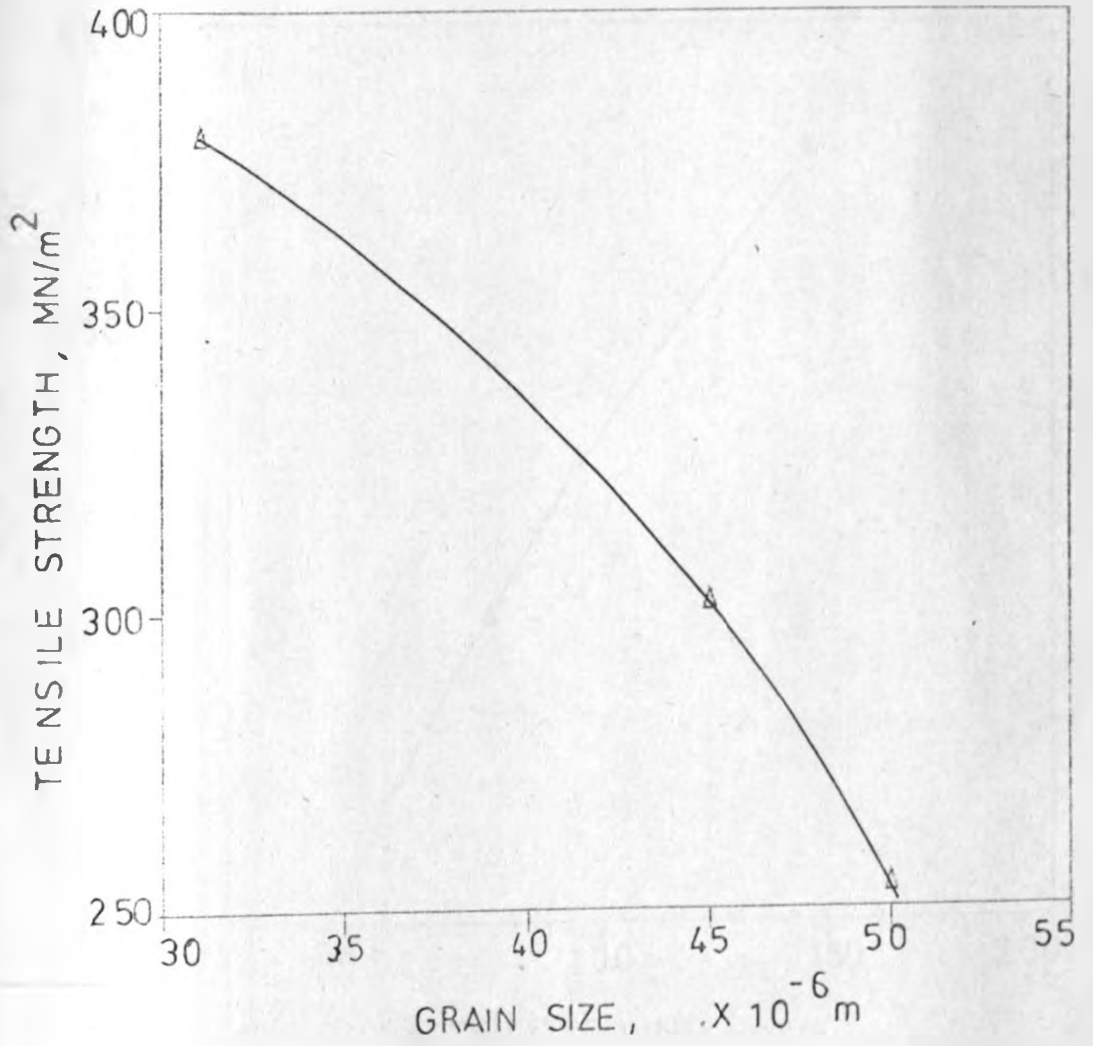


Figure 4.21 - Tensile strength versus matrix grain size

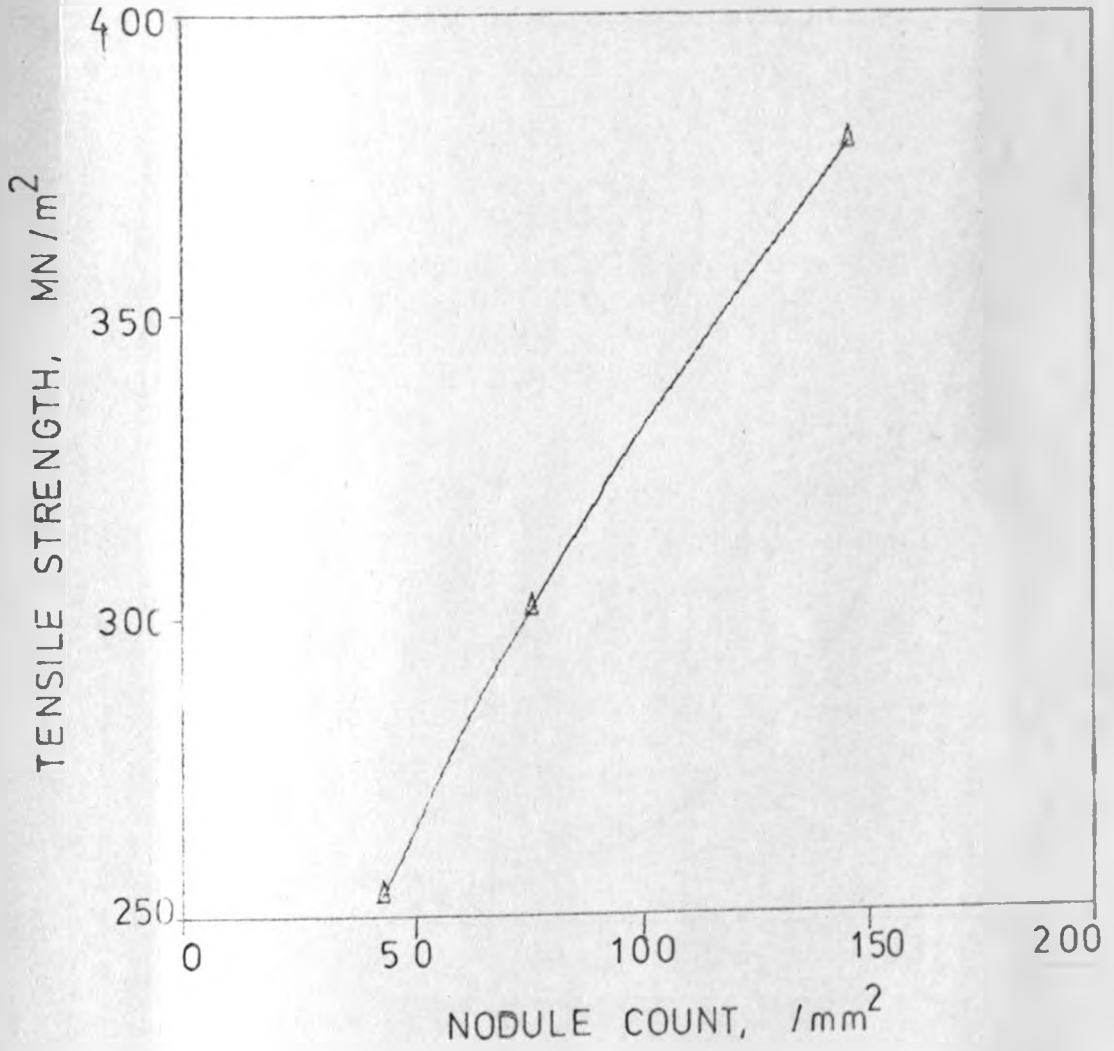


Figure 4.22 - Tensile strength versus nodule count

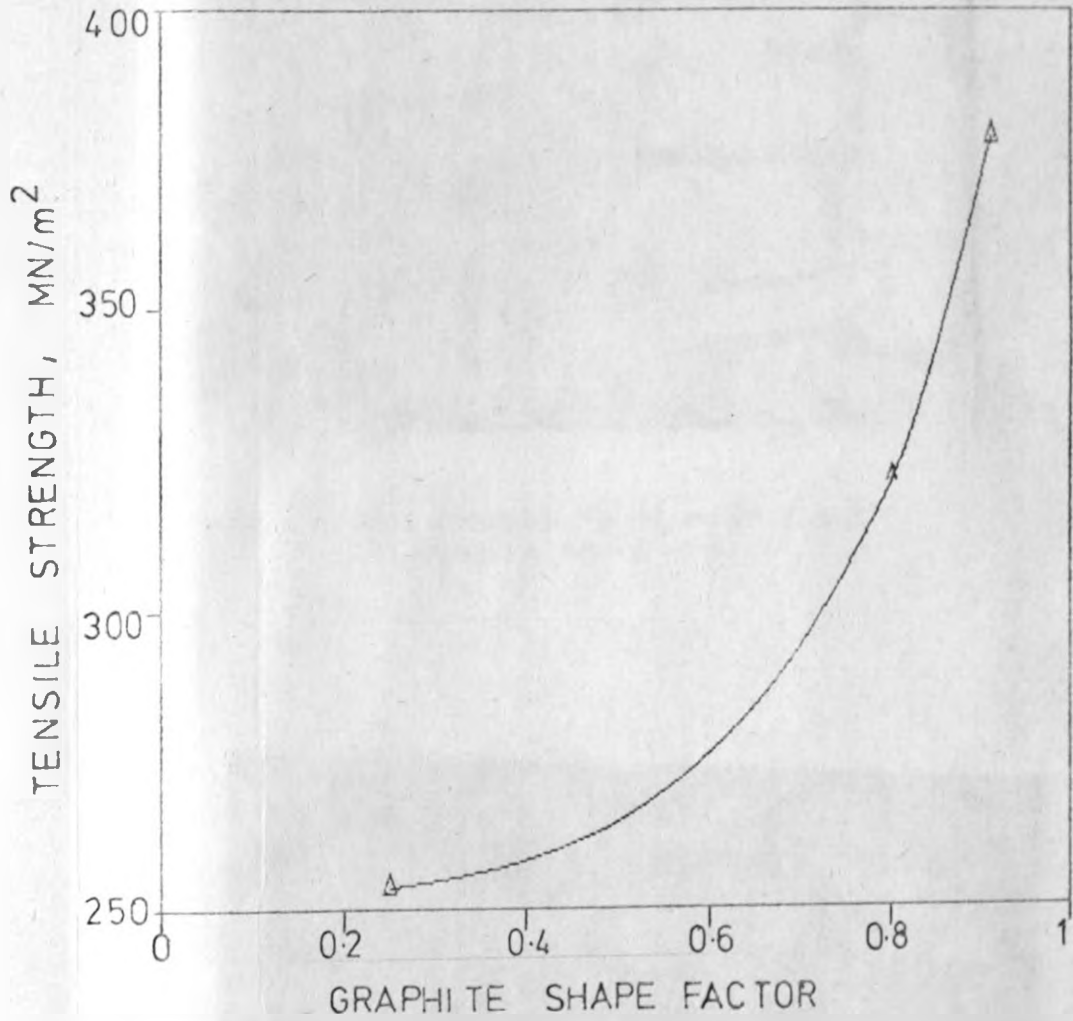


Figure 4.23 - Tensile strength versus nodularity
(graphite shape factor)

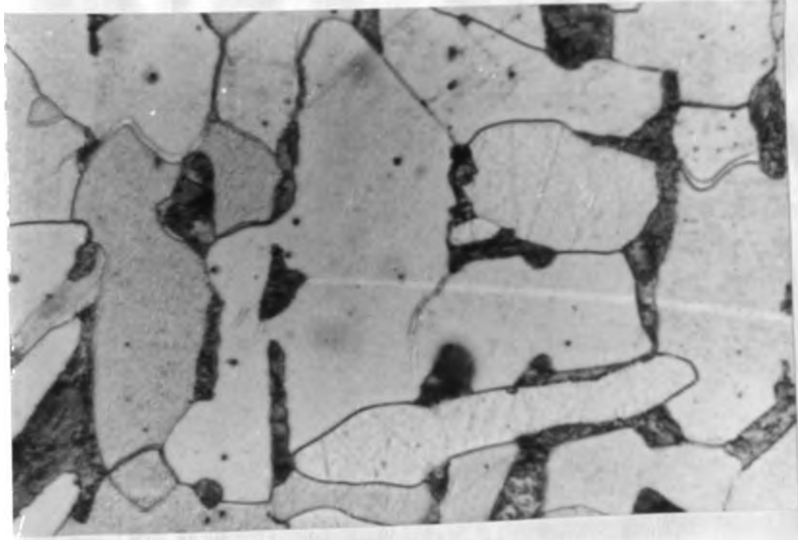


Plate 1 - Microstructure of mild steel
2% Nital etch X 400.

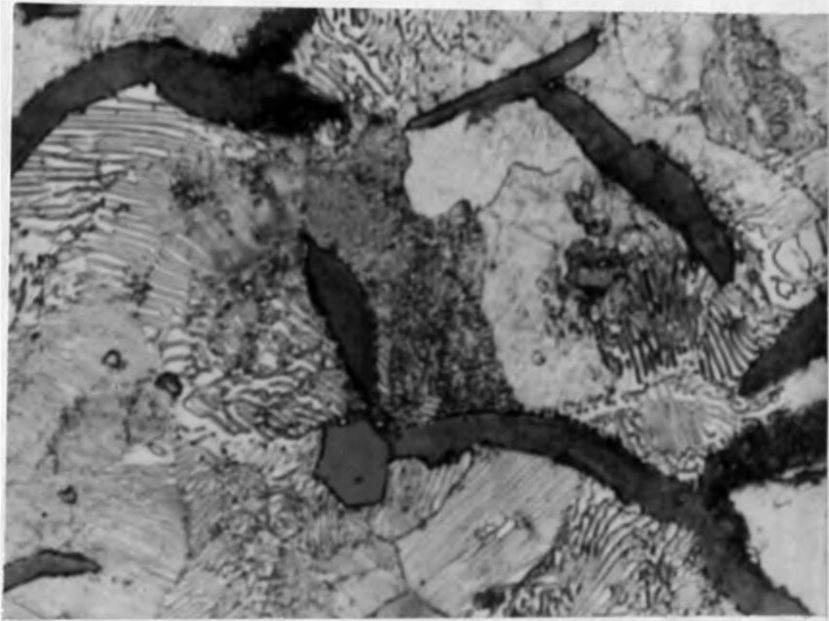


Plate 2 - Microstructure of pearlitic gray cast
(heat G1). 2% Nital etch X 400.

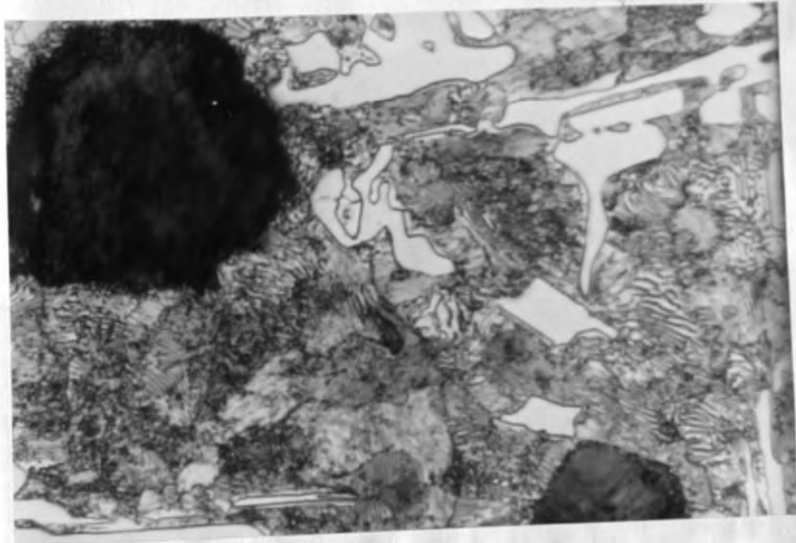


Plate 3 - Microstructure of ductile iron (heat SGC) as-cast, pearlitic, low nodularity and nodule count. Etched in 2% Nital X 400.

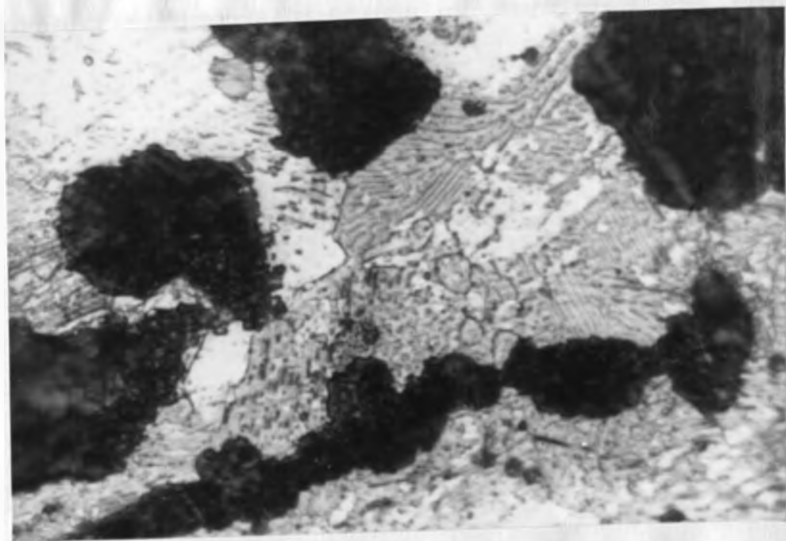


Plate 4 - Microstructure of ductile iron (heat SGC) annealed for 6 hours pearlitic-ferritic matrix. Etched in 2% Nital X 400.

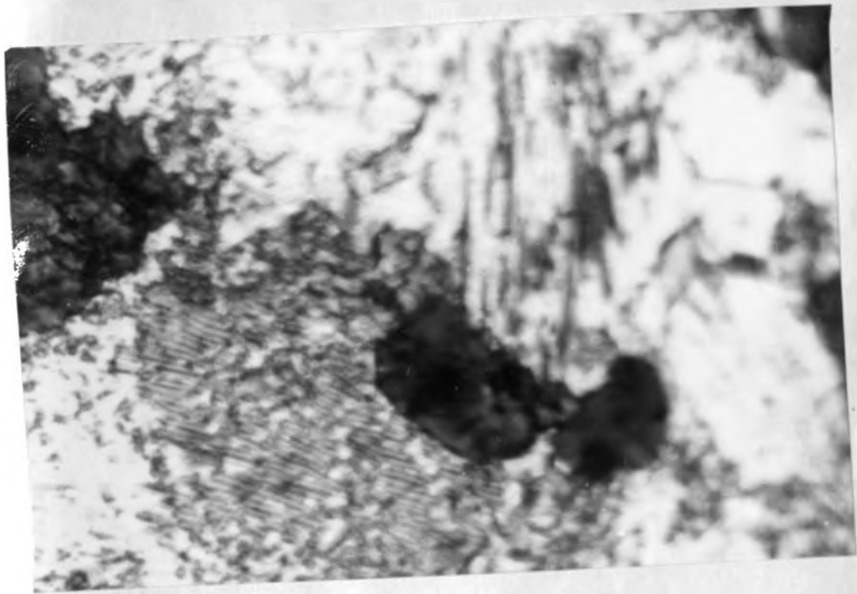


Plate 5 - Microstructure of ductile iron (heat SGC)
annealed for 24 hours, with dominating
ferritic matrix. Etched in 2% Nital.
X 400.

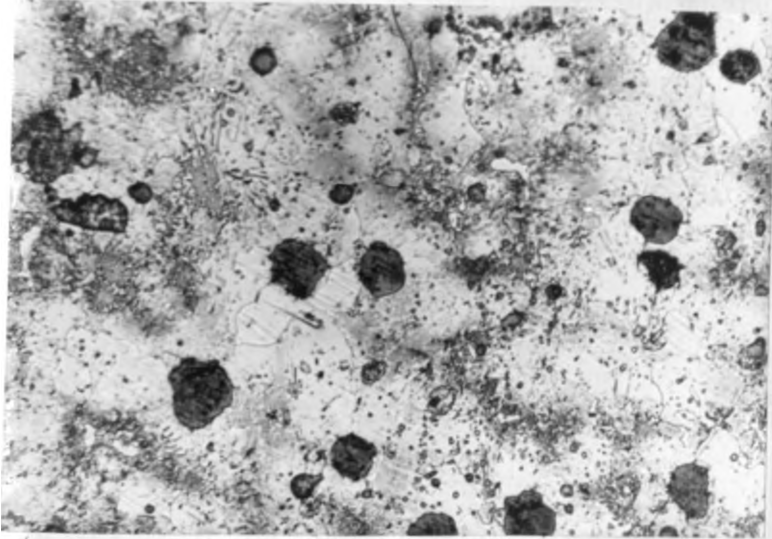


Plate 6 - Microstructure of ductile iron (heat SGB)
improved nodularity and nodule count.
Etched in 2% Nital X 100

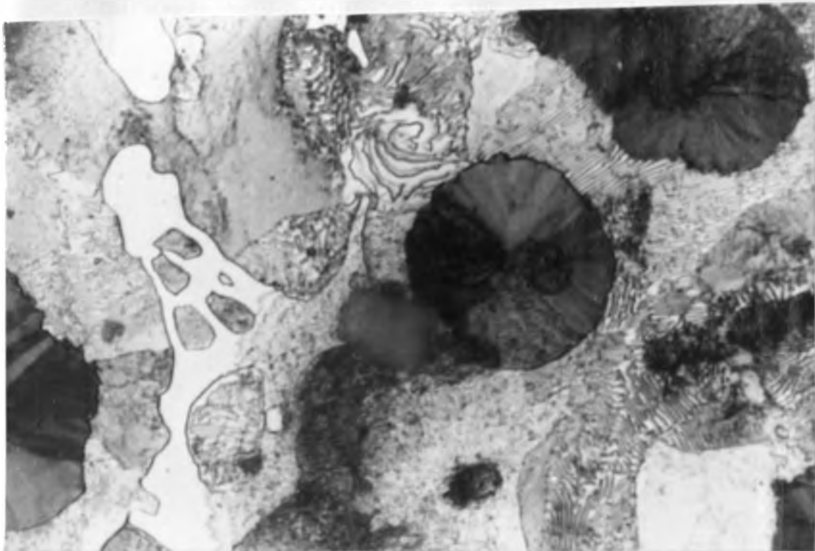


Plate 7- Microstructure of ductile iron (heat SGB)
annealed for 12 hours, pearlitic-ferritic
matrix. Etched in 2% Nital. X400

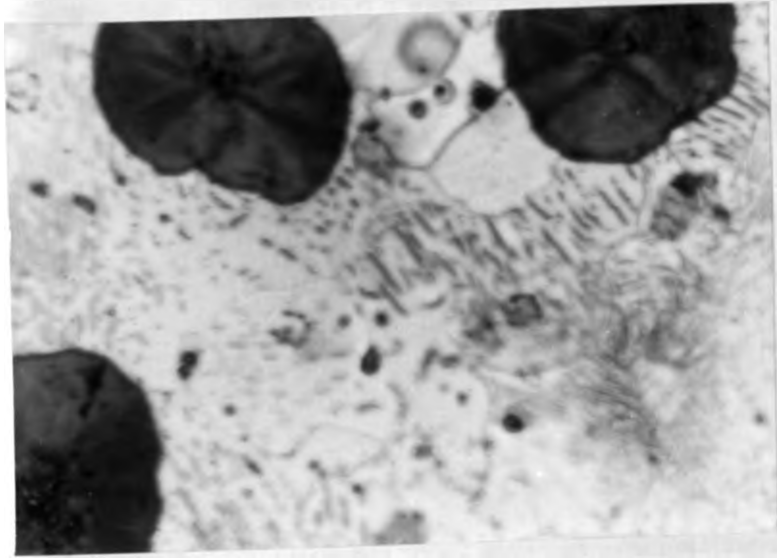


Plate 8 - Microstructure of ductile iron (heat SGB) annealed for 24 hours, ferritic matrix. Etched in 2% Nital. X 400

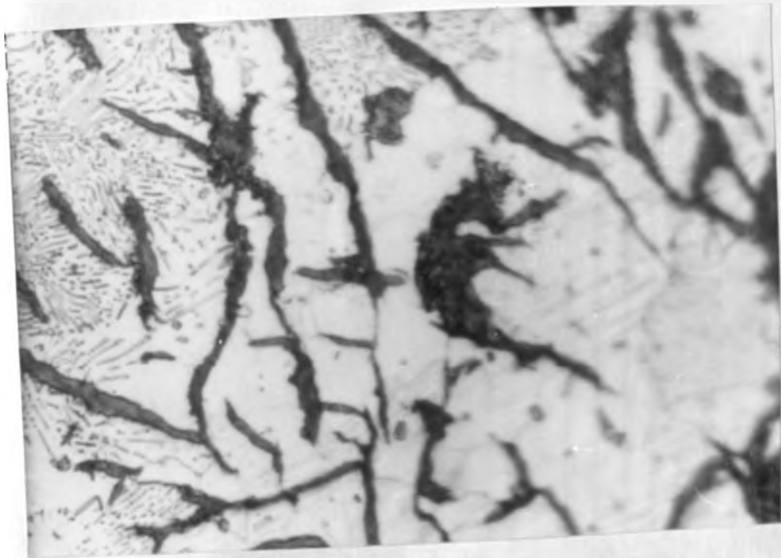


Plate 9 - Microstructure of ductile iron (heat SGB) showing graphite deterioration to slow cooling rate. Etched in 2% Nital. X 400



Plate 10 - Microstructure of ductile iron (heat SGA) as-cast pearlitic, high nodularity and nodule count. Etched in 2% Nital. X 400

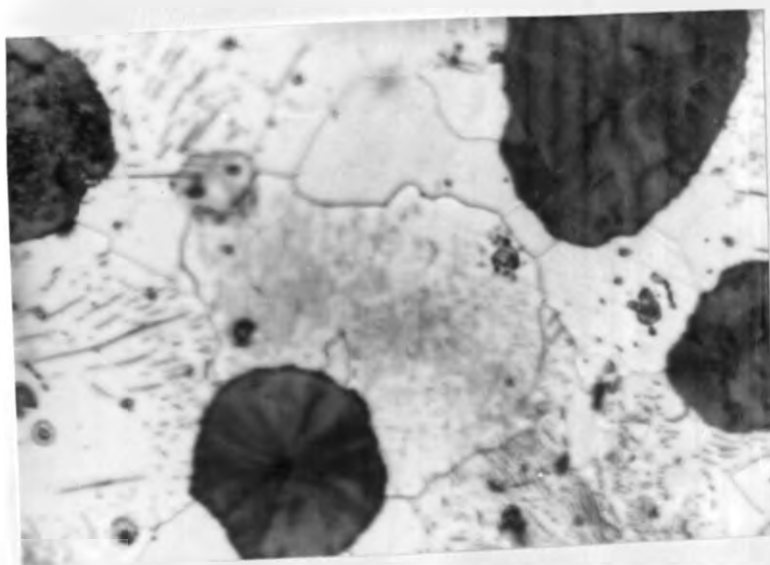


Plate 11 - Microstructure of ductile iron (heat SGA) annealed for 12 hours, dominating ferritic matrix. Etched in 2% Nital. X 400

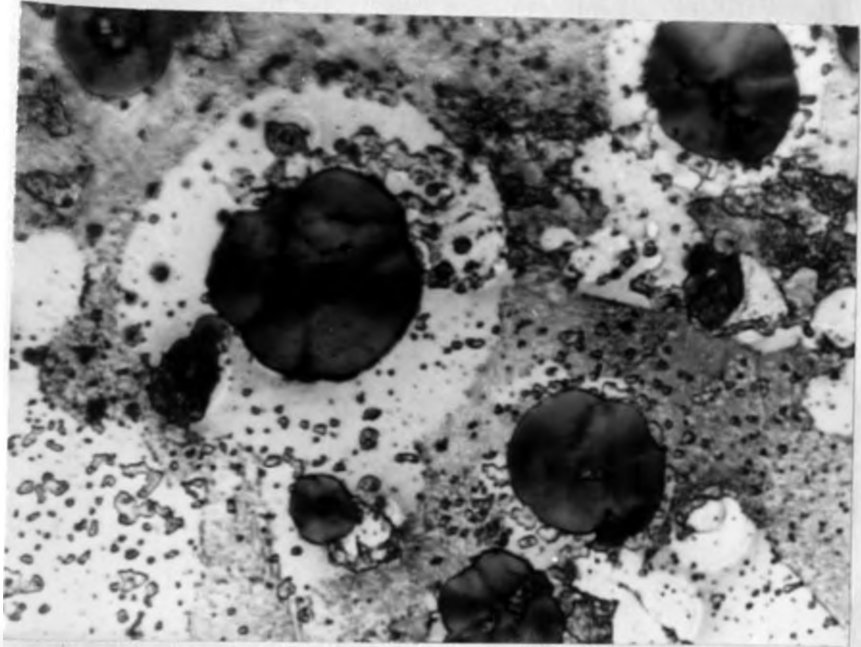
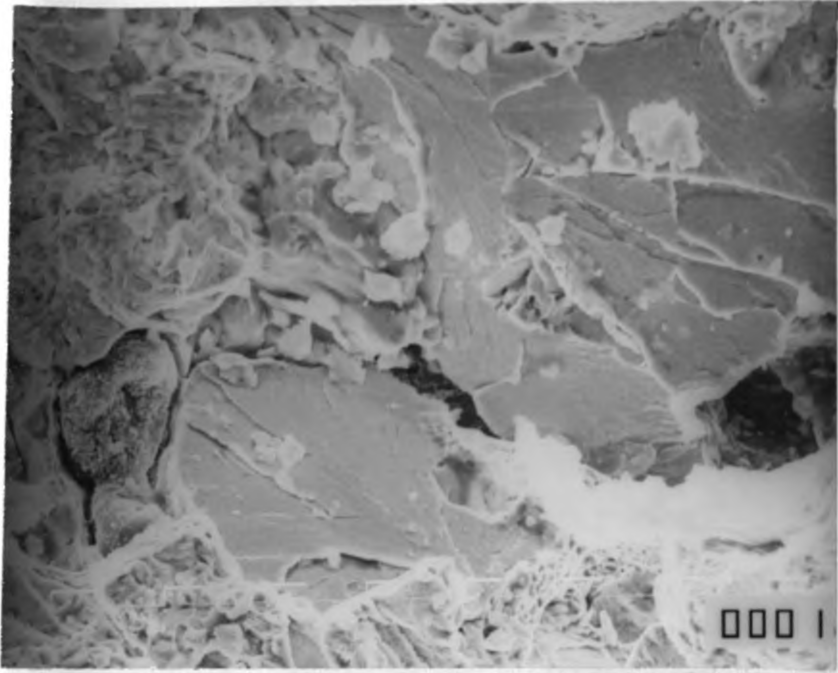
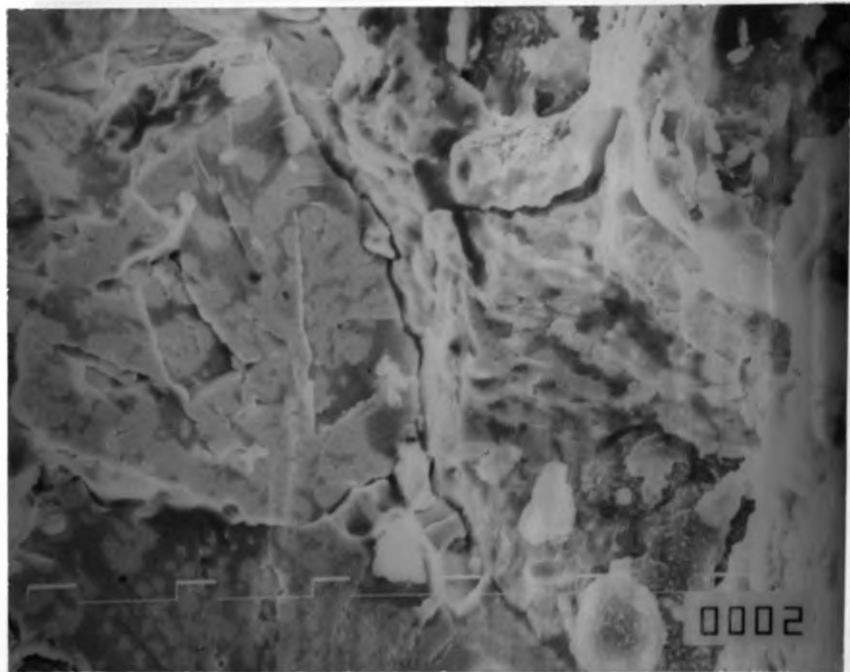


Plate 12 - Microstructure of ductile iron (heat SGA) annealed for 24 hours, with fully ferritic matrix and showing the ferrite rings surrounding the nodules (bull's-eye structure). Etched in 2% Nital. X 400

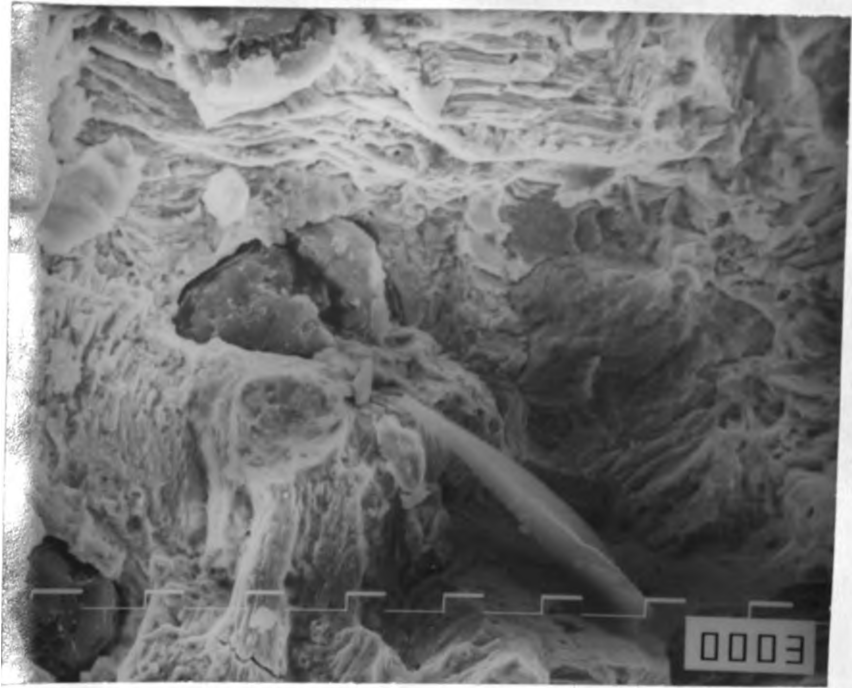


(a)

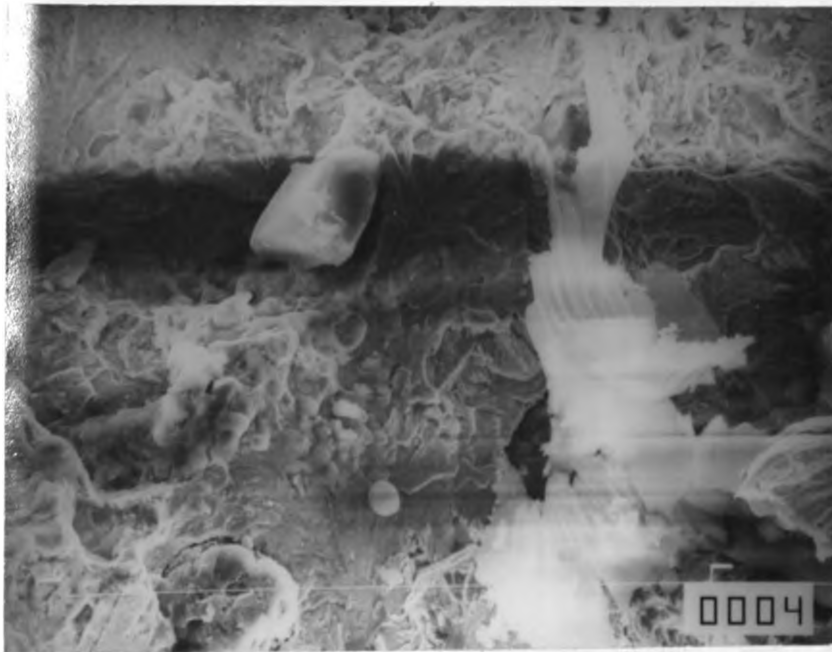


(b)

Plate 13 - SEM photos. Ductile iron (heat SGA) as-cast.
(a) Interface between fatigue and fracture region. X 1500
(b) Transgranular failure of pearlitic matrix. X 2000

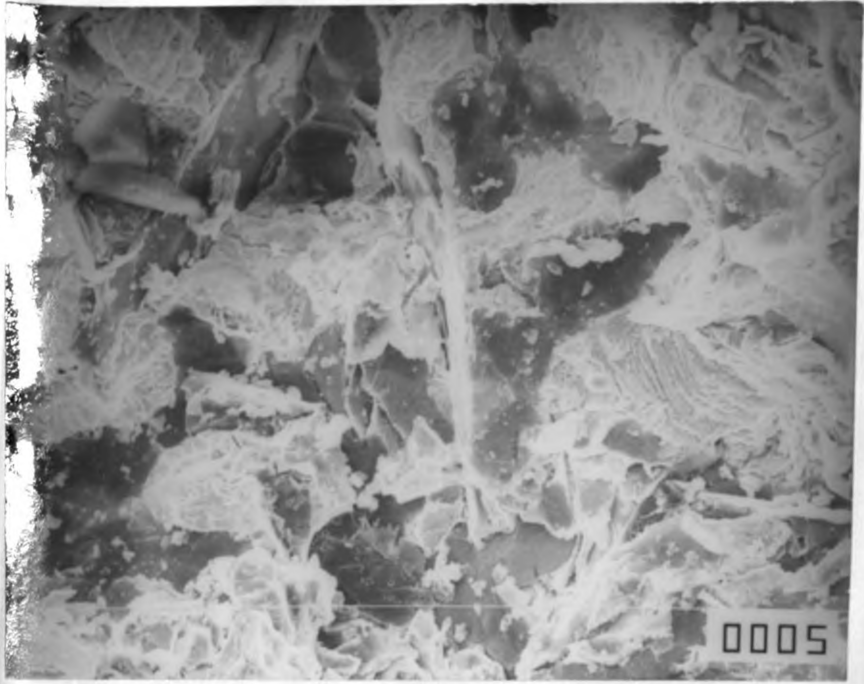


(a)

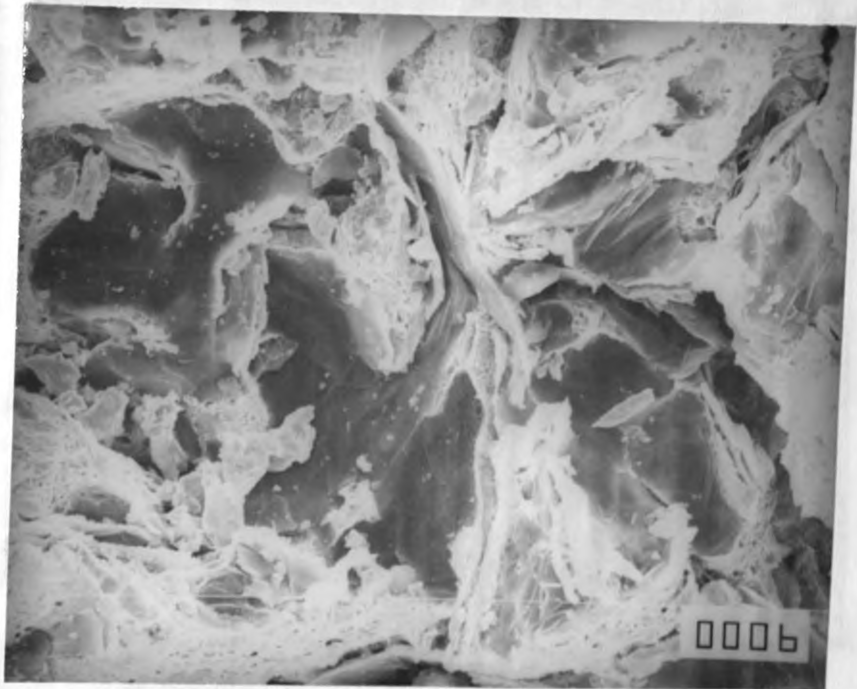


(b)

Plate 14 - SEM photos. Ductile iron (heat SGA) annealed for 12 hours, ferritic-pearlitic matrix.
(a) Fatigue/Fracture interface. X 1500
(b) Ductile behaviour of fracture. X 1000

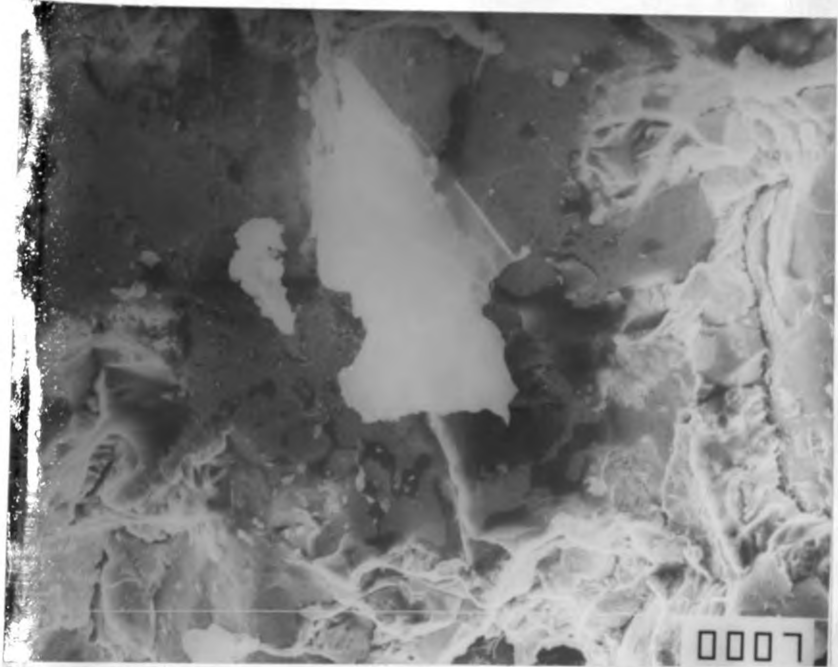


(a)

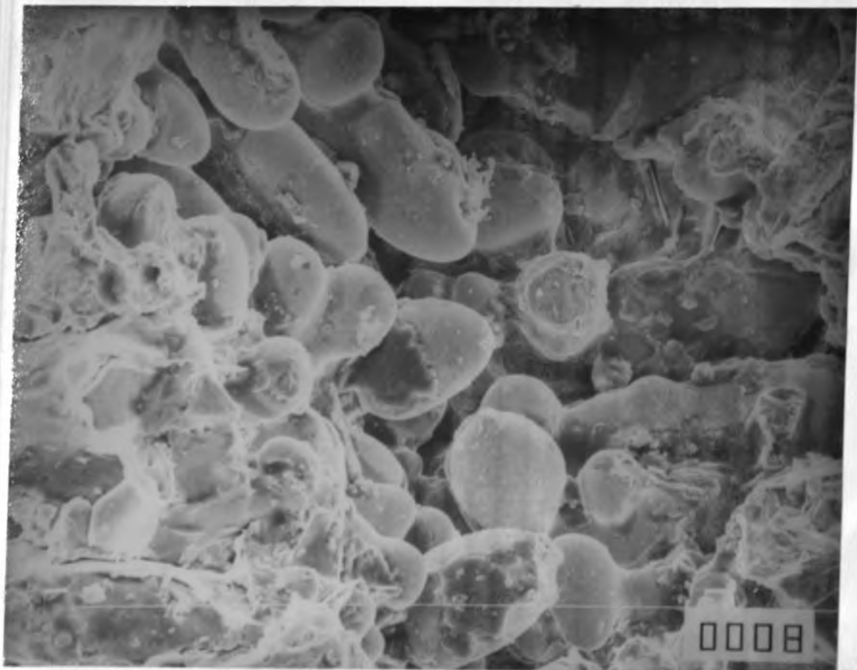


(b)

Plate 15 - SEM photos. Ductile iron (heat SGA) annealed for 24 hours, ferritic matrix. (a) Nucleation occurs at the nodule/ferrite interface, and failure occurs by microvoid coalescence. X750 (b) Extensive ductile tear in fracture. X750



(a)



(b)

Plate 16 - SEM photos. Ductile iron (heat SGB) as-cast pearlitic matrix. (a) Quasi-brittle fracture with crack branching or "channeling". X 1000
(b) Shows porosity, a result of trapped gases or turbulent flow of metal. X 500



Plate 17 - SEM photo. Ductile iron (heat SGC) annealed for 24 hours. Low nodularity, ferritic. Shows crack branching or "channeling", and river patterns. X750

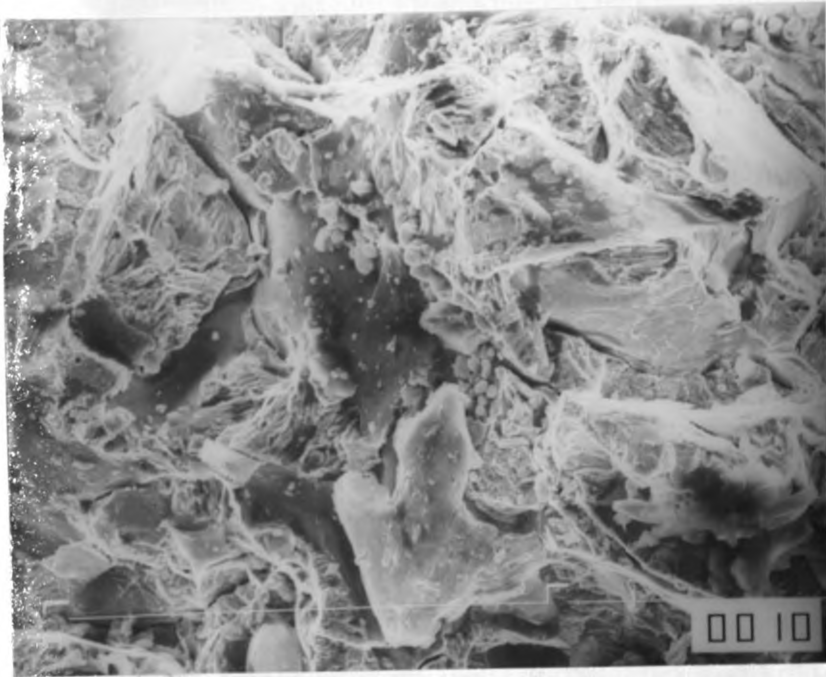


Plate 18 - SEM photo. Gray cast iron (heat G1) as-cast,
pearlitic matrix. Shows brittle fracture
appearance with tongues and river patterns.
X750.

CHAPTER FIVE

5.0 CONCLUSIONS AND RECOMMENDATIONS

5.1 CONCLUSIONS

The following conclusions may be drawn from the present work.

1. The materials under investigation are ductile cast irons of different amounts of residual magnesium content.
2. Foundry production of sound carbide-free ductile iron castings with good nodule count and high nodularity has been found to involve complex physical metallurgy of these materials. The magnesium treatment process for spheroidisation, alloying elements and heat treatment have been found to be the most important production variables which require strict control.
3. Mechanical and microstructural properties have been found to improve as the residual magnesium level increased from 0.004% in gray cast iron to 0.043% in ductile cast iron. This has been attributed to the improved nodularity and nodule count which results from the increase of the magnesium content. The same effects have been observed when the sulphur content decreases from 0.08% to 0.05% .

4. The tensile strength has been found to lie between 250 MN/m^2 and 380 MN/m^2 in low and high magnesium ductile irons respectively, while the percent elongation lies between 1 and 2.5 .

For the materials tested the values obtained for the conditional fracture toughness are as follows:

gray cast iron,	19.34 to 25.72 $\text{MN/m}^{-3/2}$
ductile iron, alloy SGA,	31.30 to 68.48 $\text{MN/m}^{-3/2}$
ductile iron, alloy SGB,	23.16 to 29.87 $\text{MN/m}^{-3/2}$
ductile iron, alloy SGC,	18.81 to 28.63 $\text{MN/m}^{-3/2}$
mild steel,	54.33 to 59.63 $\text{MN/m}^{-3/2}$

The toughness of the ductile cast irons has been found to depend on the amount of ferrite in the matrix and the thickness of the ferrite ring around the graphite nodule.

5. The microstructure has been found to govern the mechanical properties and this has been observed to be more pronounced in the fracture behaviour of the ductile irons.

Ferritic matrix structures, high nodule counts, high graphite shape factor or nodularity, small inter-nodule spacing and small matrix grain size have been observed in the materials with high fracture toughness values.

Nodule size has been observed to have little effect on the properties.

6. Alloying elements have been found to affect both production and the properties of ductile irons.
7. The specimens have been observed to fracture by ductile tear for ferritic matrix structures and by intergranular fracture for pearlitic matrix structures. The specimens with low nodularity have been observed to exhibit quasi-cleavage fracture.

5.2 RECOMMENDATIONS FOR FUTURE WORK

The following recommendations may be made from this study.

1. More work needs to be done to obtain high quality ductile cast iron and establish quality control and quality assurance procedures. It is suggested that gray cast iron scrap be mixed with some pig iron and steel scrap in the ratio 5:3:2 . Then silicon briquets and/or silicon carbide be used to boost the level of silicon and/or carbon, and desulphurisation be done before the spheroidising treatment.

Inoculation with silicon after the magnesium treatment is suggested in order to improve graphitisation and nodularity.

2. More data needs to be obtained for the fatigue and fracture toughness of the ductile irons under different environmental and temperature conditions.
3. Specific studies of the effects of the individual alloying elements on the fatigue and toughness is required so that composition optimisation can be achieved for specific applications of these materials.
4. Austempering heat treatment should be applied to these materials in order to improve their mechanical properties.
5. Attention should be given to the effects of impurities which occur as tramp elements in these materials and how they may be eliminated.
6. Other properties like creep, impact properties and damping properties should also be investigated.

APPENDIX A

A.0 THE FAMILY OF CAST IRONS

A.1 DEFINITION

The term cast iron is an alloy of iron, carbon (up to about 4.0%), and silicon (up to about 3.5%) and is the collective term for the group of engineering materials designated specifically as follows.

1. White and chilled cast iron
2. Malleable cast iron
3. Gray cast iron
4. Nodular cast iron (also known as spheroidal graphite cast iron or ductile cast iron)
5. High alloy cast iron (or alloy cast iron)

Cast iron offers a tremendous range of the metallic properties of strength, hardness, machinability, wear resistance, abrasion resistance, and corrosion resistance and other properties [61]. Further, the foundry properties of cast irons in terms of yield, fluidity, shrinkage, casting soundness, ease of production and others make it highly desirable for casting purposes.

A.2 CHEMICAL COMPOSITION

The broad limits of chemical composition of some cast irons are given in Table A.1 and the overall picture of the composition ranges in the table with respect to carbon and silicon in cast iron is illustrated in Figure A.1 .

The four basic types of cast iron are best differentiated by their chemical composition and their microstructure. The typical chemical compositions, specifications and use of a few commercial cast irons are given in reference [61] .

A.2.1 WHITE AND CHILLED CAST IRON

White cast iron is produced when the cooling rate of the metal during solidification is so rapid that the carbon in the molten metal remains chemically combined with iron. It is hard and brittle, has a high compression strength, excellent wear resistance, and retains its hardness even at red heat.

Chilled iron is formed in when rapid solidification is allowed in certain areas as of soft to form chills. An area in a casting that solidifies at an intermediate rate can contain both iron carbide and graphite and is called mottled iron.

The microstructure of white cast iron consists of pearlite and a large percentage of iron carbide.

A.2.2 MALLEABLE CAST IRON

The majority of the carbon in this iron occur in the form of irregularly shaped nodules of graphite. The graphite is formed when white iron is given a heat treatment to dissolve the iron carbide and precipitate the graphite. This form of graphite formed in the solid state during heat treatment is known as temper carbon.

A.2.3 GRAY CAST IRON

This forms the majority of the castings produced. It consists of fine graphite flakes. The flake graphite in gray iron provides it with excellent machinability at hardness levels that provide superior wear characteristics, the ability to resist galling under borderline lubrication, and unusual elastic properties which provide excellent vibration damping.

A.2.4 DUCTILE IRON

In ductile iron the graphite occurs in form of spheroids rather than as flakes. The spheroids are obtained by inoculating with a magnesium alloy, a molten iron which is of typical gray iron analysis except for a very restricted content of minor elements like phosphorus and sulphur. The metallurgy of this addition has been presented in the main text of this report.

A.2.5 HIGH ALLOY CAST IRONS

These include high alloy white irons, high alloy gray irons and high alloy ductile irons. They are used in applications with unusual requirements, such as extreme abrasive wear resistance, heat resistance, corrosion resistance or unusual physical properties such as low thermal expansion or no magnetic attraction. They are usually specified by their chemical analysis.

A.3 MICROSTRUCTURE

The structural components of cast irons differentiate the various types of irons, white, gray, malleable, and spheroidal carbon. The most important components are defined below.

A.3.1 GRAPHITE

This is carbon in the free or elemental condition. In gray iron, flakes of graphite develop as the iron freezes and may amount to about 6-17% of the total volume [5] .

Temper carbon or graphite aggregates are developed in malleable irons by heat treatment of the white irons.

Spheroidal graphite may develop when irons are treated with a small percentage of magnesium, cerium or other special element.

The amount, size, shape, and distribution of graphite in cast irons greatly influence their properties.

Graphite as temper carbon in malleable irons and as spheroidal carbon ductile irons, does not decrease ductility to the same degree as flake [61] .

A.3.2 CEMENTITE

This is a chemical compound of carbon and iron, Fe_3C . This develops during freezing of white or chilled cast irons. It also occurs as a constituent of pearlite. It is hard and brittle.

A.3.3 FERRITE

Ferrite is defined as a solution of the normal temperature body-centred cubic crystalline form of iron and small amounts of carbon. As such it is relatively soft, ductile, and of moderate strength. Silicon hardens ferrite.

Ferrite in cast irons may occur as free ferrite or as ferrite in pearlite. Ferrite predominates in malleable irons and nodular irons of maximum ductility. In gray irons it occurs as a constituent of pearlite. It contains less than 0.02% carbon. A ferritic matrix is most often desired in iron because of its excellent machinability. In ductile iron ferrite provides the high ductility.

A ferritic matrix is not suitable for applications requiring excellent wear resistance and for flame or induction hardening because of its lack of combined carbon.

A.3.4 PEARLITE

Pearlite is a mixture of ferrite and cementite arranged in alternate lamellae. It is strong and moderately hard with some ductility. The amount present in cast iron depends on the degree of graphitisation.

It contains about 0.5-0.9% combined carbon. In white irons, pearlite and cementite are the chief structural components.

A.3.5 STEADITE

This is a eutectic of iron and iron phosphide of low melting point about 950-980°C . Iron phosphide is very hard and brittle, so excessive phosphide content raises the hardness and brittleness of gray iron because of the steadite formed. Steadite contributes to decrease of machinability and increased wear resistance.

A.3.6 AUSTENITE

Austenite may be defined as a solution of carbon and the high-temperature face-centred cubic crystalline form of iron which occurs during solidification and which, during slow cooling, changes to pearlite, ferrite or a combination of the two. Austenite as a portion of the microstructure at room temperature, is encountered only in cast irons which are specially alloyed with nickel to make the austenite stable at room temperature.

A.3.7 OTHER CONSTITUENTS OF CAST IRONS

Molybdenum and nickel can cause the matrix structure to become acicular (binitic) as it cools in the mould after casting. This structure provides a very high strength at a machinable hardness without the necessity and problems of a separate heat treatment.

Iron may be alloyed so that the matrix structure is martensitic as-cast. This is characteristic of the extremely wear resistant chromium-nickel white cast iron in which carbides are surrounded by a matrix of martensite.

The sulphur that is present in iron normally occurs as manganese sulphide. This compound solidifies at a temperature above the solidification temperature of the iron, therefore it forms in separate particles [62] .

A.4 SUMMARY

Chemical composition is by far the only factor determining the microstructure of cast irons. Cooling rate, freezing mechanism and the evolution of certain gases from the metal may alter the microstructure, and properties.

In nodular cast irons the graphite shape, size, distribution and nodule count may be varied by the melting and metal-handling practice and alloying variation [63].

In malleable irons, the melting practice and heat treatment given the white iron are the major factors affecting the properties.

In all cast irons, the influence of section size and cooling rate is omnipresent.

	Gray iron Wt %	White iron Wt %	Malleable iron Wt %	Ductile iron Wt %
Carbon	2.50-4.00	1.80-3.60	2.00-2.60	3.00-4.00
Silicon	1.00-3.00	0.50-1.90	1.10-1.60	1.80-2.80
Manganese	0.25-1.00	0.25-0.80	0.20-1.00	0.10-1.00
Sulphur	0.02-0.25	0.06-0.20	0.04-0.18	0.03 Max
Phosphorus	0.05-1.00	0.06-0.18	0.18 Max	0.10 Max
Magnesium	—	—	—	0.01-0.10

Table A.1 - Range of compositions for typical unalloyed cast irons [5].

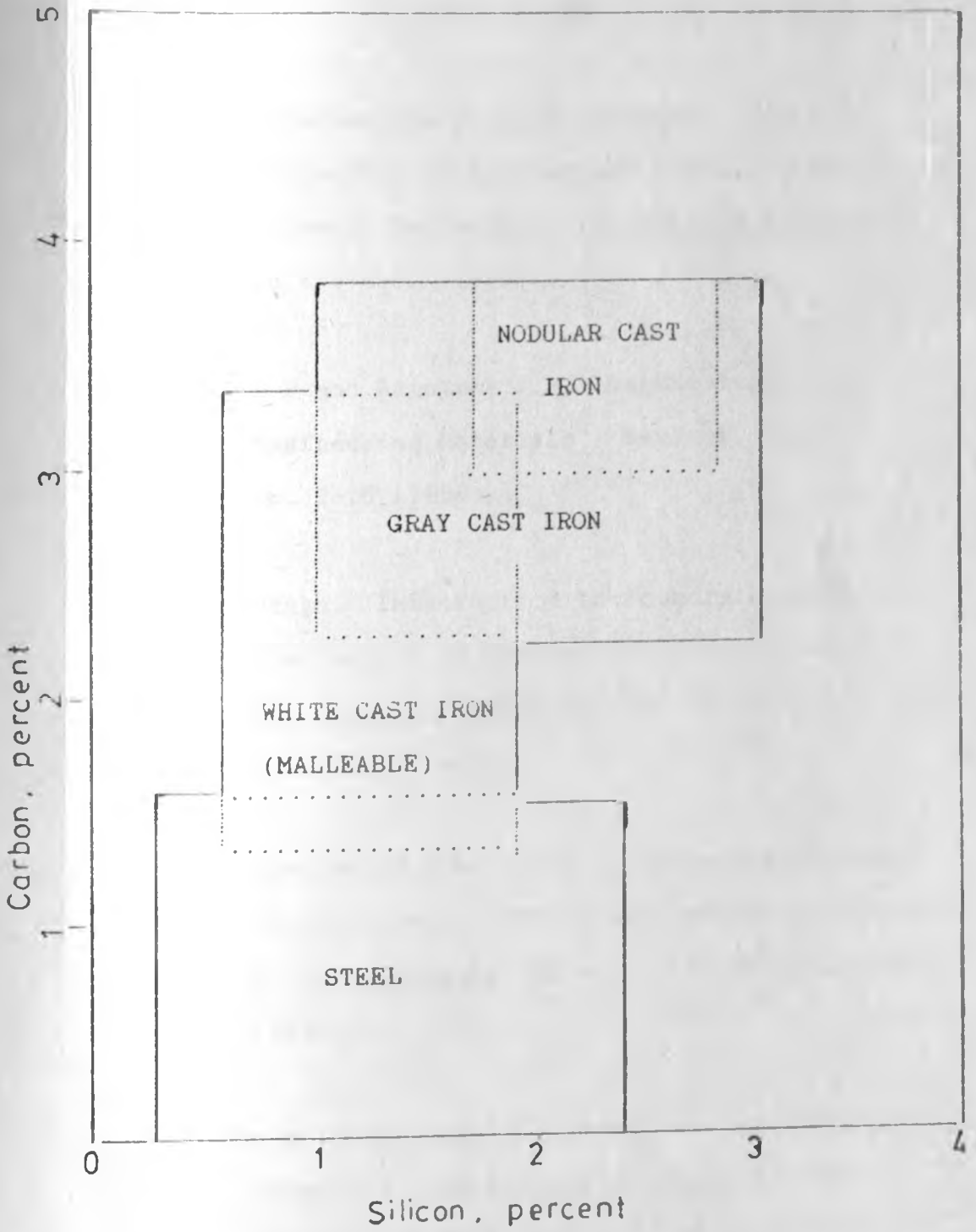


Figure A.1 - The carbon and silicon percentage ranges present in cast irons [5].

REFERENCES

1. R. A. Harding and G. N. J. Gilbert, "Why the Properties of Austempered Ductile Irons Should Interest Engineers", The British Foundryman pp.489-496, (1986).
2. Minor D.F and Seastone J.B, "Handbook of Engineering Materials", Newyork, Wiley pp. 2-15 (1955).
3. H.L. Morgan, "Introduction to Foundry Production and Control of Austempered Ductile Irons". The British Foundryman, pp. 98-108 (Feb/March, 1987).
4. R.C Voight and C.R Loper Jr., "Austempered Ductile Iron - Process Control and Quality Assurance", J. Heat Treating ASM vol. 3 No.4 pp. 291-309 (1984).
5. Richard W. Heine, Carl R. Loper, Jr. and Philip C. Rosenthal, "Principles of Metal Casting", McGraw-Hill Book Company, London, (1974).
6. UNIDO, "A Handbook of Industrial Statistics", (1985).

7. BCIRA, "Engineering Data on Nodular Cast Irons SI units", Birmingham, (1974).
8. Donaldson, E.G., "Automotive Applications of Spheroidal Graphite Cast Iron", Foundry Trade Journal Vol. 156 No. 3287, pp. 544, 548, 551, (June, 1984).
9. Gratton, R., "Forecasting the Ductile Iron Industry", Modern cast Vol 73 No 10, pp.20-23, (Oct. 1983).
10. R. Salzbrenner., "Fracture Toughness Behaviour of Ferritic Ductile Cast Iron". J. Mat. Sci. vol 22, pp. 2135-2147, (1987).
11. P.F. Weiser, C.E. Bates and J.F. Wallace, "Mechanism of Graphite Formation in Iron-Silicon-Carbon Alloys", By Malleable Founders Society Ohio, (1967).
12. M.H. Jacobs, T.S Law, D.A. Melford and M.J. Shawell. "Basic Processes Controlling the Nucleation of Graphite Nodules or Chill Cast Iron", Metal Technology Vol. 1, p.490, (1974).

13. R.J. Warrick., "Spheroidal Graphite Nuclei in Rare Earth and Magnesium Inoculated Iron", Trans AFS Vol. 74, p.722, (1966).
14. S. Yamamoto, Y. Kawano, Y. Murakimi, B. Chang and R. Ozaki, "Producing Spheroidal Graphite Cast Iron by Suspension of Gas Bubbles in Metals", Trans. AFS Vol. 83, p.217, (1985).
15. V.R.S. Murthy, Kishore and S. Seshan, "Morphology of Flake , Ductile and Compacted Graphite", Journal of Metals, pp. 24-28, (Dec. 1986).
16. Ralph Barton, "Magnesium Treatment Processes for S-g Iron Production", Foundry Trade Journal, pp.119-121, (Feb. 1987).
17. ASTM A 536-84, "Standard Specification for Ductile Iron Castings", Annual Book of ASTM Standards Vol. 01-02 section 1, pp. 325-380, (1987).
18. G.E. Else and R.H. Dixon, "The magnesium Treatment of Cast Iron for the Production of Spheroidal Graphite or Compacted Graphite Cast Irons", The British Foundryman, pp. 18-23, (Jan. 1988).

19. R.W. Heine, "Oxidation - Reduction Principles Controlling the Composition of Molten Cast Iron", Trans. AFS Vol. 59, (1951).
20. S.L. Gartsman, "Desulphurisation of Iron and Steel", Foundry Vol. 86, p.46, (1958).
21. Charles F. Walton, "Gray and Ductile Iron Castings Hand Book", Published by Gray and Ductile Iron Founders' Society, (1971).
22. H. W. Lownie, Jr., "Ladle Inoculation Improves Gray Iron Properties and Structures", Foundry Vol. 71, (Nov.-Dec., 1943).
23. S. Vasudevan, S. Seshan and K. Chattopadhyay, "A Study of the Influence of Manganese Additions on Austenitic Ductile Iron", The British Foundryman, pp.243-251, (June, 1984).
24. D. Argo and M Gagne, "The Effects of Manganese on the Microstructure and the Mechanical Properties of compacted Graphite Irons", The British Foundryman, pp.172-177, (May, 1985).

25. K.I. Washcherko and A.P. Rudoy, "Surface Tension of cast Iron", Trans. AFS. Vol. 70, p855, (1962).
26. B.F. Dyson, "The Surface Tension of Iron and some Iron Alloys", Trans. AIME Vol. 227, p1098, (Oct., 1963).
27. Stanp D.W. Kennedy J., "Development of Magnesium Treatment for S-g Iron Production Using Sliding Gate Valve Injection", Paper presented at BCIRA international Conference, S-g Iron - The next 40 years. Warwick University, (April, 1987).
28. Horiuchi, Y., "Ductile Iron Application and Production Method in Japan", AFS/DIS Quality Ductile Iron production, Rosemont, Illinois (14-16 Oct. 1975).
29. Best, K.J., "Metallurgical Treatment of Molten Iron by Means of Inoculant Wire and Magnesium Treatment Wire", Giesserei - Praxis Vol. 21, pp.313-320, (6 Nov., 1983).

30. Whitecomb, R.C., "Flow-through Process Makes Ductile Iron", Foundry Management and Techniques, pp.30-32, (Feb., 1984).
31. Palmer P.V. and Wright D.V., "The Imconod Process for Nodular Graphite Cast Iron batch Production", Foundry Trade Journal, pp. 323-325, (April, 1985).
32. Remondino M., Pilastro F. and Natale E., "Quality and Economic Aspects of In-mould Iron Treatment", 43rd International Foundry Congress, Bucharest, Paper No. 11, (1976).
33. Arun M. Rao, K.S.S. Murthy, M.R. Seshadri, "Feeding of Nodular Iron in Shell Moulds", The British Foundryman, pp.131-139, (1985).
34. J.V. Anderson and S.I. Karsay, "Pouring Rate, Pouring Time and Choke Design for S-g Iron Castings", The British Foundryman, pp.492-498, (Dec. 1985).
35. H.Roedter, "An Alternative Method of Pressure-control Feeding of Ductile Iron Castings", Foundry Trade Journal Int., pp.174-178, (Sept., 1986).

36. S. Nishi, T. Kobayashi, S. Taga, "The Effect of Microstructure on the Toughness of Ferritic Nodular Cast Iron", Journal of Materials Science Vol.11, pp.723-730,(1976).
37. D.A. Shockey, K.C. Dao, R.L. Jones, "Effect of Grain-size on the Static and Dynamic Fracture Behaviour of α -Titanium", Mechanisms of Deformation and Fracture, Edited by K.E. Easterling, University of Lulea, Sweden, (1978).
38. H. Conrad, "Iron and its Dilute Solid Solutions", Interscience, Newyork, p. 314(1963).
39. Stephen I. Karsay, "Ductile Iron I - Production. The State of the Art", Quebec Iron and Titanium corporation, Canada, (1976).
- 40 D.E. Diesburg, "Fracture Toughness Test Methods for Abrasion Resistant White cast Irons using Compact specimens", Fracture Toughness and Slow-stable Cracking, Proceedings of the 1973 National Symposium of Fracture - Proceedings of the ASTM STP 559, p3. (1974).

41. J.F. Knott, "Fundamentals of Fracture Mechanics",
Published by the Butterworth Group, London,
(1973).
42. D.J. Hayes, "Origins of the Stress Intensity
Factor Approach to Fracture", A general
introduction to fracture mechanics, A Journal
of Strain Analysis Monograph Mechanical
Engineering Publishing Ltd London, p.9, (1978).
43. Geoffrey R. Egan, "Techniques for Assessing
Fracture Toughness", The mechanics and
physics of Fracture, The metals
society/Institute of Physics, (1975).
44. V.J. Colangelo and F.A. Heiser, "Analysis of
Metallurgical Failures", John Wiley and sons,
Newyork, London, (1974).
45. J.C. Radon and A.A. Pallock, "Development of Fast
Fracture in Low Alloy Steel", Fracture
Toughness and slow-stable cracking -
proceedings of the 1973 National Symposium of
Fracture Mechanics Part 1. ASTM STP 559
p.15, (1974).

46. D.K. Verma and J.T. Verry, "Microstructural and Macrostructural Modeling of the Fracture Behaviour of Pearlitic Gray Irons", Trans. ASME. Journal of Engineering Materials and Technology Vol. 104, pp 262-266, (Oct. 1982).
47. BSI Handbook No. 19., "Methods for the Sampling and Analysis of Iron, Steel and Other Metals", (1978).
48. Frost N.E, Marsh J.K. and Pook L.P., "Metal Fatigue", Oxford University Press, Ely House, London , (1974).
49. BS 5447., "Methods of Testing for Plane Strain Fracture Toughness (K_{Ic}) for Metallic Materials", (1979).
50. ASTM E 399 - 81., "Standard Test Method for Plane Strain Fracture Toughness of Metallic Materials", Annual Book of ASTM Standards Part 10, (1980).
51. BS 3846., "Methods for the Calibration and Grading of Extensometers for Testing of Metals", (1979).

52. ASTM E 10-78., "Standard Test Method for Brinell Hardness of Metallic Materials", Annual Book of ASTM Standards Part 10, (1981).
53. ASTM E 8-81., "Standard Methods of Tension Testing of Metallic Materials", Annual Book of ASTM Standards Part 10, (1981).
54. ASTM E3 - 80, "Standard Methods of Preparation of Metallographic Specimens", Annual Book of ASTM Standards Part 11, (1981).
55. ASTM E 112 - 81, "Standard Methods for Estimating the Average Grain Size of Metals", Annual Book of ASTM Standards Part 11, (1981).
56. ASTM E2 -62, "Standard Methods of Preparation of Micrographs of Metals and Alloys; Including Recommended Practice for Photography as applied to Metallography", Annual Book of ASTM Standards Part 11, (1981).
57. Jen Kei-Peng, Scardina, Joseph T. Smith, Dallas G., "Fracture Behaviour of As-cast Pearlitic Nodular Iron", Eng. Fract. Mech. Vol. 22, No 2 pp. 227 - 236, (1985).

58. R.K. Nanstad, F.J. Worzala and C.R. Loper Jr.,
"The Fracture Characteristics of Nodular Cast
Iron", Trans AFS Vol. 82, pp.473-486, (1974).
59. A. Little and H.J. Heine, "The Fracture Toughness
of Malleable and Ductile Iron", Trans. AFS
Vol. 82, (1974).
60. Paulo da Silva Pontes, Nivado Lemos Cupini, Atsumi
Ohuo., "Grain Refinement by Gas Bubble
Stirring During Solidification", The British
Foundryman Vol. 178, Part 4, p.178, (May, 1985).
61. American Foundryman's Society, "Cast Metals
Handbook, 4th Edition", Newyork Wiley. (1957).
62. I. Minkoff "The Physical Metallurgy of Cast
Iron", Published by John Wiley and sons,
(1984).
63. M.H. Jacobs, T.S. Law, D.A. Melford & M.J. Shawell,
"Basic Processes Controlling the Nucleation of
Graphite Nodules or Chill Cast Iron", Metal
Tech. Vol. 1, p.490, (1974).